

**UCSF**

**UC San Francisco Electronic Theses and Dissertations**

**Title**

Adaptation and recovery from adaptation in the auditory nerve of the cat

**Permalink**

<https://escholarship.org/uc/item/1w15s8wj>

**Author**

Chimento, Thomas C.

**Publication Date**

1989

Peer reviewed|Thesis/dissertation

Adaptation and recovery from adaptation in the auditory nerve of the cat.

by

Thomas C. Chimento Jr.

**DISSERTATION**

**Submitted in partial satisfaction of the requirements for the degree of**

**DOCTOR OF PHILOSOPHY**

in

Speech and Hearing Science

in the

**GRADUATE DIVISION**

of the

**UNIVERSITY OF CALIFORNIA**

**San Francisco**

DEGREE  
CONFERRED

5 1 1988



Date

University Librarian

Degree Conferred: . . . . .

**This work is dedicated to my parents, who gave me the moral and financial support to complete my undergraduate studies and begin my graduate studies, and to my wife, Catherine, who continued that support through the completion of my doctorate.**

## **ACKNOWLEDGEMENTS:**

As one progresses through an academic career, many individuals provide insights and perspectives which aid in choosing a field of investigation and, finally, a dissertation project. In my case, John Williston was the person who introduced me to the field of electrophysiology. I was able to continue along that path by working with Don Jewett and John Gardi.

The study that follows was my third attempt at a dissertation topic. I thank Mike Merzenich for allowing me the freedom to try the initial two projects even though they did not fall strictly within the framework of ongoing research in his laboratory. Although these initial attempts did not lead to a dissertation, they added to my understanding of the auditory system and the difficulties inherent in developing new research procedures.

I want to thank Russell Snyder for suggesting the framework of the present study and for his assistance in the surgical procedures and use of the data collection system.

I especially want to thank Christoph Schreiner for his guidance and patience. There are few scientist as easy to work with as Dr. Schreiner. He is willing to listen to suggestions and allow one to do experiments that he may not completely agree with, as long as a reasonable justification can be presented. Having Chris as my mentor was truly a pleasure.



## **ABSTRACT:**

This study examined the time course of adaptation and recovery from adaptation of the auditory nerve neurophonic (ANN) and single auditory nerve fiber responses. The conditions studied were: 1) adaptation response using low level, 800 Hz or characteristic frequency (CF) stimuli; and 2) onset recovery and whole-tone response recovery following a masker of equal frequency with variable silent intervals between the masker offset and probe onset.

The auditory nerve neurophonic (ANN) reflects the ensemble response of phase-locked firing in single auditory nerve fibers to sustained signals. Consequently, neural response properties such as adaptation and recovery from adaptation of these coherent following responses can be studied in this experiment. ANN and single unit responses to 290 ms long, 800 Hz or CF tones presented at 10-30 dB SL were recorded from the auditory nerve of the cat. Adaptation properties were determined and fit to the equation:  $A(t_p) = Y_r * (\exp(-t_p / \text{Tau}A_r)) + Y_s * (\exp(-t_p / \text{Tau}A_s)) + A_{ss}$ . Recovery from adaptation was determined by recording the response of a probe tone following a 100 ms masker tone equal in frequency to the probe, ranging from -5 to 30 dB relative to the probe amplitude. Both the onset recovery and the whole tone recovery were determined for the ANN and single unit responses. The onset data were analyzed and fit to either the equation:  $A(\Delta t) = A_{\max} - Y_r * (\exp(-\Delta t / \text{Tau}R_r)) + Y_s * (\exp(-\Delta t / \text{Tau}R_s))$  or  $A(\Delta t) = A_{\max} - Y * (\exp(-\Delta t / \text{Tau}R))$ . The whole tone response could be fit to either the adaptation equation or to the two-time-constant recovery equation, depending on the relative amplitude of the masker and the length of the silent interval between masker offset and probe onset.

The results of this study indicate that ANN time constants are comparable to those measured for single fibers. The pattern of recovery of the whole tone response for the ANN is comparable to the single fiber response. Models which have been used to describe synaptic transduction in the auditory nerve are presented and compared to the results of this study. Possible sites and mechanisms for adaptation and recovery from adaptation taking into account recent data from electrical stimulation studies and receptor channel morphology and kinetics are discussed.

## **Table of Contents:**

<b>ACKNOWLEDGEMENTS:</b> .....	iii
<b>ABSTRACT:</b> .....	iv
<b>LIST OF FIGURES:</b> .....	vii
<b>INTRODUCTION:</b> .....	1
Adaptation: .....	1
Recovery from Adaptation:.....	4
Auditory Nerve Neurophonic (ANN): .....	8
<b>METHODS:</b> .....	10
General: .....	10
Signal Generation and Control:.....	11
Response Recording and Analysis:.....	13
ANN-.....	13
Single fibers-.....	13
Data Analysis: .....	14
ANN-.....	14
Single fibers-.....	16
<b>RESULTS:</b> .....	17
Single Fiber Response Characteristics:.....	17
Adaptation: .....	17
Recovery: .....	19
Onset Recovery: .....	21
Whole Tone Recovery: .....	39
Auditory Nerve Neurophonic Response Characteristics: .....	47
Adaptation: .....	47
Onset Recovery: .....	53
Whole Tone Recovery: .....	56
<b>DISCUSSION:</b> .....	64
Adaptation: .....	70
Onset Recovery: .....	71
Whole Tone Recovery: .....	74
Comparison of ANN to Single Fiber Responses:.....	75
Where and How?.....	78
Previous Models: .....	85
Features of a model of synaptic transduction:.....	97
<b>BIBLIOGRAPHY:</b> .....	99

## **LIST OF FIGURES:**

Fig. M1.	Schematic of stimuli .....	12
Fig. R1.	PSTH to 290 ms 800 Hz. pure tone.....	18
Fig. R2.	Adaptation examples .....	20
Fig. R3.	Time constants of adaptation vs. stimulus probe level.....	22
Fig. R4 .	Time constants of adaptation vs. CF.....	23
Fig. R5.	Time constants of adaptation vs. CF.....	24
Fig. R6.	Time constants of adaptation vs. CF.....	25
Fig. R7.	TauAr vs. TauAs. ....	26
Fig. R8.	TauA vs. each unit. Another form of the previous Figure ....	27
Fig. R9.	Two-tau onset recovery examples. ....	29
Fig. R10.	One-tau onset recovery examples.....	30
Fig. R11.	Two-tau onset recovery time constants vs. relative masker/probe level.....	31
Fig. R12.	Two-tau onset recovery time constants vs. masker level. ....	32
Fig. R13.	Two-tau onset recovery time constants vs. probe level. ....	33
Fig. R14.	Two-tau onset recovery time constants vs. CF.....	34
Fig. R15.	One-tau onset recovery time constants vs. relative masker/probe level.....	35
Fig. R16.	One-tau onset recovery time constants vs. masker level. ....	36
Fig. R17.	One-tau onset recovery time constants vs. probe level. ....	37
Fig. R18.	One-tau onset recovery time constants vs. CF. ....	38
Fig. R19.	Single unit whole tone recovery.....	42
Fig. R20a.	Examples of whole tone recovery in four units.....	43
Fig. R20b.	Examples of whole tone recovery in four units.....	44
Fig. R20c.	Examples of whole tone recovery in four units.....	45

Fig. R20d. Examples of whole tone recovery in four units..... 46

Fig. R21. Examples of averaged ANN data..... 49

Fig. R22. ANN adaptation time constants. .... 50

Fig. R23a. RMS amplitude values and model values for adaptation. .... 51

Fig. R23b. RMS amplitude values and model values for adaptation. .... 52

Fig. R24. ANN recovery time constants. .... 54

Fig. R25. ANN data and model for recovery from adaptation. .... 55

Fig. R26. ANN whole tone recovery..... 58

Fig. R27. ANN whole tone recovery at  $\Delta t = 0$ . .... 59

Fig. R28a. Examples of whole tone recovery in four animals..... 60

Fig. R28b. Examples of whole tone recovery in four animals..... 61

Fig. R28c. Examples of whole tone recovery in four animals..... 62

Fig. R28d. Examples of whole tone recovery in four animals..... 63

Fig. D1. Schematic of adaptation and onset recovery ..... 66

Fig. D2. Schematic of whole tone recovery traces. .... 68

Fig. D3. Same as D2 with masker louder than the probe ..... 69

Fig. D4. Electrically stimulated auditory nerve fiber responses. .... 81

Fig. D5. Schematic of Brachman model. .... 88

Fig. D6. Schematic of Eggermont model. .... 90

Fig. D7. Schematic of magnitude of adaptation. .... 91

Fig. D8. Results of Eggermont model for whole tone recovery..... 93

Fig. D9. Schematic of Meddis model. .... 95

## **INTRODUCTION:**

Knowledge of the time course of adaptation and recovery from adaptation of the auditory nerve are critical for the analysis of how the auditory system handles the flow of information of complex, time varying stimuli, e.g. of running speech. The primary sources of such data for the peripheral auditory system, e.g. for the design of models of speech processing, has been the responses of single auditory nerve fibers and compound action potentials (CAP) (Delgutte, 1982; Sachs et al., 1982; Miller and Sachs, 1983; Sachs et al., 1983; Sinex and Geisler, 1983, 1984; Delgutte, 1984; Delgutte and Kiang, 1984a,b,c,d). Although the results of these two methods produce similar values for a given species (Eggermont and Spoor, 1973a,b; Spoor et al., 1976), the stimuli used in easily accomplished measurement of CAPs have been restricted to short duration, high frequency tones. For the development of accurate models which can be applied to human speech perception, the adaptation and recovery from adaptation for longer duration, low frequency tones need to be taken into account. Ideally, human auditory nerve responses would be utilized for the development of these models. The auditory nerve neurophonic (ANN) can be recorded in humans, and can provide a measure of longer-term, low frequency adaptation and recovery responses.

### **Adaptation:**

The process of adaptation following an intensity step in the input produces a large initial response followed by a gradual reduction to a constant sustained level (steady state). This reduction displays an exponential decay from the initial response magnitude toward the steady state response

level. The analysis of single auditory fiber responses and CAP responses to tone bursts has led to quantitative estimates of the time constant(s) of adaptation. The majority of previous studies that have attempted to describe adaptation quantitatively have used a single time constant (Kiang et al., 1965; Smith and Zwislocki, 1975; Smith, 1979; Harris and Dallos, 1979; Huang, 1981). Values ranged from approximately 10 msec in cat to 60 msec in Mongolian gerbil. Several investigators have applied an equation with two exponential processes (i.e. two time constants) to more accurately fit the adaptation process (Brachman 1980; Smith and Brachman 1982; Westerman and Smith 1984; Westerman, 1985).

Recording from single units is a relatively difficult and time consuming procedure which is not feasible in humans for the foreseeable future. It is less difficult to place an electrode on the round window and record the CAP volume conducted from the auditory nerve. In this way Abbas and Gorga (1981) measured "perstimulatory adaptation" in cats with a modified forward masking paradigm. An 8 kHz masker of varying duration was followed after a delay of 5 msec by a short 8 kHz probe. The CAP amplitude elicited by the probe was measured as a function of masker duration. It was assumed that no significant recovery from the masker had occurred when the probe was presented, and that the magnitude of adaptation at the end of the masker was therefore being measured. The CAP response pattern across stimulus amplitude was similar to PSTHs for single unit responses, and was interpreted as reflecting the frequency specific response of a limited population of auditory fibers.

The adaptation of CAP responses of humans and guinea pigs recorded with identical stimuli have been compared (Spoor et al., 1976; Eggermont and Spoor, 1973a). Trains of stimuli presented at varying inter-

stimulus intervals (ISIs) were used. The relative amplitude and absolute latencies of auditory nerve responses ( $N_1$ ) to 4 and 6 kHz tones were measured. The interstimulus interval needed for  $N_1$  to reach a given relative amplitude or latency was four times greater in man than in guinea pigs.

A comparison of the adaptation time constant of auditory nerve fiber responses and CAPs was conducted using Mongolian gerbils (Westerman, 1985). Stimuli were 4 kHz tones of varying duration followed after a 10 msec delay by a brief 4 kHz probe tone. Again it was assumed that no significant recovery had occurred between the masker offset and the probe onset, and that the probe tone was therefore measuring the magnitude of adaptation at the end of the masker tone as a function of stimulus duration. A good correlation was found between the CAP and single fiber responses. By applying a curve-fitting algorithm to the CAP data, a mean rapid time constant of adaptation of 2 msec and a mean short term time constant of adaptation of 58 msec was estimated. A single recovery time constant equation was applied to the single unit data and a mean value of 48 msec estimated.

Kiang et al. (1965) described the single unit response pattern to tone bursts as having "a sharp peak at the onset with a gradual 'adaptation' to a relatively stable rate of discharge." A similar response pattern was produced with long duration noise bursts. Changes in the discharge rate reached a plateau approximately 30 ms after stimulus onset. However, if very long (1 min) stimuli were used, a continuous gradual reduction in firing rate proceeds throughout the stimulus presentation.

In 1975, Smith and Zwislocki published a more detailed account of single unit adaptation. 200 ms tones were presented to guinea pigs at the CF of the fiber being studied. A quasi-steady firing rate occurred within 150



ms of stimulus onset and the decline in firing rate followed an exponential function with a time constant of approximately 40 ms. Later work from this group demonstrated two adaptation time constants produced a more accurate description of the decline in firing rate (Smith and Brachman, 1980,1982; Brachman, 1980; Westerman, 1985; Westerman and Smith, 1984).

In summary, an adaptive process which follows an exponential time course has been observed in all CAP and single fiber studies of the vertebrate peripheral auditory system. The decline in response amplitude or firing rate can be defined by the time constant of adaptation. The exact value and number of time constants which most accurately describes the data varies between studies. This variation may be caused by interspecies differences or methodological constraints.

### **Recovery from Adaptation:**

When two stimuli of equal amplitude and frequency are sequentially presented, the second stimulus elicits a response of decreased amplitude for some time after completion of the first stimulus. In general terms, the fiber has adapted to the first stimulus and needs some time to recover from the adaptation before a response of equal amplitude can be elicited by the second stimulus. If the amplitude of two stimuli are unequal, and the first stimulus is sufficiently louder than the first, the response to the second stimulus may be completely suppressed, at least for a short time. Depending on the relative amplitude and duration of the masker this effect may be referred to as forward masking, residual masking, poststimulatory threshold shift or temporary threshold shift. The recovery process appears to follow roughly an exponential time course but there is some disagreement

whether there are one or two time constants and whether these time constants are level dependent. For stimuli of equal (moderate) levels the recovery time constant is longer than the adaptation time constant (Smith, 1977; Harris and Dallos, 1979; Eggermont, 1985).

Harris and Dallos (1979) found that the recovery time constant in single nerve fibers increased as the relative masker/probe level increased. For higher masker levels, they also observed a second time constant in the recovery process. However, Westerman (1985) observed only a single time constant in their single unit onset recovery functions. The relative masker/probe levels used by Westerman (1985) ranged from -30 to 0 dB while those in the Harris and Dallos (1979) study ranged from -10 to 40 dB. The latter used only one probe level to make their assessment. These differences in the applied stimulus conditions may be a source of the different results.

Recovery of the CAP from adaptation has been measured in humans and guinea pigs using pure tone or white noise maskers followed by brief probe tones (Eggermont and Spoor, 1973b; Spoor et al., 1976). Spoor et al. (1976) compared the recovery in humans and guinea pigs using identical stimuli. The time to complete recovery was four times longer in man than in the guinea pig and the shape of the recovery function was different.

Westerman (1985) observed a two stage recovery function in the CAP of Mongolian gerbils using a 300 msec masker followed after a variable silent interval by a test tone of equal frequency. The short term recovery had a time constant of approximately 400 msec while the value of the rapid time constant of recovery varied as a function of the relative masker/probe intensity. For a constant level masker at 60 dB SPL and probe amplitudes of

30 to 60 dB SPL, the rapid time constant of recovery varied from 200 to 20 msec, respectively. The rapid recovery results were similar to single fiber onset results, although no variation in the time constant with probe amplitude was seen in the single fiber data. In contrast, Abbas and Gorga (1981) found no variation in the recovery time constant as a function of relative masker/probe level, using CAPs recorded with 4 probe levels and 7 masker levels.

There are two basic methods for examining the effects of adaptation on subsequent single unit firing patterns. The simplest form is comparable to the CAP methods discussed above. An adapting tone is presented followed by a short probe tone. The amplitude of the response is examined as a function of the relative level of the two tones, the silent interval between the masker offset and probe onset and the duration of the masker. The more detailed method is to present long probe tones and examine the same set of parameters as above, but instead of a gross measurement of total response amplitude, a fine grain measurement of the change in probe amplitude during the stimulus presentation is done. By using one to three ms analysis windows the dynamic response properties of the unit could be described as the stimulus parameters are systematically varied.

The first method of analysis was employed by Smith (1977,1979) using gerbil auditory nerve responses. He concluded that the decrement of the probe response produced by a masker was independent of the intensity of the probe tone, i.e. "the (masker) produced a simple shift of the rate-intensity function along the rate coordinate, and (probe) and (masker) responses differed only by an additive constant." The recovery of the 40 ms probe response followed an exponential time course with an average time constant of 115 ms.

A similar examination of forward masked responses was conducted by Harris and Dallos (1979) in chinchilla auditory nerve fibers. They measured the recovery of response magnitude to a 15 ms probe as a function of the silent interval between masker offset and probe onset while varying the relative masker/probe level and the duration of the masker. A masker duration of 100 ms produced the maximal suppression of the probe response. As the silent interval was increased the response magnitude recovered with an exponential time course which varied as a function of relative masker level. In cases where the masker was 10 dB or more louder than the probe, a second time constant was observed in the recovery data.

In the studies described above, the recovery from adaptation was restricted to relatively long duration probes which were thought to describe the onset of the forward masked response. Under these condition any differential recovery of the onset vs. steady state portions of the response would remain undetected.

In summary, recovery from adaptation have been studied in the auditory nerve of several animal species and in humans. The results demonstrate similarities across species in the shape of the processes, i.e. they are all exponential. There are differences in: 1) the actual time constants obtained; 2) the number of time constants invoked to produce a good fit to the data; and 3) the relationship between stimulus level and the estimated time constants. Additionally, many of the investigations have been restricted to high frequency stimuli and short duration probe tones. The detailed pattern of recovery of a forward masked response to a sustained probe as a function of the silent interval between masker offset and probe onset has not been studied. This limitation in procedures was used as a starting point for the collection and analysis of data in the present study.

### **Auditory Nerve Neurophonic (ANN):**

All of the above described data reported in the literature originated from high frequency auditory nerve fibers. None of the cited studies used long duration probe tones to measure whole-nerve phase locked responses. In this study the ANN to long, low frequency tones (in the speech range) is compared to single unit responses recorded in the same species using the same stimuli and analysis methods.

One reason CAPs were limited to short duration, high frequency stimuli is that recording from the round window or promontory using long probe tones introduces cochlear microphonic (CM) responses along with the neural response from the auditory nerve. When recording onset responses to short tone pips, the CM can be eliminated by alternating the phase of the stimulus (Spoor et al., 1976) or by rolling the phase (Abbas and Gorga, 1981) while having little effect on the CAP. This is because the onset response reflects the spectral composition of the rapid initial intensity change and is not phase locked to the stimulus frequency. However, for long duration stimuli, that generate phase locked responses to the stimulus frequency, such as the ANN, rolling the phase of the stimulus cancels the response, while alternating the phase of the stimulus produces a severely altered spectrum of the neural response (Gardi et al., 1979; Chimento and Schreiner, 1989). An effective method for reducing CM contamination without altering the spectrum of the neural response is to record the ANN with bipolar electrodes placed directly on the eighth nerve (Snyder and Schreiner, 1984; 1985). The ANN represents the spatially summed response of synchronized, phase locked auditory nerve fibers. There is evidence that

at low probe levels the magnitude of the ANN accurately reflects the response of a frequency selective population of auditory nerve fibers. Since the ANN can be recorded with low frequency, long duration tones, it provides detailed information about the time course of phase locked responses. With the ANN, adaptation and the recovery from adaptation can be examined with the same stimuli that have been used in single unit studies. The ANN provides a direct view of the coherent ensemble firing characteristics of the auditory nerve. By selectively including only those neurons which are in mutual synchrony and phase locked to the stimulus, the ANN offers a direct method for measuring the threshold, dynamic range, and time constants of adaptation and recovery of the ensemble firing of auditory fibers. In addition, the ANN can be recorded from humans and, consequently, allows a direct estimate of basic physiological characteristics of the human auditory nerve (Møller and Jho, 1988).

The goal of this thesis was to record the auditory nerve neurophonic and single auditory nerve fiber responses in the cat and measure the time constants of adaptation and recovery from adaptation using long duration, low frequency tones. In this study, the ANN is compared to single unit responses recorded in the same species using the same stimuli and analysis methods. The results are fit to a two-time-constant model of adaptation and recovery.

## **METHODS:**

### **General:**

All experiments were conducted on adult cats obtained from a breeding colony on the University of California Davis campus. Animals were free of external and middle ear infections and obstructions. Food and water were provided ad lib to gang-housed animals maintained on a dark-light cycle. The animals were initially anesthetized with an i.m. injection of ketamine HCl (10 mg/kg) and acepromazine (0.1 mg/kg). An i.v. line was inserted into the cephalic vein and a surgical level of anesthesia maintained by continuous infusion of a 10:1 solution of lactated Ringer's and Sodium Pentobarbital (6-7 mg/kg\*hr). Anesthetic level was confirmed by observing the "ear-flick" response to tapping the opening of the outer ear canal with a sharp probe or retraction of the paw following a pinch between the toes with a hemostat.

A tracheotomy was performed to reduce the buildup of fluid in the lungs and allow easy access for acute resuscitation in the event of anesthetic overdose. The left pinna was removed exposing the external auditory canal. The canal was cut approximately 3 mm distal to the tympanic membrane and a hollow ear bar was sealed into the canal for stimulus presentation (see below). The auditory nerve was exposed by opening the cranium posterior to the pinna and retracting the cerebellum medially. The base of the auditory nerve as it exits the internal auditory meatus and enters the cochlear nucleus (CN) can be visualized with either gentle retraction of the nerve by placing small cotton wads between the CN and the lateral wall of the skull or by the CN and auditory nerve being pulled gently medially with retraction of the cerebellum.

### **Signal Generation and Control:**

Stimuli were generated with a Texas Instruments TMS32010 16-bit Digital Signal Processor and output via a Burr-Brown DAC running at an output rate of 60 kHz. The antialiasing filter had an upper cut-off frequency of 15 kHz. The signal was delivered via STAX 54 electret headphones encased in a grounded metal container, which was acoustically coupled to a hollow ear bar sealed into the cats external ear canal. The system was calibrated with a Bruel and Kjaer 1/2 inch microphone. A transfer function for the system was measured with a General Radio Wave Analyzer (model 1521-B) and Graphic Level Recorder (model 1000-A). The amplitude of the stimuli varied less than  $\pm 6$  dB from 100 Hz to 14 kHz.

Probe signals were 800 Hz tones with a total duration of 290 ms including a 5 ms linear rise/fall. Masker tones were 100 ms in duration including a 5 ms linear rise/fall (Fig. M1). Relatively long (5 ms) rise/fall times were used to reduce contamination from an abrupt stimulus onset. The following averaged responses were collected during the ANN experiments: (1) a response to the probe tone alone using a stimulus 10 to 30 dB SL (i.e. above the animal's electrophysiological threshold), (2) a response to a probe following a forward masker after silent intervals ( $\Delta t$ ) of 0, 3, 6, 12.5, 25, 50, 100, 200, and 400 ms. The forward masker was at the same frequency as the probe with an amplitude of -5 to 20 dB relative to the probe, and was always 100 ms in duration because of physiological evidence that masker durations longer than 100 ms do not produce significant additional suppression of the probe (Harris and Dallos, 1979). An interstimulus interval (measured from



**Fig. M1. Schematic of stimuli. A) Maskers were 100 msec tones at 800 Hz. with 5 msec linear rise/fall. Masker tones were presented at levels not more than 30 dB above the probe to avoid neural fatigue. The silent interval ( $\Delta t$ ) varied from 0 to 400 msec (see text for values). Masker frequency was equal to probe frequency in all cases. 500 or 800 Hz probe tones had a total duration of 290 ms with 5 msec linear rise/fall.  $t_p$  equals the time after probe onset. Maximum probe level was 30 dB above the animals threshold (dB SL) and interstimulus intervals (ISI) of 1000 msec were used in all experiments to avoid fatigue. B) Stimuli for adaptation. All characteristics of the probe stimuli were as above, except no masker was present.**

probe offset to masker onset) of 1000 ms was used throughout to avoid fatigue of the neural response.

In the single unit experiments, probe tones were also 10 to 30 dB SL. However, the relative masker level was restricted to 20 and 30 dB above the probe level. The silent intervals used for single unit forward masked responses were the same as the ANN, except the 3 ms silent interval was omitted. The time restrictions inherent in recording single unit responses, i.e. holding a unit for long periods, was often the limiting factor in deciding how many parameters could be studied in each fiber.

### **Response Recording and Analysis:**

#### **ANN-**

To record the ANN, platinum/iridium electrodes were placed on opposite sides of the auditory nerve as it exits the internal acoustic meatus and were secured to the skull with dental acrylic. The signal from the auditory nerve electrodes was initially amplified 1000X with a Princeton Applied Research 113 preamplifier then further amplified with a 3A9 plug-in amplifier for a Tektronix 565 oscilloscope. The bandpass was 300 to 3000 Hz for both amplifiers (6 dB/octave for each filter). The total gain varied with the recording conditions, the usual gain being either 50,000 or 200,000. The signal was digitized with a 12-bit converter at 10 kHz. Two hundred responses were collected for each averaged response.

#### **Single fibers-**

For recording single unit responses from the auditory nerve, glass microelectrodes with impedances of 15 -50 M $\Omega$  were inserted into the nerve under visual control with a Kopf hydraulic microdrive. Glass pipets (WPI

TW130-F) 1.0 mm in diameter were drawn on a Brown-Flaming electrode puller and filled with 3 M KCl. The signal was initially amplified 1000X with a Princeton Applied Research 113 preamplifier then further amplified with a 3A9 plug-in amplifier for a Tektronix 565 oscilloscope. The bandpass was 300 to 3000 Hz for the PAR amplifier and 1000 to 3000 Hz for the Tektronix amplifier. The signal was passed through a BAK window discriminator to isolate the spikes from background noise. Acceptance pulses were collected at 100 kHz. Twenty to forty responses were collected for each post stimulus time histogram (PSTH). The computer system was restricted to a maximum of 1500 spikes per PSTH and the number of traces was varied to work within this limitation.

The center frequency (CF), and threshold were determined for each unit with audio-visual examination of the response to tones. The spontaneous rate was measured by recording a series of 300 ms responses with the signal input disconnected.

### **Data Analysis:**

#### **ANN-**

The RMS amplitude of a two cycle (2.5 ms) segment of the unmasked response was measured at twenty post-onset times. In the masked condition the onset response represented by a 2.5 ms segment at the same time ( $t_p$ ) as the first segment in the unmasked response was measured for each silent interval ( $\Delta t$ ). The resulting time course of the response magnitude was interpreted as the sum of two exponential processes. We assumed that the two processes begin at time zero, i.e., at the beginning of the probe for adaptation, and at the end of the masker for recovery from adaptation. Two

time constants of adaptation,  $\text{TauA}_{\text{rapid}}$  ( $\text{TauA}_r$ ) and  $\text{TauA}_{\text{short term}}$  ( $\text{TauA}_s$ ) and recovery from adaptation,  $\text{TauR}_{\text{rapid}}$  ( $\text{TauR}_r$ ) and  $\text{TauR}_{\text{short term}}$  ( $\text{TauR}_s$ ) were extracted using a linear least-squares best fit on log transformed data. A line was fit through the later series of points for each trace and the resulting values for the initial points subtracted from the initial data values. This was necessary to properly apply the equations presented below. If the longer time constant effects are not subtracted from the initial data (i.e. the rapid time constant data) the  $\text{Tau}_r$  and  $\text{Tau}_s$  are not being calculated as two linearly summed, independent processes as implied in the equation, and the result will not properly fit the data. This can be made clear by putting values into equation 1, performing the log transformation and fitting the data with straight lines. The calculated values will differ from the entered values unless the above subtraction is done. The corresponding Y-intercepts of the rapid ( $Y_r$ ) and short term ( $Y_s$ ) process were also determined after the appropriate subtraction was done. The time course for adaptation is then described by:

$$A(t_p) = Y_r * (\exp(-t_p / \text{TauA}_r)) + Y_s * (\exp(-t_p / \text{TauA}_s)) + A_{ss} \quad (1)$$

where  $A(t_p)$  equals the RMS amplitude if the response at  $t_p$  ms after probe onset, and  $A_{ss}$  equals the magnitude of the steady state response (see Westerman and Smith, 1984; Westerman, 1985). Recovery from adaptation as measured by the probe onset response is described by:

$$A(\Delta t) = A_{ss} - Y_r * (\exp(-\Delta t / \text{TauR}_r)) + Y_s * (\exp(-\Delta t / \text{TauR}_s)) \quad (2)$$

(modified from Harris and Dallos, 1979) where  $A(\Delta t)$  equals the RMS amplitude of the onset response after a silent interval of  $\Delta t$  ms.

### **Single fibers-**

The equations used for analysis of the single unit data was the same as used in the ANN experiments. The analysis of spike number followed a similar sequence as above except that longer segments were used in later segments of the response to reduce the variability of the data. Data collected with 800 Hz tones is expressed in number of spikes per 2.5 ms window (equal to 2 cycles of the standard stimulus), with the longer segments being divided by an appropriate factor to keep the effective analysis window at 2.5 ms. Therefore, if a 10 ms window, from 90 to 100 ms was used, the total number of spikes would be divided by 4 ( $10 / 4 = 2.5$ ). When data was collected with CF stimuli, the analysis window was adjusted to equal an integral number of stimulus cycles as near to 2.5 ms as possible.

It was discovered that the onset recovery data could be fit to either a two-time-constant recovery equation (Eq. 2) or to a one time constant recovery equation:

$$A(\Delta t) = A_{SS} - Y*(\exp(-\Delta t/\text{TauR})) \quad (3)$$

## **RESULTS:**

### **Single Fiber Response Characteristics:**

#### **Adaptation:**

A typical response to an 800 Hz tone is shown in Fig. R1. In the upper window the entire 300 ms response is displayed while the lower window contains the first 50 ms expanded to clearly demonstrate the phase locking of the response to the probe tone. The onset time of the first analysis window was selected to precede the two cycles which produced the maximum amplitude. Using the two-time-constant exponential decay equation to model each trace produced accurate fits to the data as demonstrated in Fig. R2. It was relatively easy to estimate time constants for the single unit adaptation data as the responses were robust and had minimal variation within each trace. (This was not the case for whole tone recovery responses-details are presented in later sections). Six examples are presented in Fig. R2, each shifted vertically by 10 spikes for ease of viewing. The open symbols are the result of entering the two-time-constants, the Y-intercepts and the steady state estimated from each trace into the equation. Solid symbols are the data. TauAr starting with the top traces was 3.6, 7.3, 1.8, 2.2, 5.4, and 4.7 ms. The corresponding TauAs values were 137.1, 176.2, 99.0, 62.3, 80.2 and 92.3 ms. For each case a single time constant exponential equation was applied which failed to produce a reasonable fit to the data. The initial three to five points were seriously underestimated by the one Tau equation.

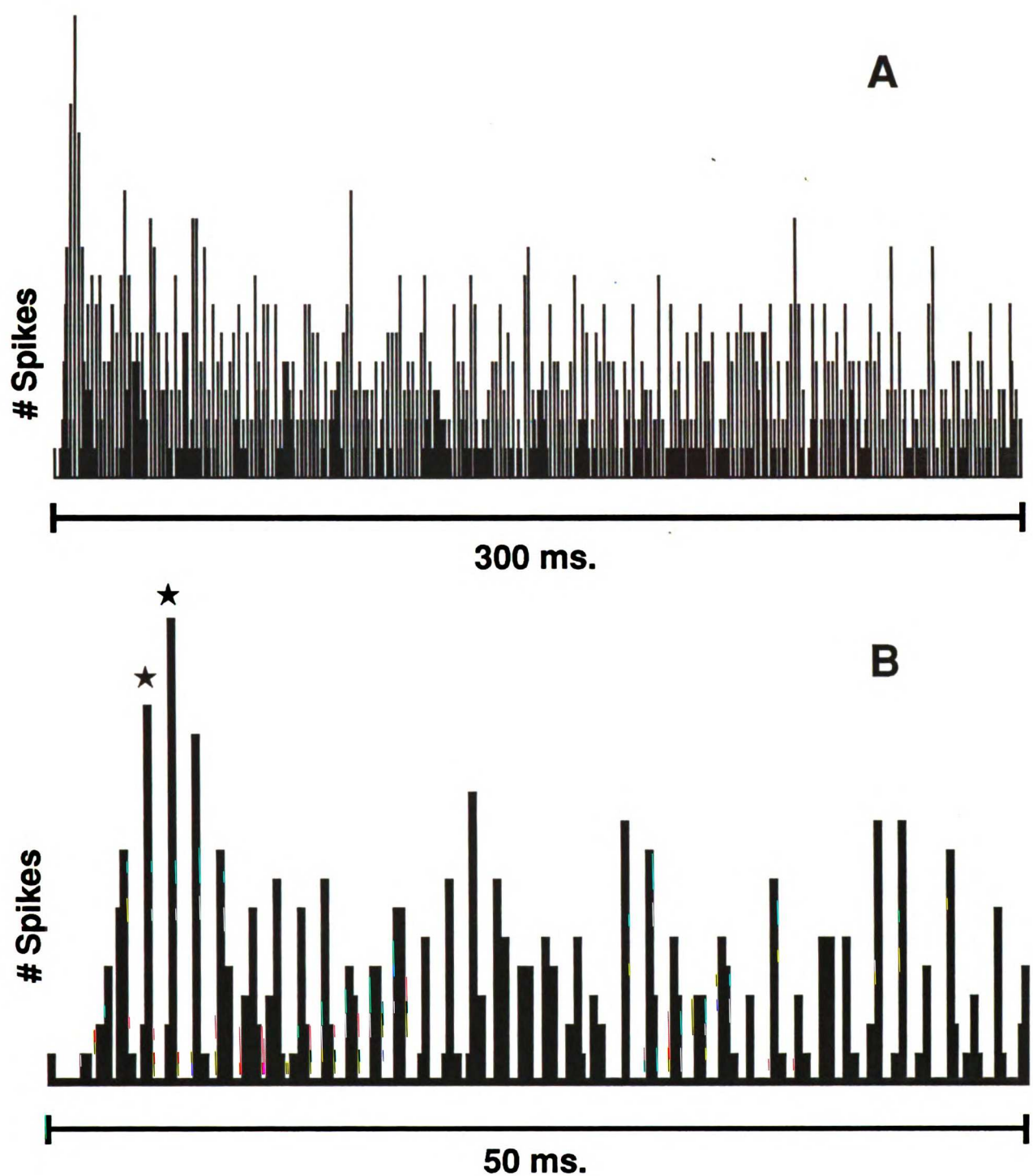


Fig. R1. PSTH to 290 ms 800 Hz. pure tone. A) entire response showing large onset and decay to steady state. B) first 50 msec of response expanded to demonstrate phase locking of response. The two bins with stars are cycles which produced the maximum amplitude. In the example shown the two bins marked with stars would be selected as the "zero time" for all subsequent analysis (adaptation, onset recovery, and whole tone recovery).

The rapid and short term adaptation time constants (TauAr and TauAs) did not vary as a function of probe level (Fig. R3). TauAr had a mean of  $5.5 \pm 3.4$  ms and TauAs had a mean of  $93.7 \pm 29$  ms. In order to separate the effects of stimulus level from unit CF the data were sorted to plot increasing CF at each probe level. No systematic change was observed.

TauAr or TauAs were systematically examined to determine if they varied with any other parameter. Fig. R4 plots TauA vs. CF of the unit. The visual impression is confirmed by regression analysis which produces nonsignificant p values for TauAr and TauAs. However, this data combines cases where the stimulus frequency equals CF and cases where the stimulus frequency equals 800 Hz regardless of the units CF. If these two groups are separated and analyzed there is still no significant change in TauAr or TauAs with unit CF (Fig. R5 and R6). Finally the data were examined to determine if the variation within TauAr was correlated with TauAs. Two methods of graphically representing the data are presented. In Fig. R7 TauAr is plotted vs. TauAs The axes have equal lengths so that the 45 degree line represents a correlation of 1.0. Obviously no such correlation exists. Fig. R8 sorts the data according to increasing values of TauAr, maintaining the appropriate pairing of TauAr and TauAs. TauAs remains a scattered horizontal grouping, not a positively sloping line correlated to TauAr.

### **Recovery; General:**

A response which has asymptoted to a steady state firing level is followed by a period of recovery from adaptation. This recovery of the fiber's ability to respond after having adapted can be studied by measuring the response to a probe stimulus presented after a silent interval. By



## Adaptation Plots: Data and Model

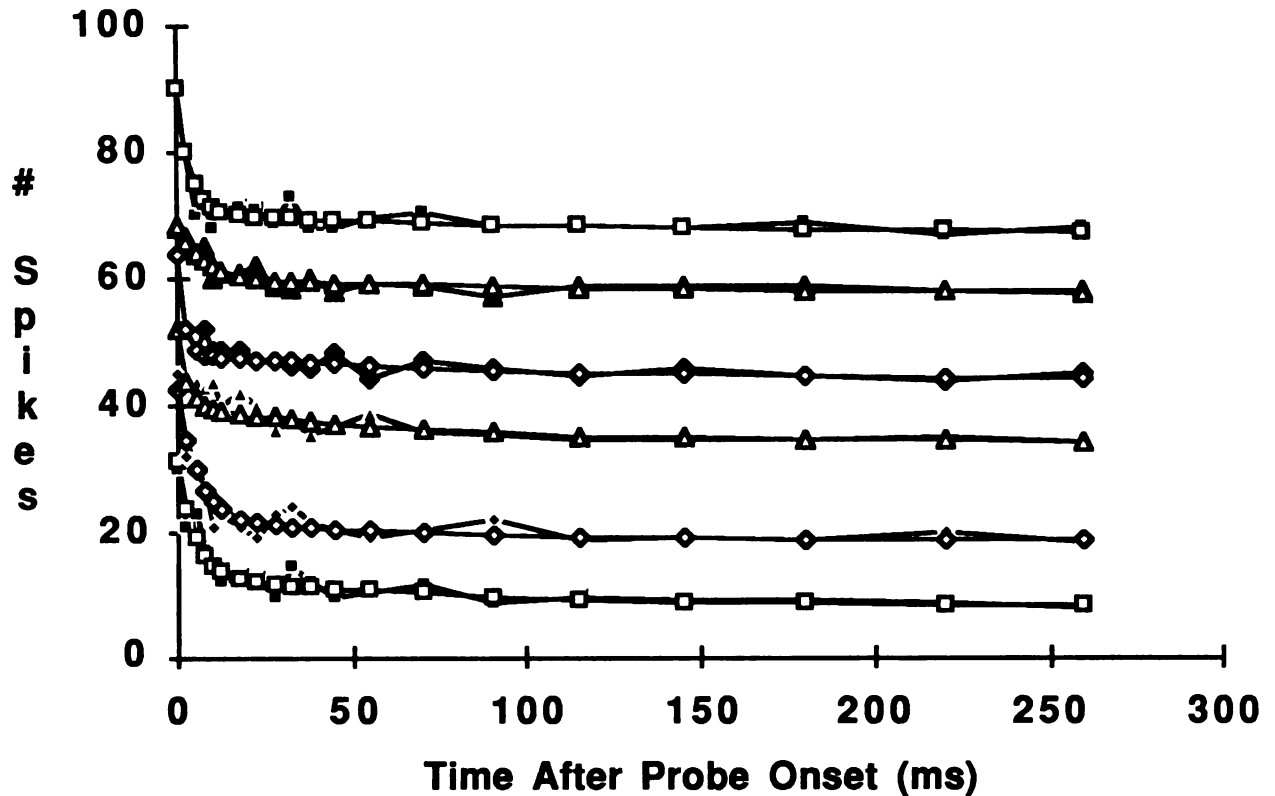


Fig. R2. Adaptation examples. Six examples of PSTH data converted into 20 amplitude values. The filled symbols are data values and the open symbols are the model fit to the data employing the two-time-constant adaptation equation (Eq. 1). This convention is used in all Fig.s. The first five points in each trace are positioned at the onset time of the analysis window while all other points are positioned in the center of the analysis window. The later analysis windows (which are longer; see text) have been normalized to 2 cycles of the stimulus (2.5 msec for 800 Hz.).

presenting a set of probe stimuli preceded by ever increasing silent intervals, the recovery from adaptation can be plotted. In this study two forms of recovery were examined: 1) recovery of the onset response to a probe tone and 2) recovery of the whole tone. In the first case the amplitude of the onset analysis window (2.5 ms) was used while in the latter case the same set of 20 analysis windows as used to measure adaptation were applied.

### **Onset Recovery:**

Fig. R9 plots the onset recovery of six different units, the top five shifted vertically for ease of viewing. All of these were fit to an exponential equation with two-time-constants (Eq. 2). Fig. R10 is a similar plot, except that the units are best fit with a single time constant exponential equation (Eq. 3). All onset recovery data were entered into both the one and two-time-constant equations to confirm the existence of two independent groups. In cases where two-time-constants were chosen as the best fit, using the one time constant equation resulted in a model with points which systematically exceeded the data values for the first two to five points. Conversely, when data best fit with a one time constant equation were tested with the two-time-constant equation the attempt failed completely because the necessary subtraction of the short term time constant effect from the initial data points produced negative values causing a computational error (calculating the log of a negative number). In two cases presented in Fig. R10 the first two points of the model are flat. The model calculation produced negative values in these cases, which were changed to zero as a "negative number of spikes" is meaningless.

### TauA Time Constants

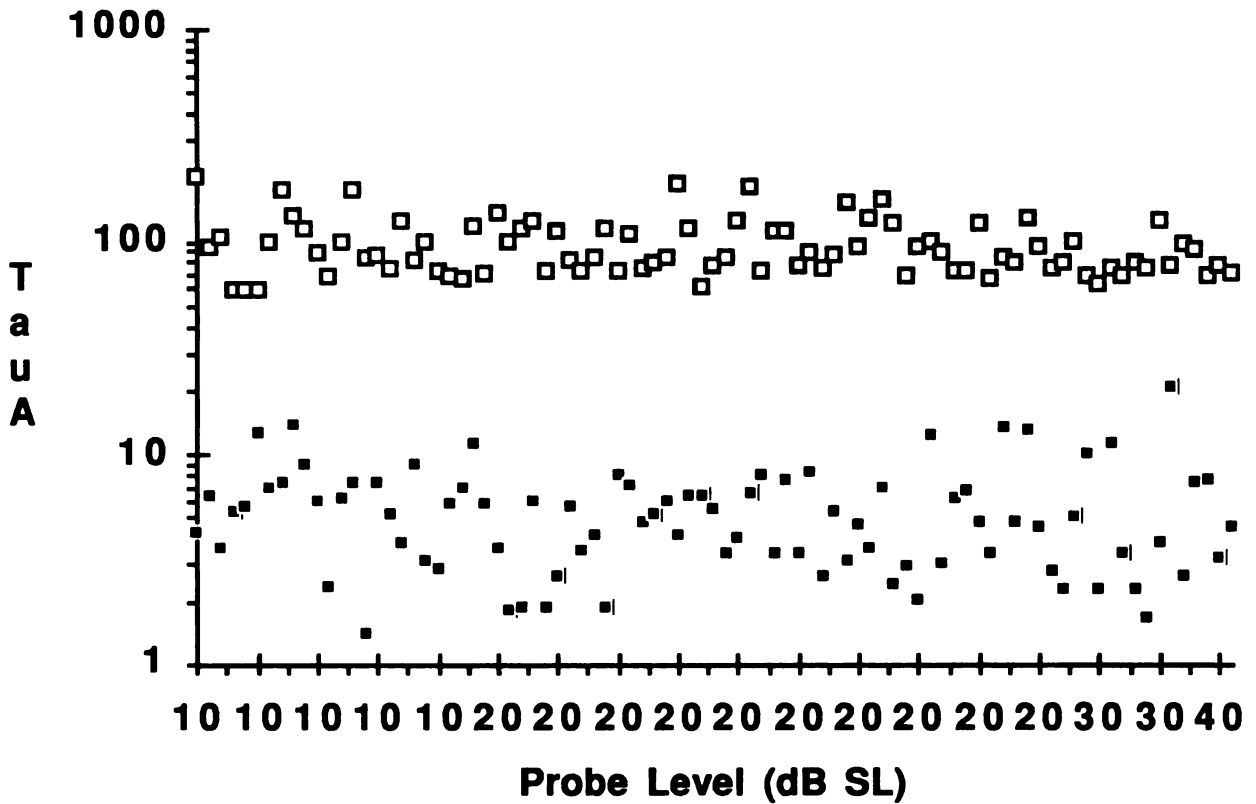


Fig. R3. Time constants of adaptation vs. stimulus probe level. Filled symbols are the rapid adaptation time constant values (TauAr) and the open symbols are the short term adaptation time constants values (TauAs). This convention is maintained in all Fig. that follow. Note that there is no change in either TauAr or TauAs as the probe level is increased.

### TauA Time Constants

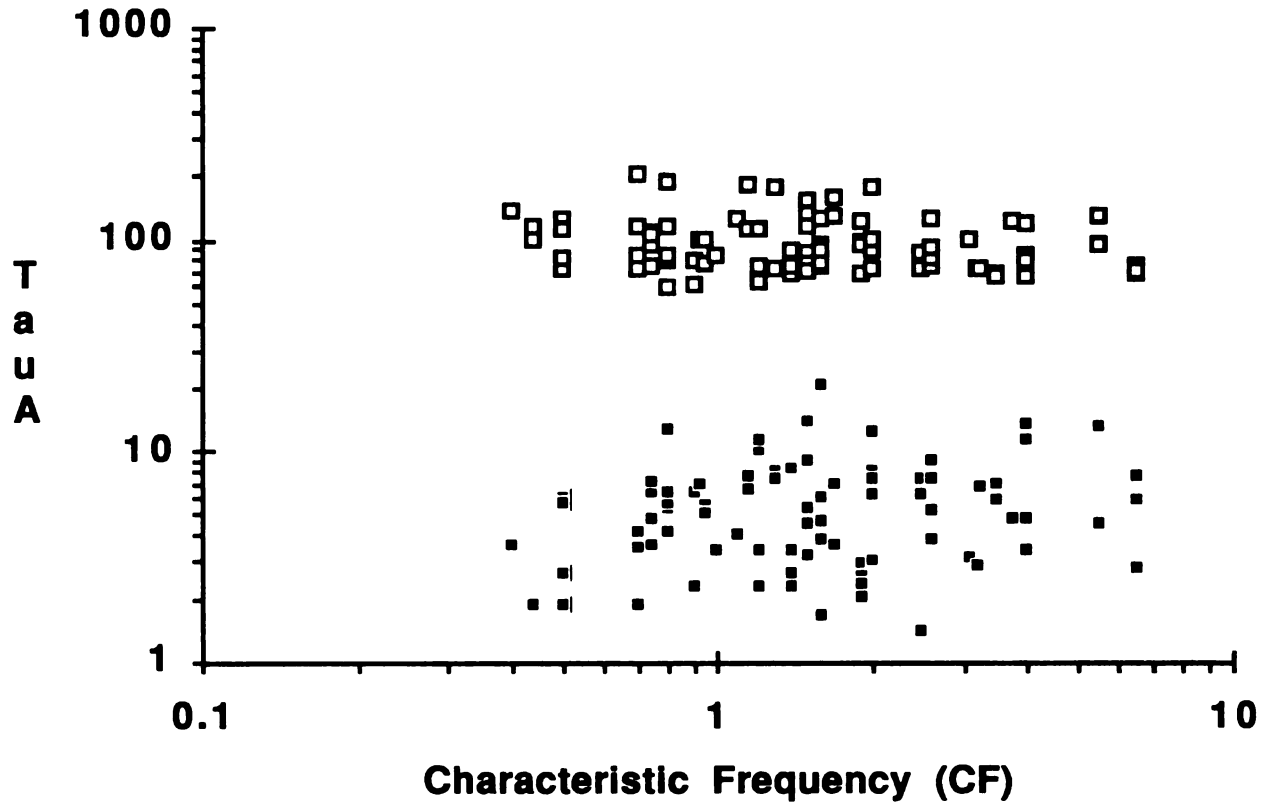


Fig. R4 .Time constants of adaptation vs. CF. Symbols as in Fig. R3. Note that there is no change in either TauAr or TauAs as the CF increases.

**Stimulus frequency = C.F.**

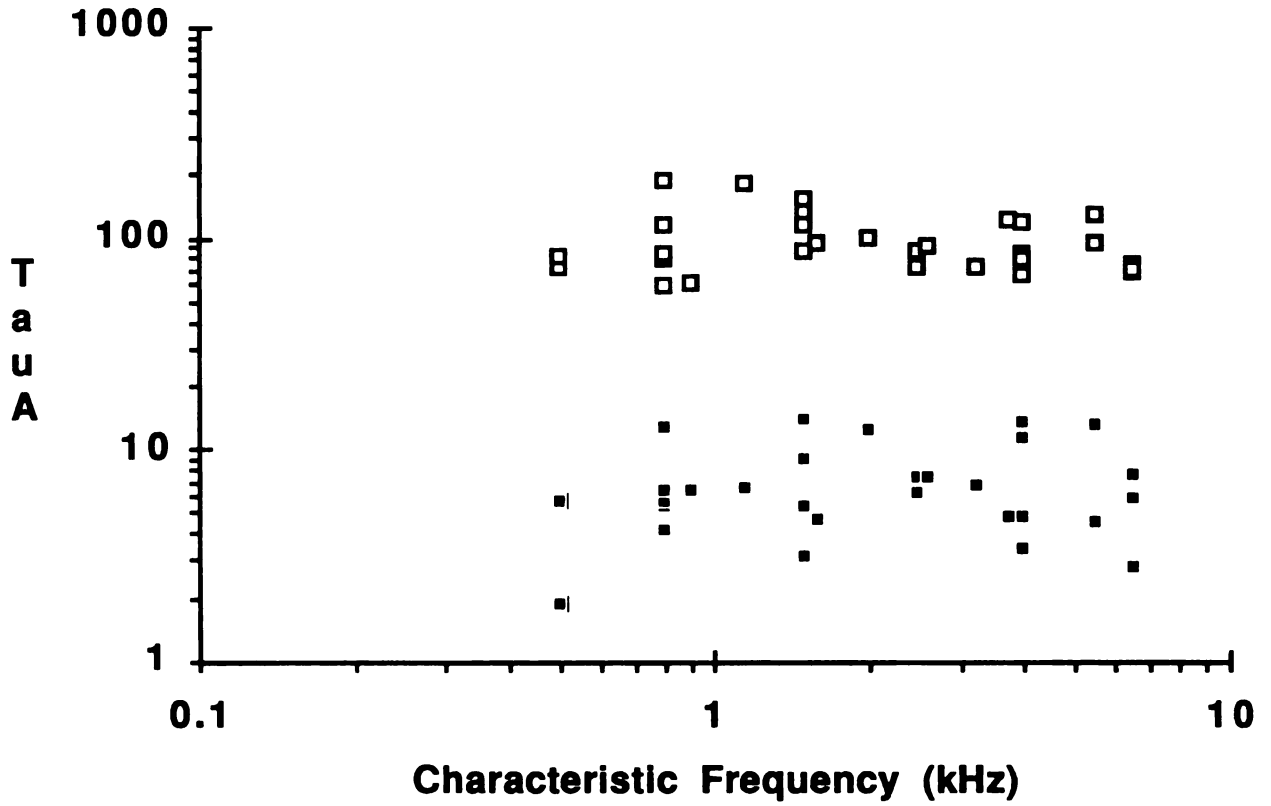


Fig. R5. Time constants of adaptation vs. CF. Only data in which the stimulus frequency was equal to the CF are plotted.

**Stimulus frequency = 800 Hz.**

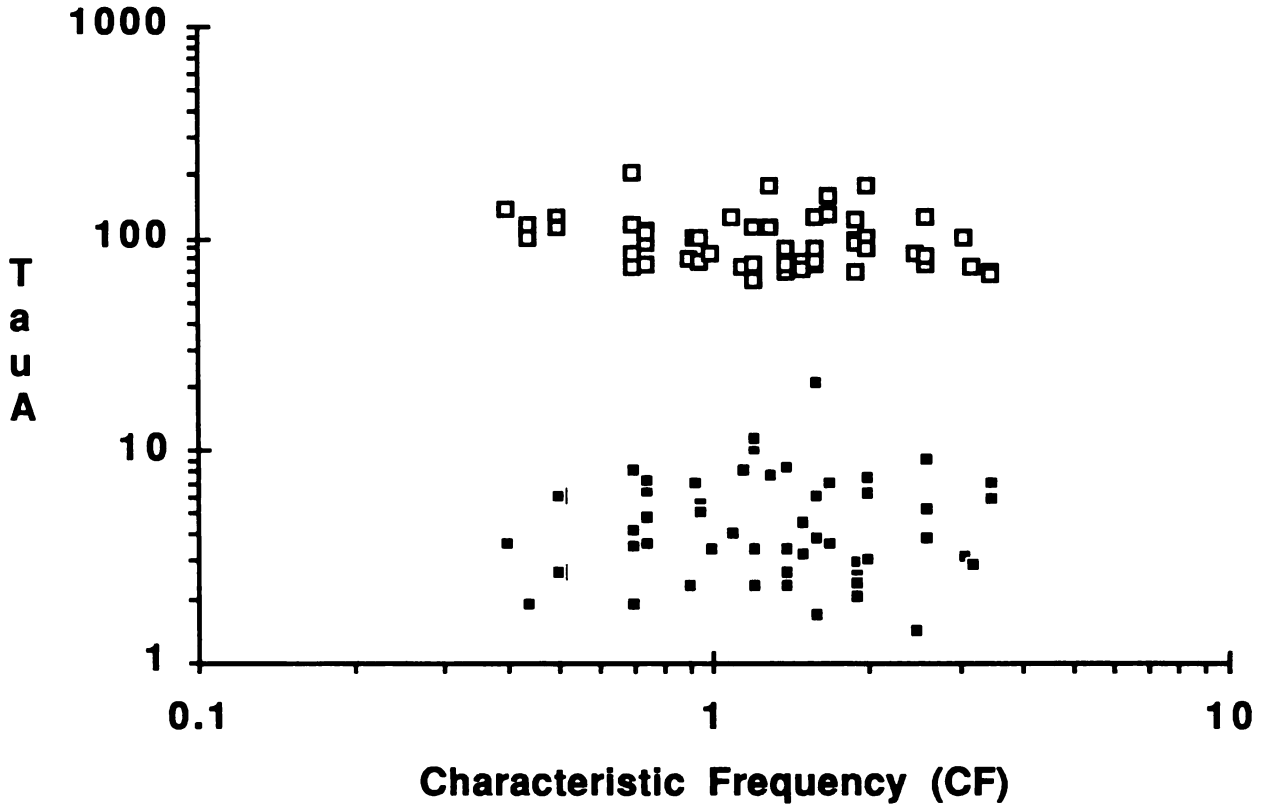


Fig. R6. Time constants of adaptation vs. CF. Only data in which the stimulus frequency was 800 Hz are plotted.

### TauAs vs. TauAr

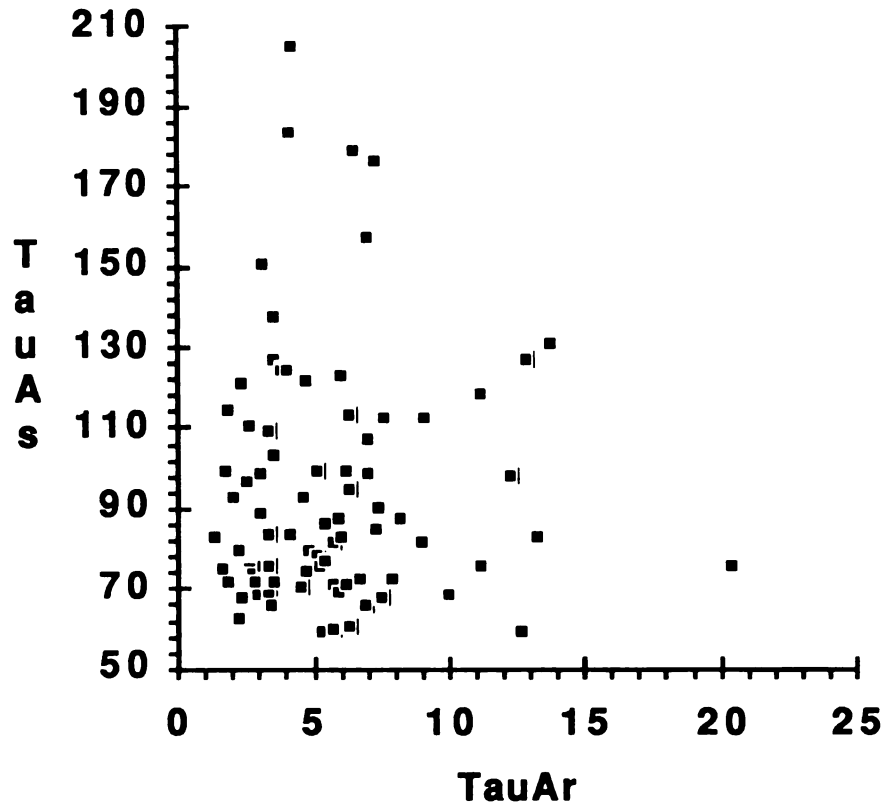


Fig. R7. TauAr vs. TauAs. The rapid and short term time constants of adaptation are plotted on equal length axes to determine if the values are covariant. The large scatter demonstrates that there is no correlation between TauAr and TauAs.

### TauAs & TauAr vs. Single Fibers

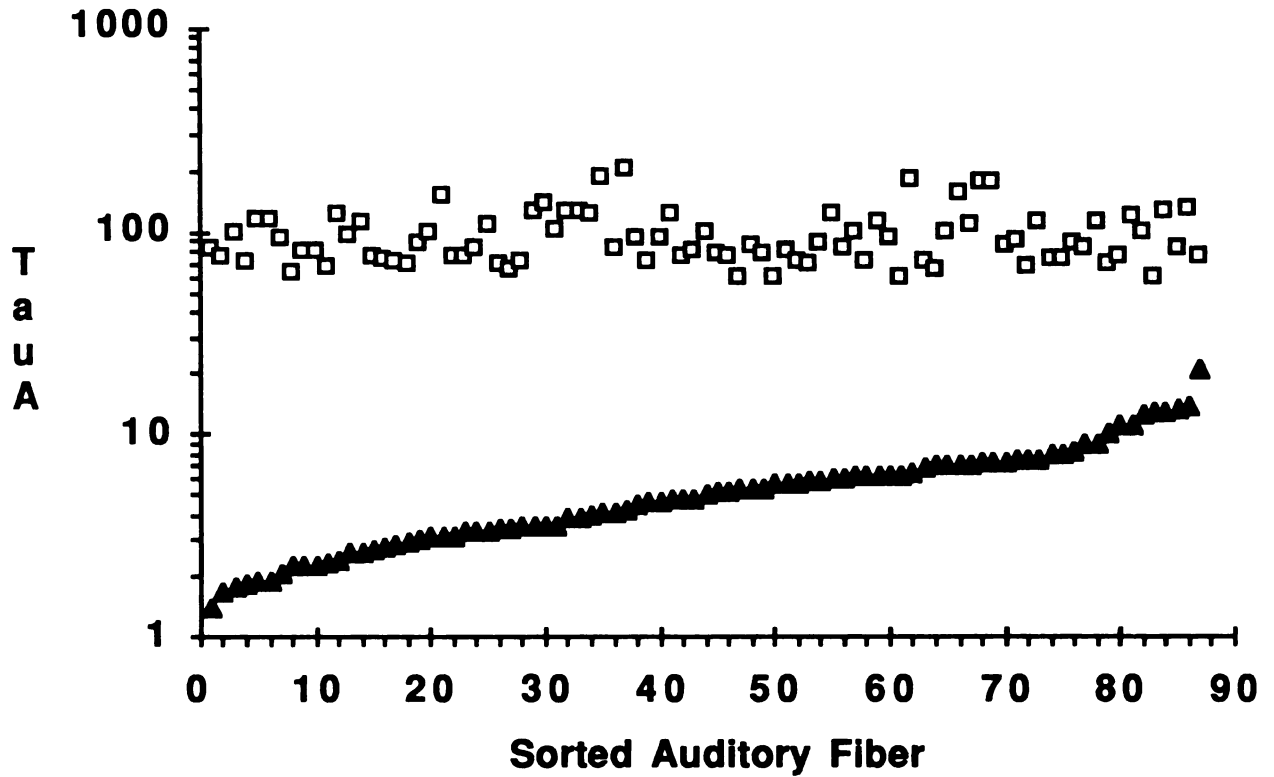


Fig. R8. TauA vs. each unit. Another form of the previous Figure.. In this case the TauAr values have been sorted according to increasing value. The corresponding TauAs value is plotted above each TauAr value. It is clear that TauAs does not vary with TauAr.



The TauRr values for the two-time-constant traces were 25.8, 17.1, 11.2, 60.4, 12.7, and 14.1 ms from the top to the bottom of Fig. R9. TauRs was 172.3, 132.0, 103.3, 471.4, 114.2, and 114.6 ms for the corresponding traces. For the one time constant traces presented in Fig. R10 TauR values starting at the top were 108.8, 106.0, 61.5, 110.9, 50.8 and 119.4 ms.

The time constants for the two TauR cases are plotted as a function of masker level minus probe level in Fig. R11. TauRr and TauRs do not vary significantly as a function of relative masker/probe level. The mean value of TauRr is  $22.0 \pm 9.6$  ms and the mean value of TauRs is  $184.1 \pm 144.8$  ms. The two TauR results are plotted vs. masker level in Fig. R12. No significant change in either TauRr or TauRs exists. Likewise, no significant change exists when probe level or CF is the dependent variable (Figs R13 and R14)

The same analysis which was conducted with the two TauR data was applied to the one TauR data. As in the two TauR cases, no significant change in the time constant existed as a function of relative masker probe level, masker level, probe level, or unit CF (Figs. R15-R18) . The mean value of TauR was  $94.6 \pm 31.2$  ms, which falls between the values of TauRr and TauRs in the two TauR cases.

## 2 Tau Onset Recovery: Data and Model

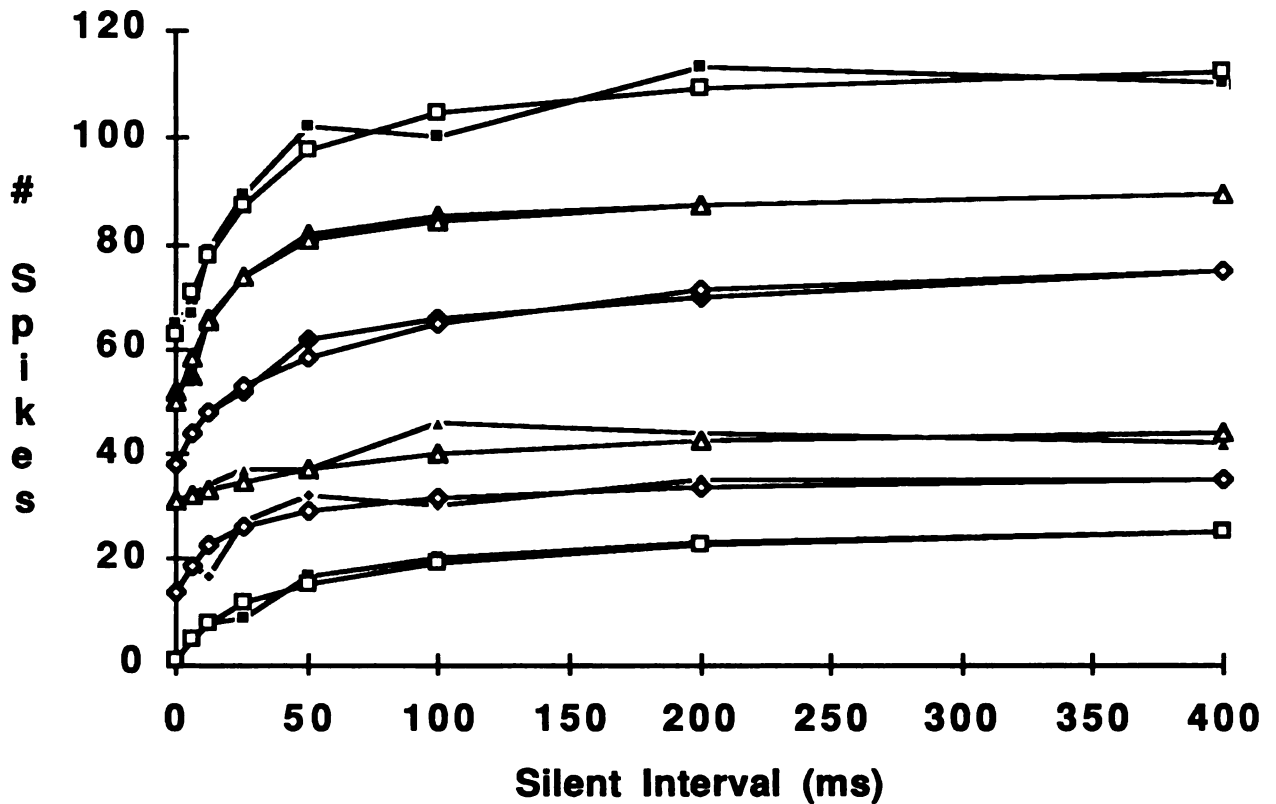


Fig. R9. Two-tau onset recovery examples. Six examples of the onset amplitude after 8 silent intervals (0, 6, 12.5, 25, 50, 100, 200, and 400 ms). The data are fit with a two-time-constant exponential recovery equation. Results have been shifted vertically for ease of viewing.

## 1 Tau Onset Recovery: Data and Model

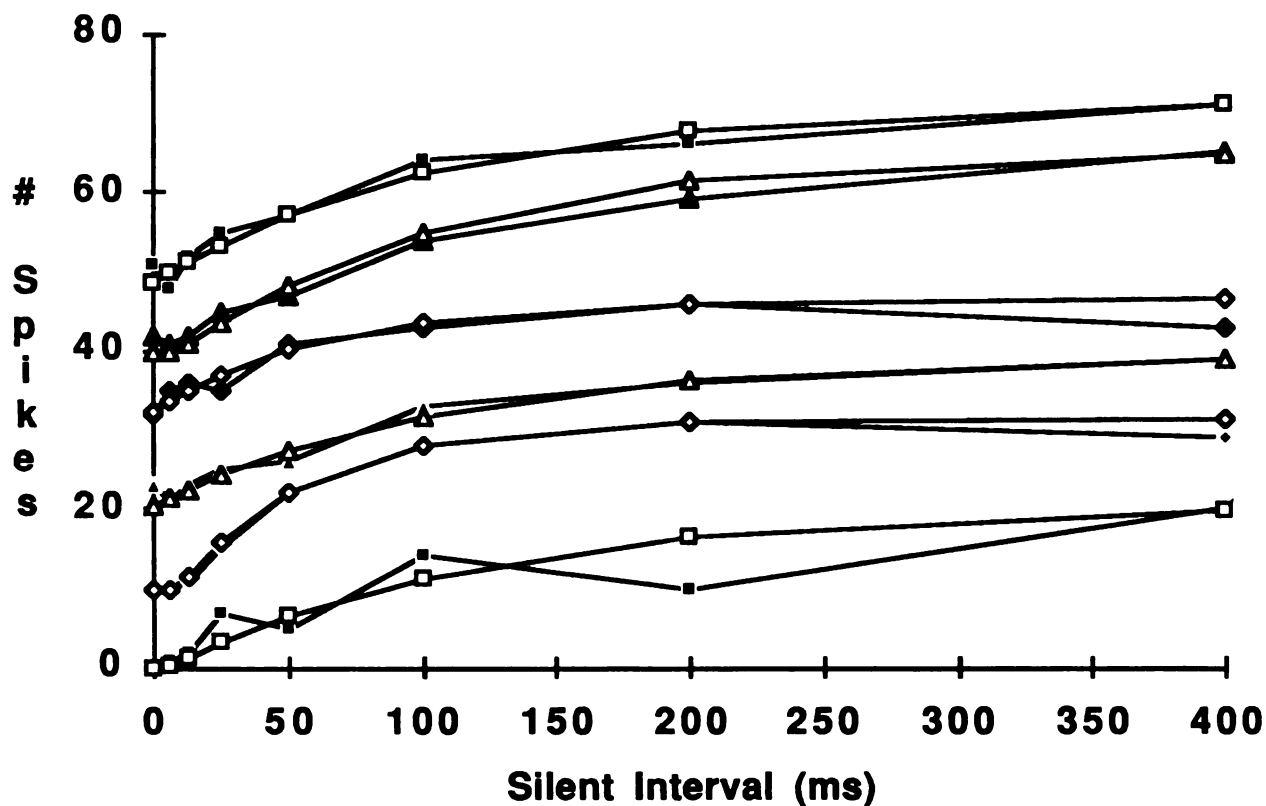


Fig. R10. One-tau onset recovery examples. Six examples of the onset amplitude after 8 silent intervals (0, 6, 12.5, 25, 50, 100, 200, and 400 ms). The data are fit with a one time constant exponential recovery equation. Results have been shifted vertically for ease of viewing.

## 2 Tau Onset Recovery Time Constants

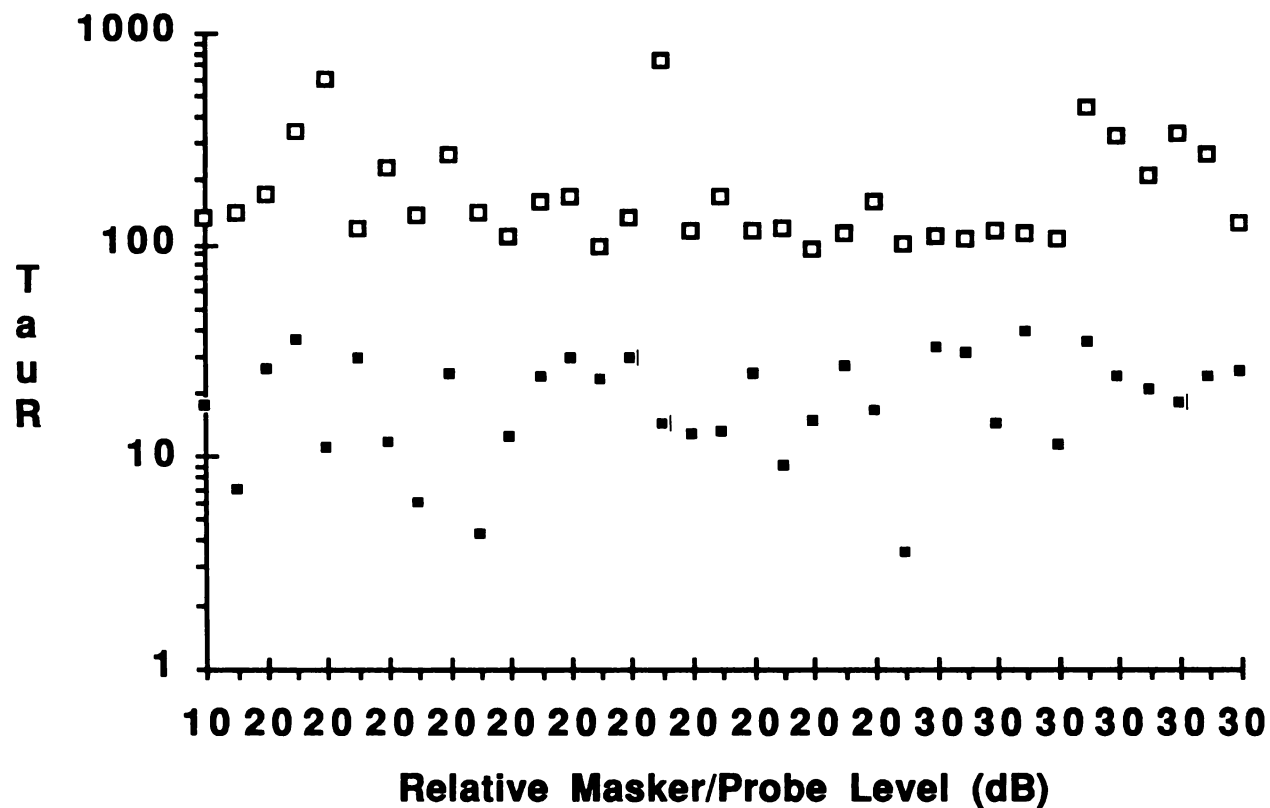


Fig. R11. Two-tau onset recovery time constants vs. relative masker probe level. TauRr and TauRs as a function of the difference between the masker level and the probe level. No change in either time constant with relative masker/probe level is seen.

## 2 Tau Onset Recovery Time Constants

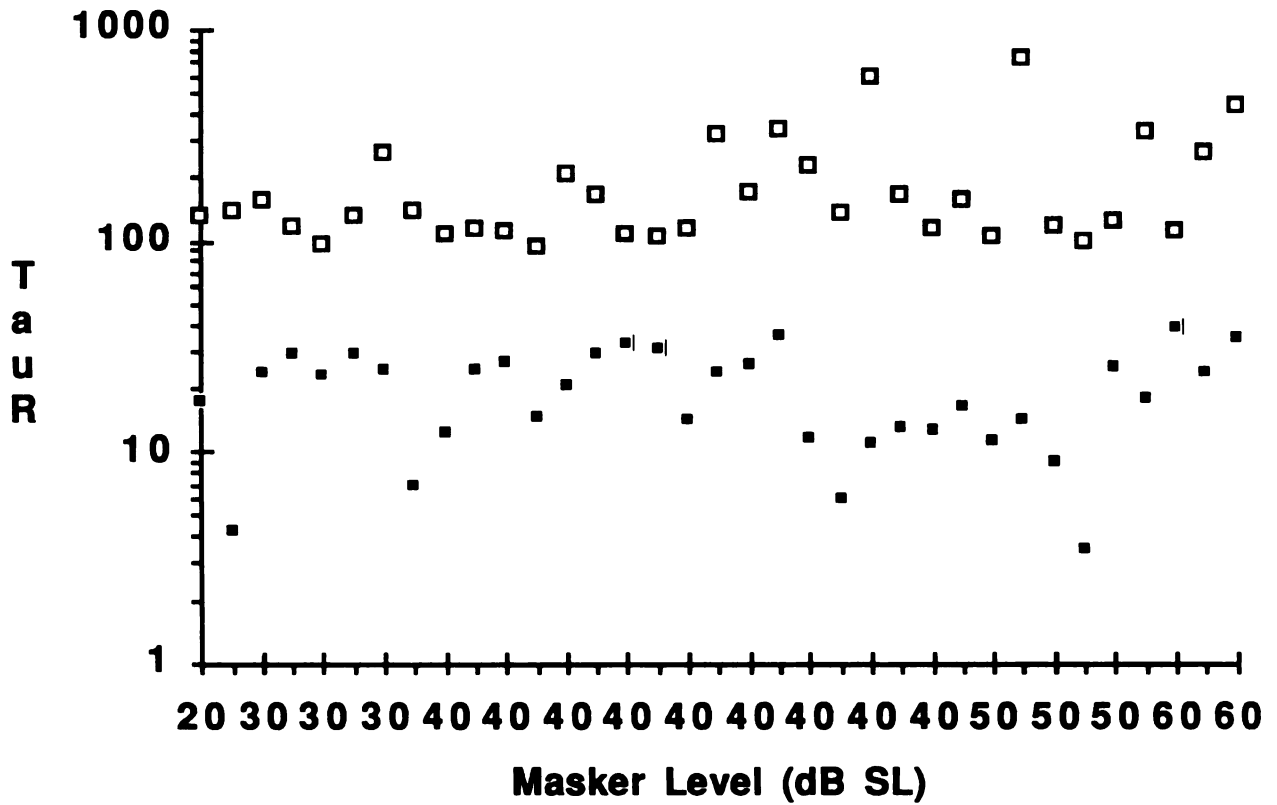


Fig. R12. Two-tau onset recovery time constants vs. masker level.  $\tau_{Rr}$  and  $\tau_{Rs}$  as a function of the masker level. No change in either time constant with masker level is seen.

## 2 Tau Onset Recovery Time Constants

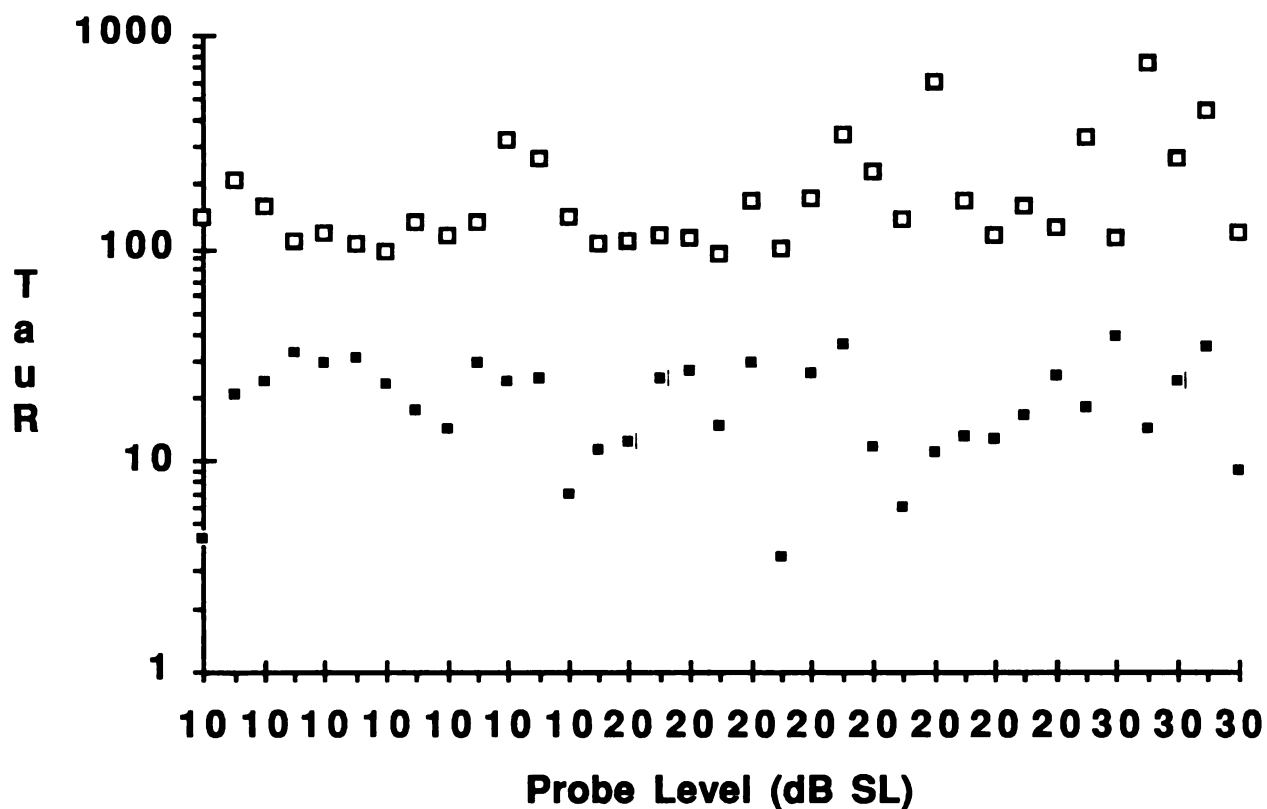


Fig. R13. Two-tau onset recovery time constants vs. probe level. TauRr and TauRs as a function of the probe level. No change in either time constant with probe level is seen.

## 2 Tau Onset Recovery Time Constants

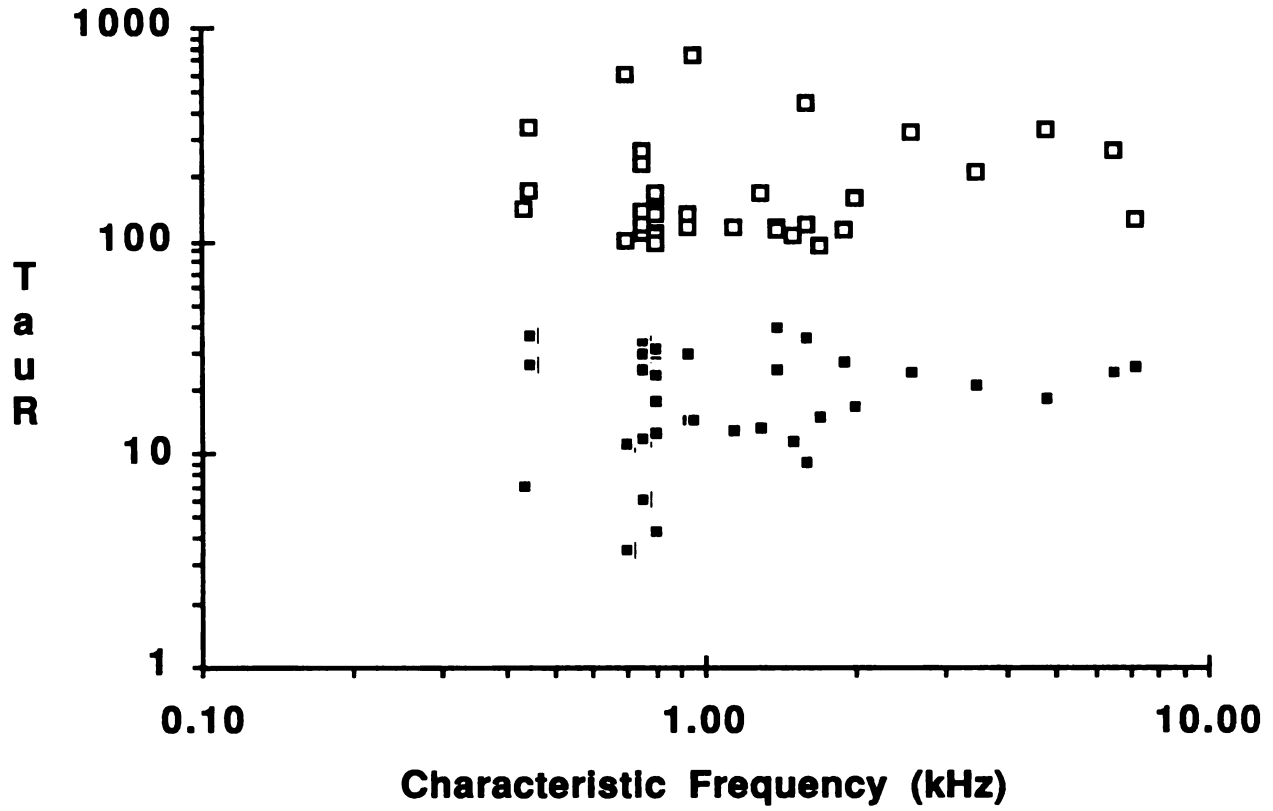


Fig. R14. Two-tau onset recovery time constants vs. CF. TauRr and TauRs as a function of CF. No change in either time constant with CF is seen.

### 1 Tau Onset Recovery Time Constants

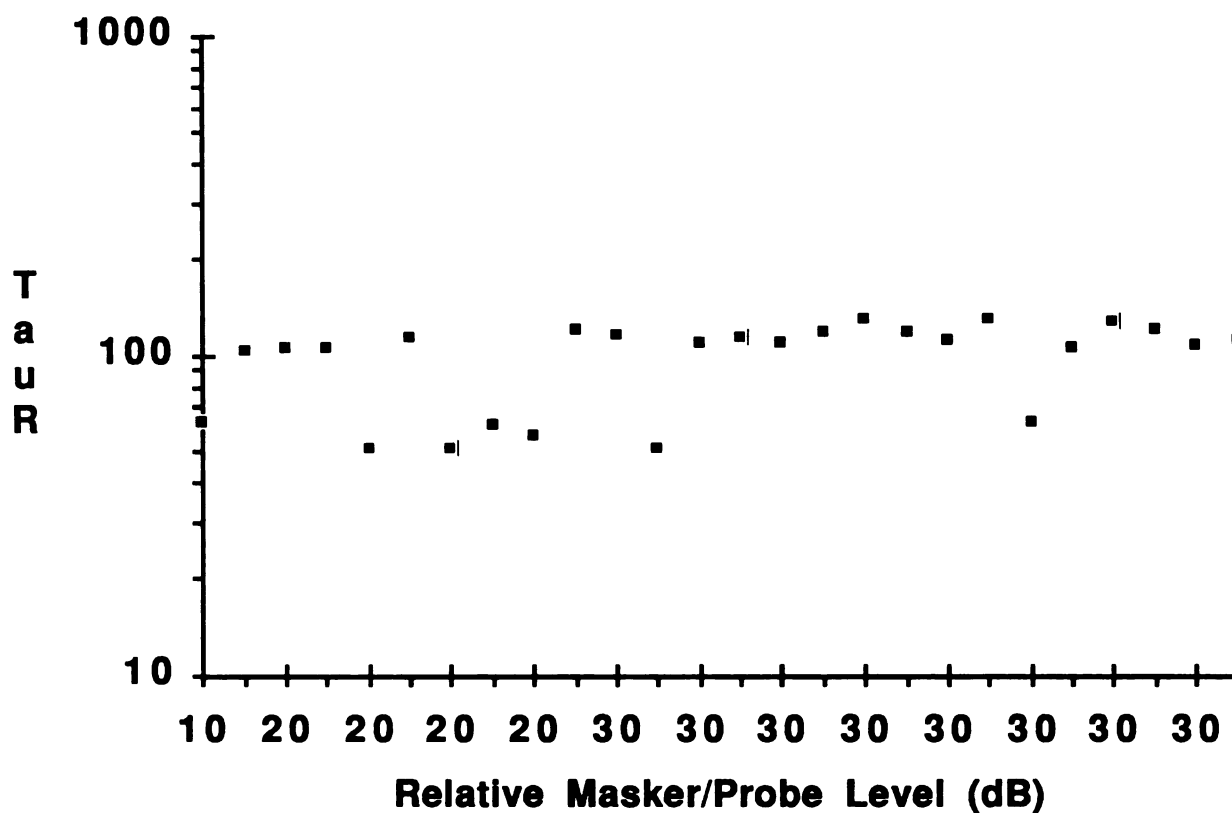


Fig. R15. One-tau onset recovery time constants vs. relative masker/probe level. TauR as a function of the difference between the masker level and the probe level. No change in the time constant with relative masker/probe level is seen. Two groups are evident. No correlation of these two groups with any other parameter was observed.



### 1 Tau Onset Recovery Time Constants

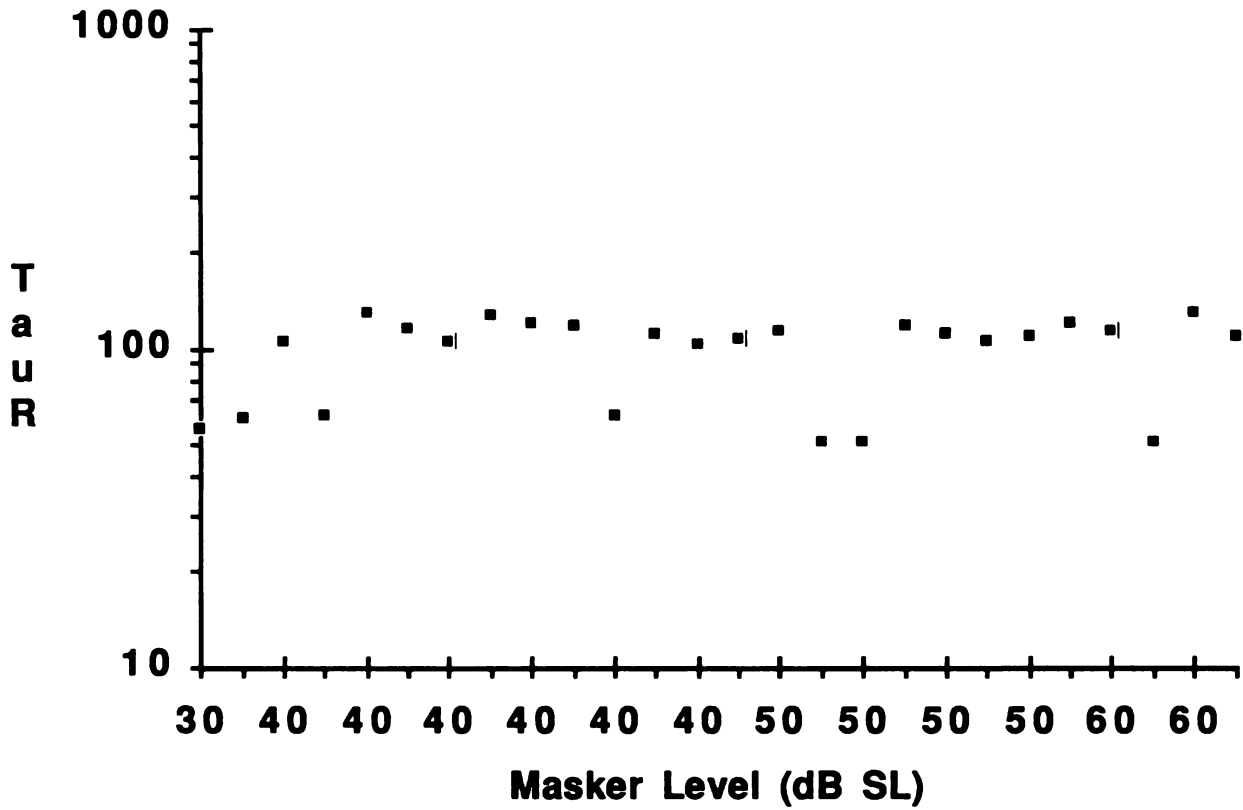


Fig. R16. One-tau onset recovery time constants vs. masker level. TauR as a function of the masker level. No change in the time constant with masker level is seen.

### 1 Tau Onset Recovery Time Constants

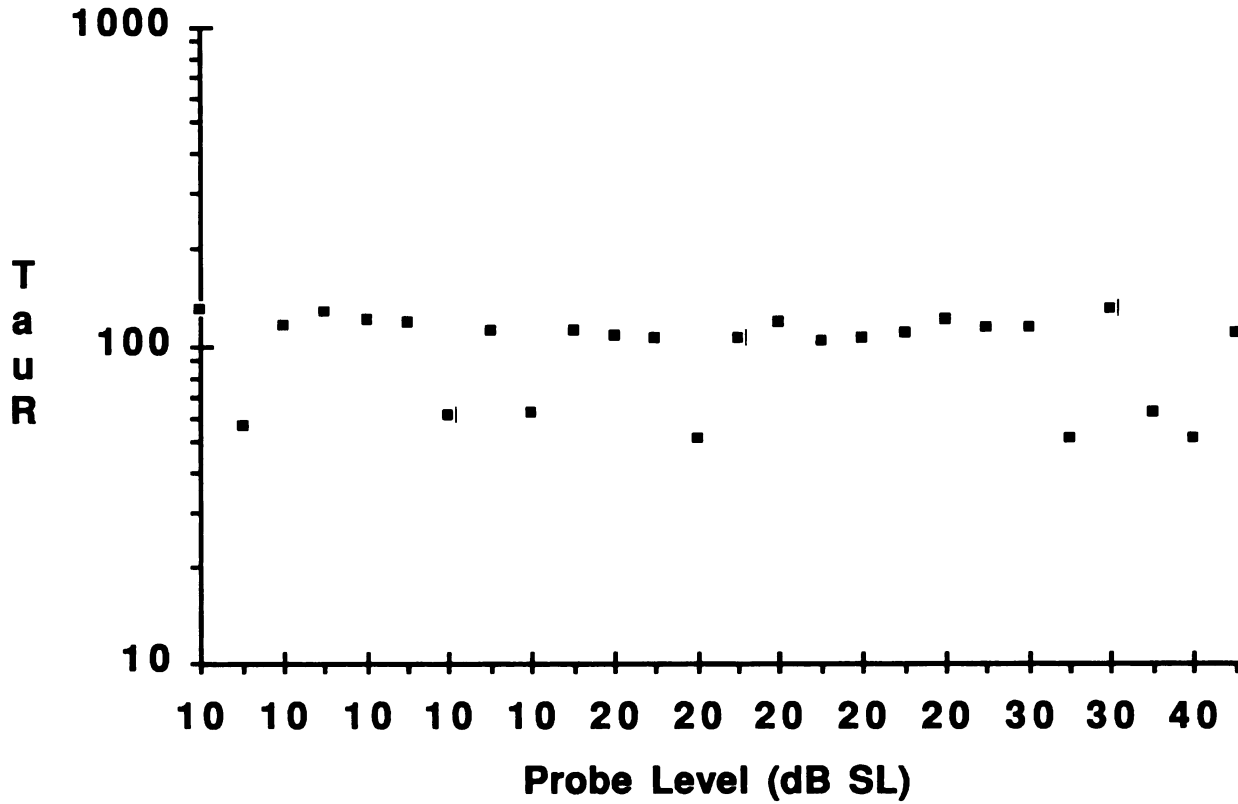


Fig. R17. One-tau onset recovery time constants vs. probe level. TauR as a function of the probe level. No change in the time constant with probe level is seen.

### 1 Tau Onset Recovery Time Constants

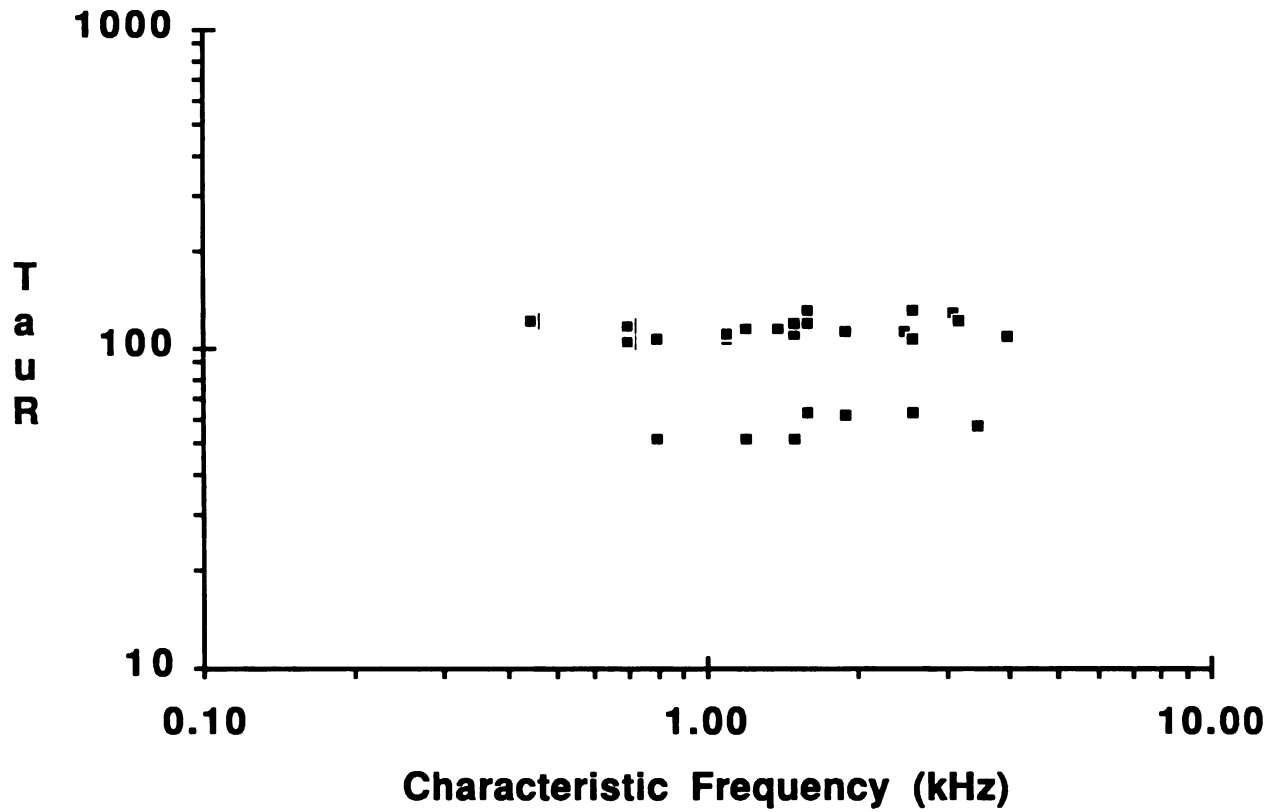


Fig. R18. One-tau onset recovery time constants vs.CF. TauR as a function of unit CF. No change in the time constant with CF is seen.

### **Whole Tone Recovery:**

Whole tone recovery in single auditory nerve fibers is displayed in Fig. R19. The traces are the sum of 19 fibers normalized by converting the spike counts to percent of maximum for each trace. The probe amplitudes varied from 10 to 30 dB above audio-visual threshold and the relative masker/probe level was always 20 dB. The probe frequency was either 800 Hz or equal to the unit's CF and the masker and probe frequencies were always equivalent. In all cases the audio-visual threshold for the stimulus used was measured and the probe stimulus chosen relative to this threshold, whether at CF or 800 Hz. The results from these two groups were compared and no systematic difference in the response characteristics were observed, therefore all the cases were combined. At the shortest silent interval ( $\Delta t = 0$  ms) the response onset is suppressed followed by a recovery to a steady state level. As the silent interval increased to  $\Delta t = 6$  ms the response became essentially flat. At  $\Delta t = 12.5$  ms the response has begun to display adaptation. Nearly complete recovery is seen at  $\Delta t = 400$  ms. For intervals longer than 10 ms, the time course of the response envelope could be described by the sum of two exponential adaptation responses with different time constants (Eq. 1). The rapid adaptation time constant for the 400 to 12.5 ms silent interval responses does not vary systematically while the short term component decreases as the interval increases. When the response finally approaches a flat line the rapid component cannot be calculated and is omitted from the model equation. The  $\tau_{Ar}$  values for the 400 to 12.5 ms silent interval traces were 5.3, 8.6, 6.5, and 7.0 ms, respectively. The  $\tau_{As}$  values for the same set of traces were 77.4, 107.0, 125.0, and 267.0 ms. At  $\Delta t = 6$  ms a single  $\tau_{As}$  of 2595.0 ms was estimated. For the interval  $\Delta t = 0$  ms, a recovery behavior was observed that

could be fitted with a two-time-constant exponential process with a  $\tau_r$  value of 8.3 ms and a  $\tau_s$  value of 682.0 ms.

The results presented in Fig. R19 demonstrate that the two exponential components in adaptation and recovery of the whole tone response are differentially effected by changing the silent interval between the masker offset and probe onset. The rapid component displays a constant dynamic behavior while the short term component is dependent on the state of adaptation. However, the influence of the rapid component on the time course diminishes with decreasing time intervals.

Fig. R20 displays representative responses from four single units. The responses follow a pattern similar to the average displayed in Fig. R19. Several features of the responses are worthy of note. In all cases the response changes from a "recovery function" at a silent interval of zero ms to an "adaptation function" at a silent interval of 400 ms. The silent interval at which the switch occurs varies between units. No correlation between the silent interval at which the switch occurs and the relative masker/probe level, masker level, or probe level was found. The responses at short silent intervals had a much greater variability in successive traces than did the unmasked responses or responses which followed a long silent interval. Of significant interest is the suppression of the response during the first few ms after onset followed by an onset response which decreased to the steady state ( Fig R20c; 12.5 ms and 50 ms.). This was observed in the vast majority of units although the exact silent interval and magnitude of the suppression at which it occurred varied. In Fig. R19 at  $\Delta t = 12.5$  ms, this phenomenon is evident in the first data part of the normalized, summed response. This observation will be returned to in the ANN whole tone recovery results and discussion sections.

It should be mentioned that the decrease in variability of all the traces in Fig. R20 after 50 ms is caused by the analysis method which used increasing window durations to measure the response amplitude. The effect is to add an additional level of averaging to the analysis.

## Whole Tone Recovery

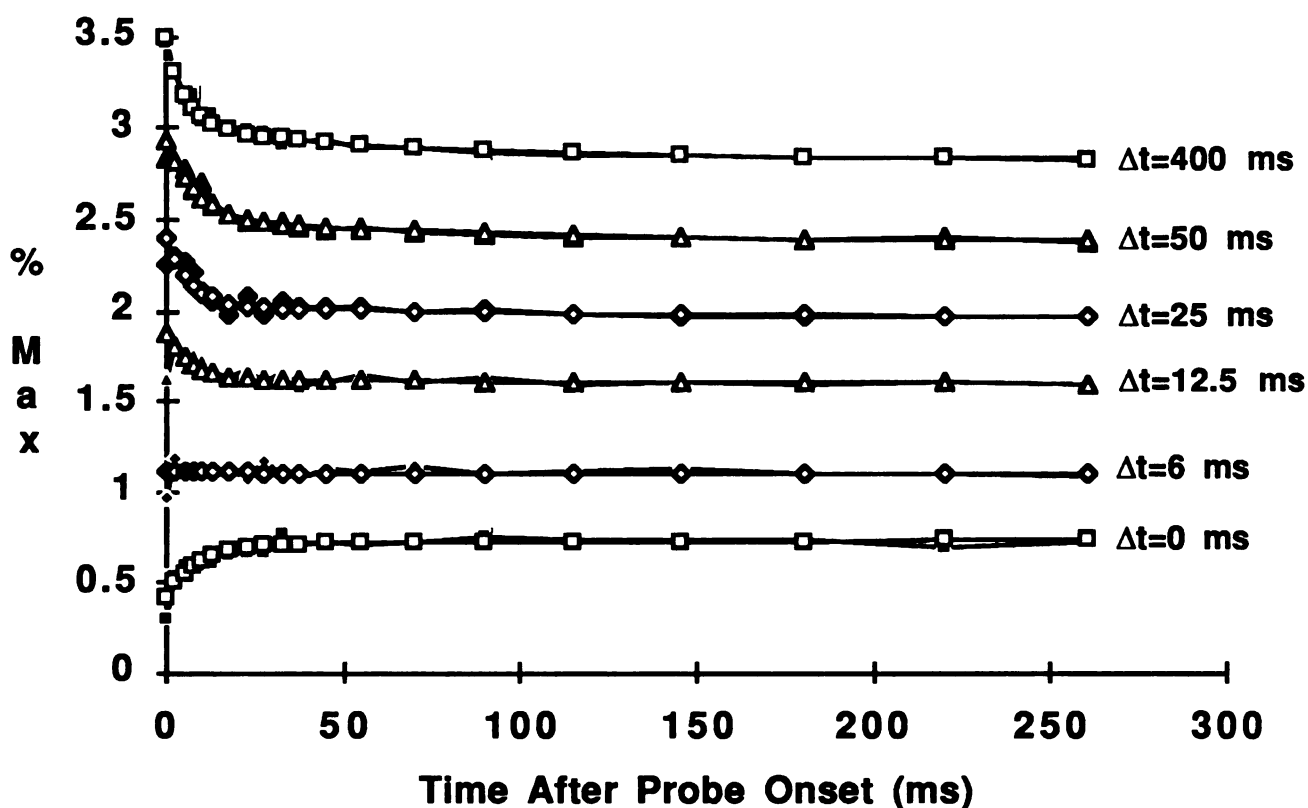


Fig. R19. Single unit whole tone recovery. Normalized, averaged data for 19 units with the masker 20 dB louder than the probe. Value to the right of each trace is the silent interval between masker offset and probe onset. Data was fit with a two-time-constant exponential adaptation equation for the top four traces (Eq. 1). At  $\Delta t = 6$  ms only a single time constant could be used. The bottom trace is fit with a two-time-constant exponential recovery equation (Eq. 2). All traces have been shifted vertically for ease of viewing.

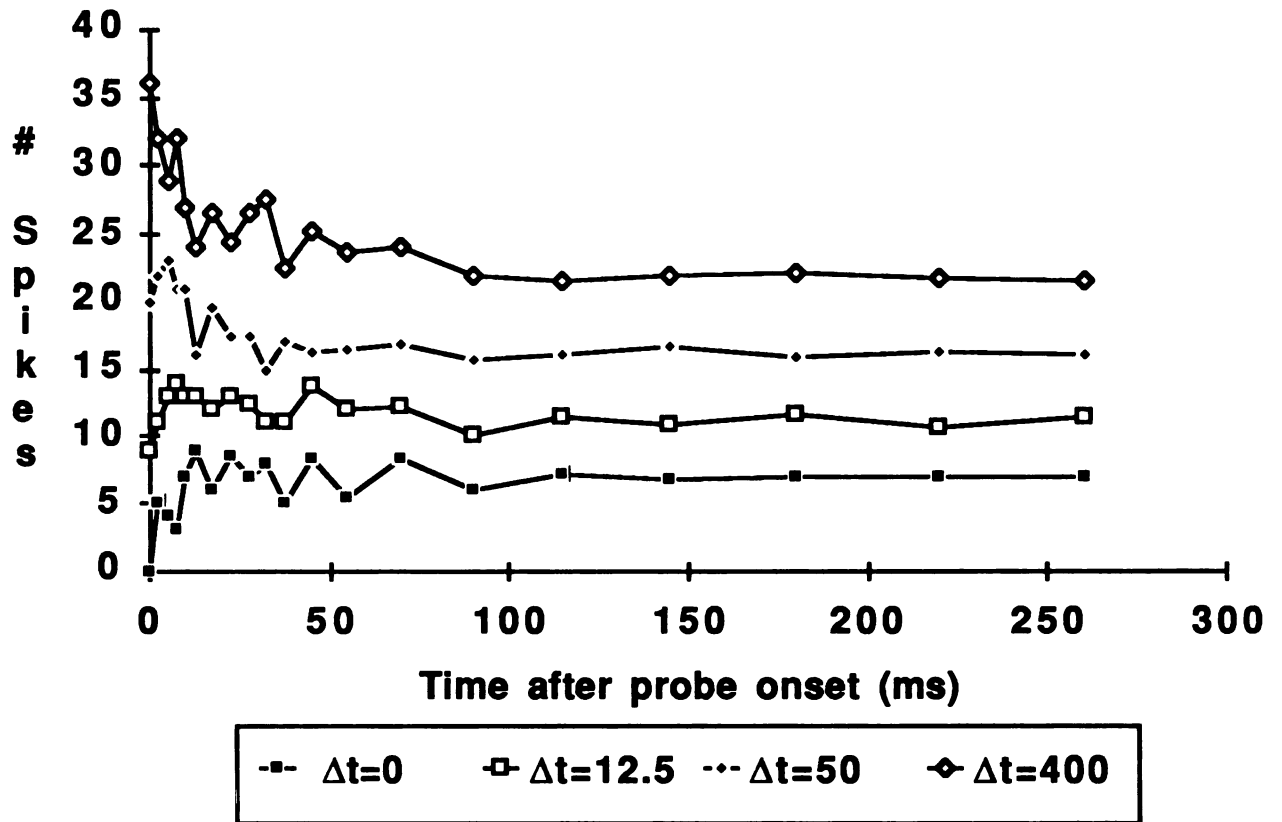


Fig. R20a. Examples of whole tone recovery in four units. All traces have been shifted vertically. A)Masker level 40 dB SL, probe 10 dB SL. B)Masker level 50 dB SL, probe 20 dB SL. C)Masker level 40 dB SL, probe 20 dB SL. D)Masker level 30 dB SL, probe 10 dB SL.



7/13 U4 50;20

B

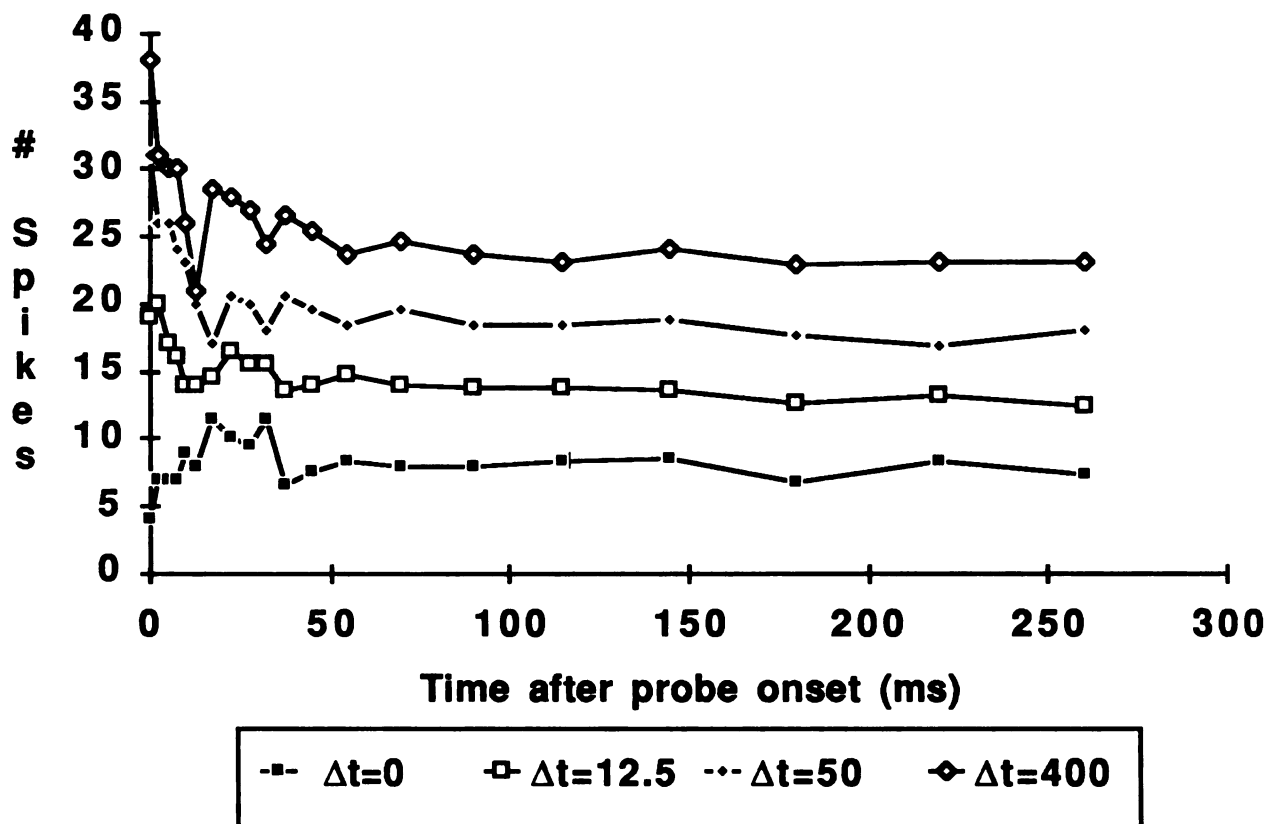


Fig. R20b. Examples of whole tone recovery in four units. B)Masker level 50 dB SL, probe 20 dB SL.

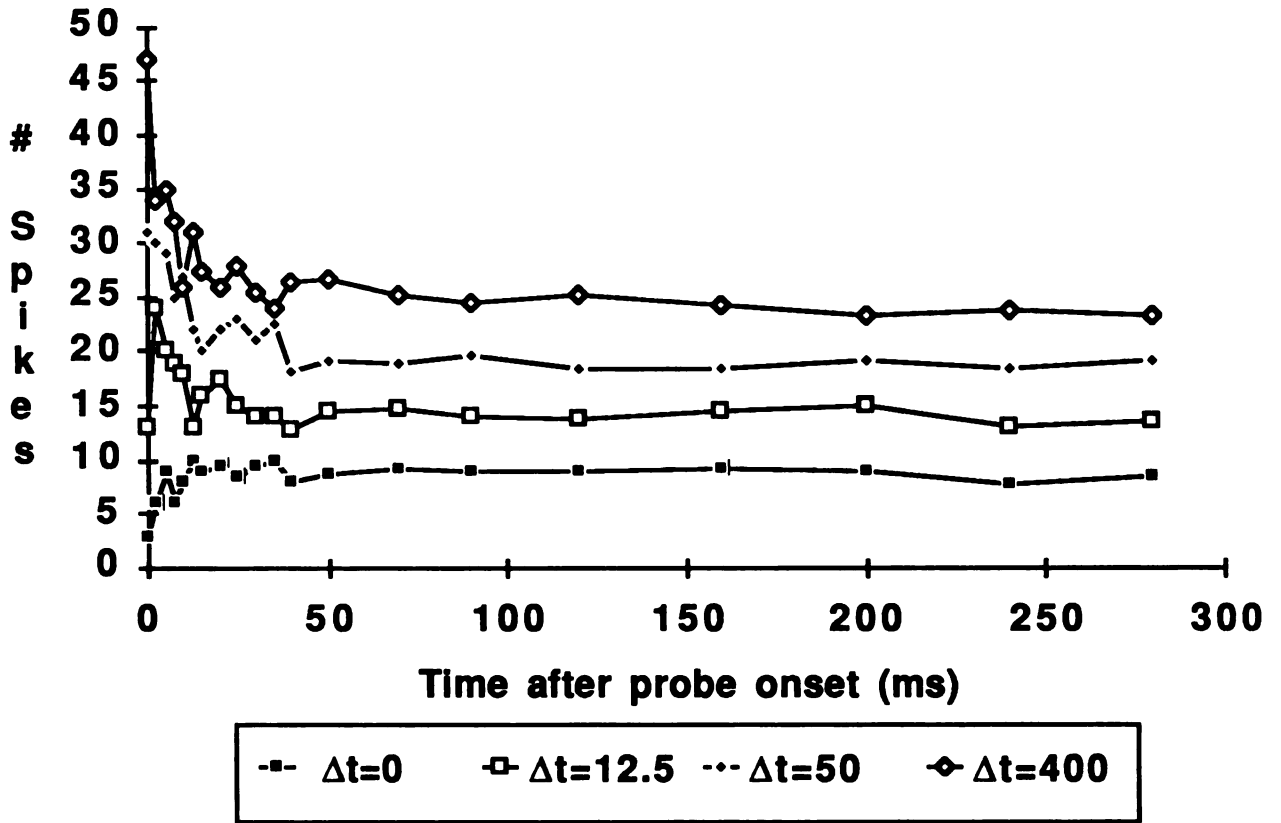


Fig. R20c. Examples of whole tone recovery in four units. C)Masker level 40 dB SL, probe 20 dB SL.

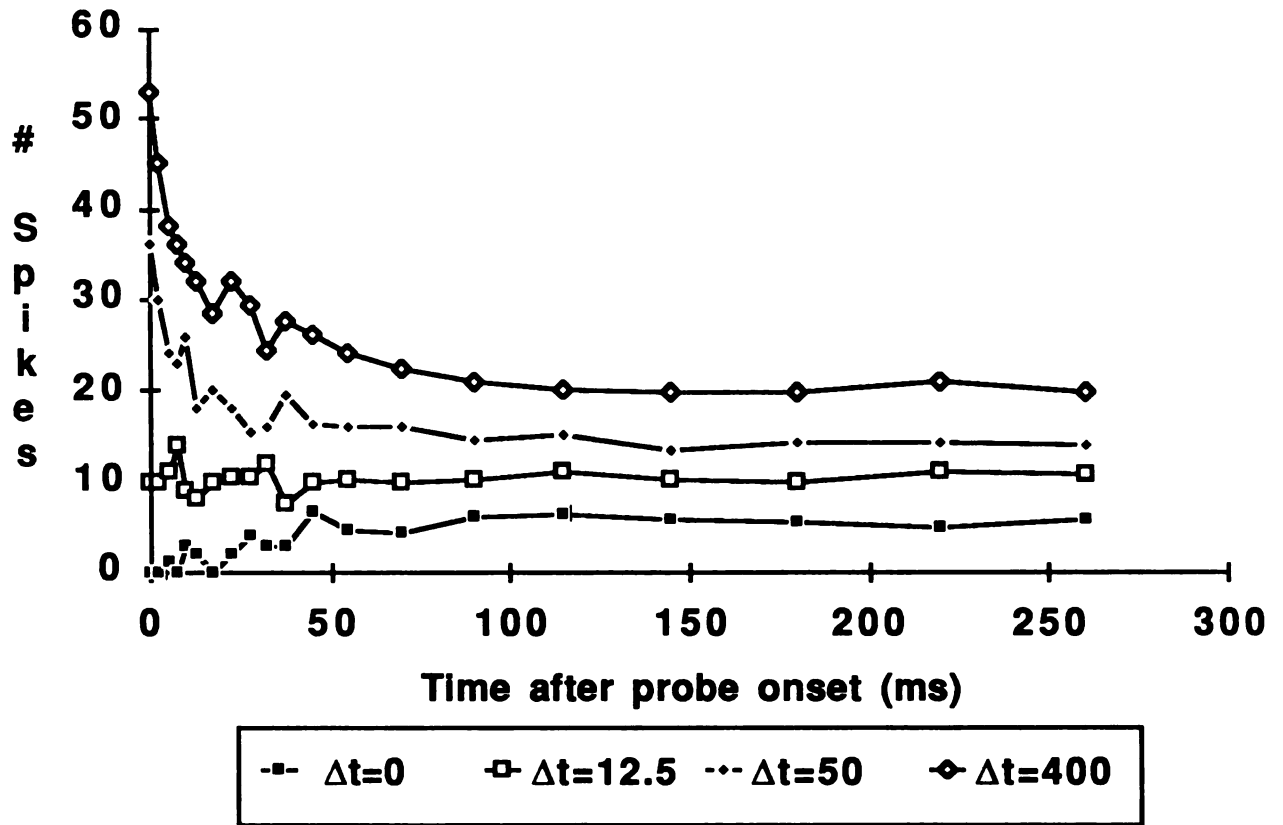


Fig. R20d. Examples of whole tone recovery in four units. D)Masker level 30 dB SL, probe 10 dB SL.

## **Auditory Nerve Neurophonic Response Characteristics:**

Typical ANN responses to a pure tone of 800 Hz are shown in Fig. R21a for two signal levels. In both cases, the response magnitude displayed a large onset which decreased during the course of the tone toward a constant steady state magnitude reflecting the temporal adaptation of the phase-locked firing rate of auditory nerve fibers. The phase of the ANN did not vary with stimulus intensity. In Fig. R21B, 9 probe responses are displayed, each preceded by an identical masker but varying in silent interval. In this case the masker was 40 dB SL and the probe was 20 dB SL. With a silent interval of 0 ms between masker and probe, the onset response was almost completely suppressed. As  $\Delta t$  was increased, the onset response recovered to a level equal or nearly equal to the unmasked condition. Along with the significant reduction in the onset amplitude of the response with zero delay there was also a phase shift in the responses with the shortest silent interval. In this example the phase recovered within six cycles after the start of the analysis window. As the silent interval increases, the phase recovery occurs sooner. In many other cases no measurable phase delay was detected following the masker offset.

### **Adaptation:**

During each experiment a series of unmasked responses were collected at each probe level before and after each masking series. The time constants were calculated for each averaged trace, at each level. The results at all probe levels are displayed as circles in Fig. R22. The squares are the average time constants across animals at each probe level and the triangles connected by dashed lines are the linear least-squares fit to the data. The rapid time constant of adaptation ( $\tau_{A_T}$ ) showed no significant change with stimulus

level, while the short term time constant of adaptation ( $\text{TauA}_S$ ) showed a 20.6 ms decrease with each 10 dB increase in probe amplitude ( $R=0.613$ ,  $N=13$ ,  $p>0.02$ ). The mean  $\text{TauA}_T$  for all cases was  $4.8(\pm 1.7)$  ms and the mean  $\text{TauA}_S$  was 115.5 ms at 10 dB SL, 83.2 ms at 20 dB SL and 73.5 ms at 30 dB SL.

When the calculated time constants of adaptation for each case were entered in Equation 1 there was a good fit to the data as illustrated in Fig. R23. Traces from four animals are displayed. The filled symbols are data and open symbols the result of fitting Eq. 1 to the data. Equally good fits were seen in all other cases.

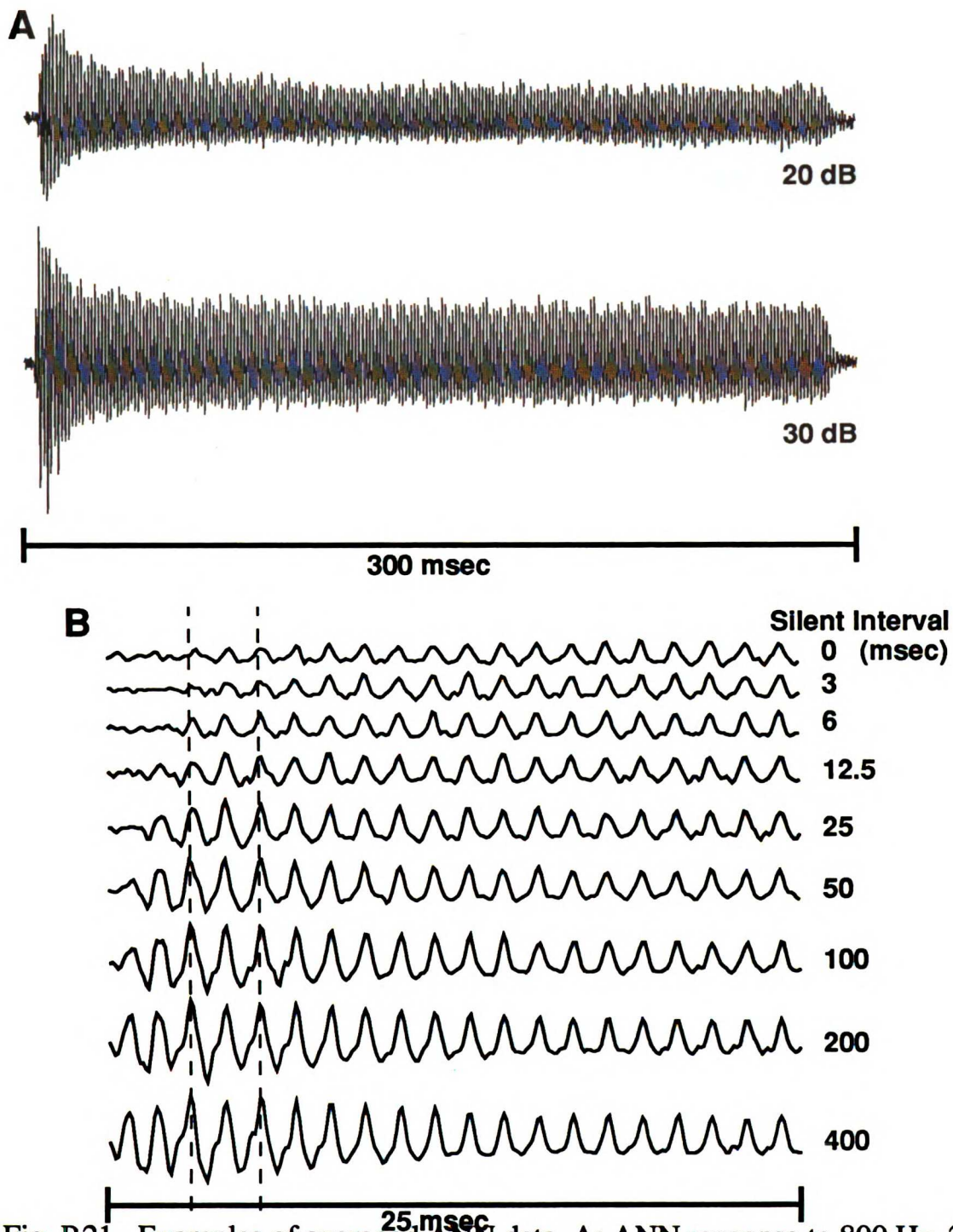


Fig. R21. Examples of averaged ANN data. A: ANN response to 800 Hz, 290 msec tone at 20 and 30 dB above the animals threshold (dB SL). Note the large onset amplitude followed by a reduction to a steady state level. B: Response to a 20 dB SL probe preceded by a 40 dB SL masker. A 25 msec window is displayed. The RMS amplitude of the 2 cycles between the vertical dashed cursors is used to measure the recovery from masking. The silent intervals between masker offset and probe onset are listed to the right of the averaged traces and are used throughout the study.

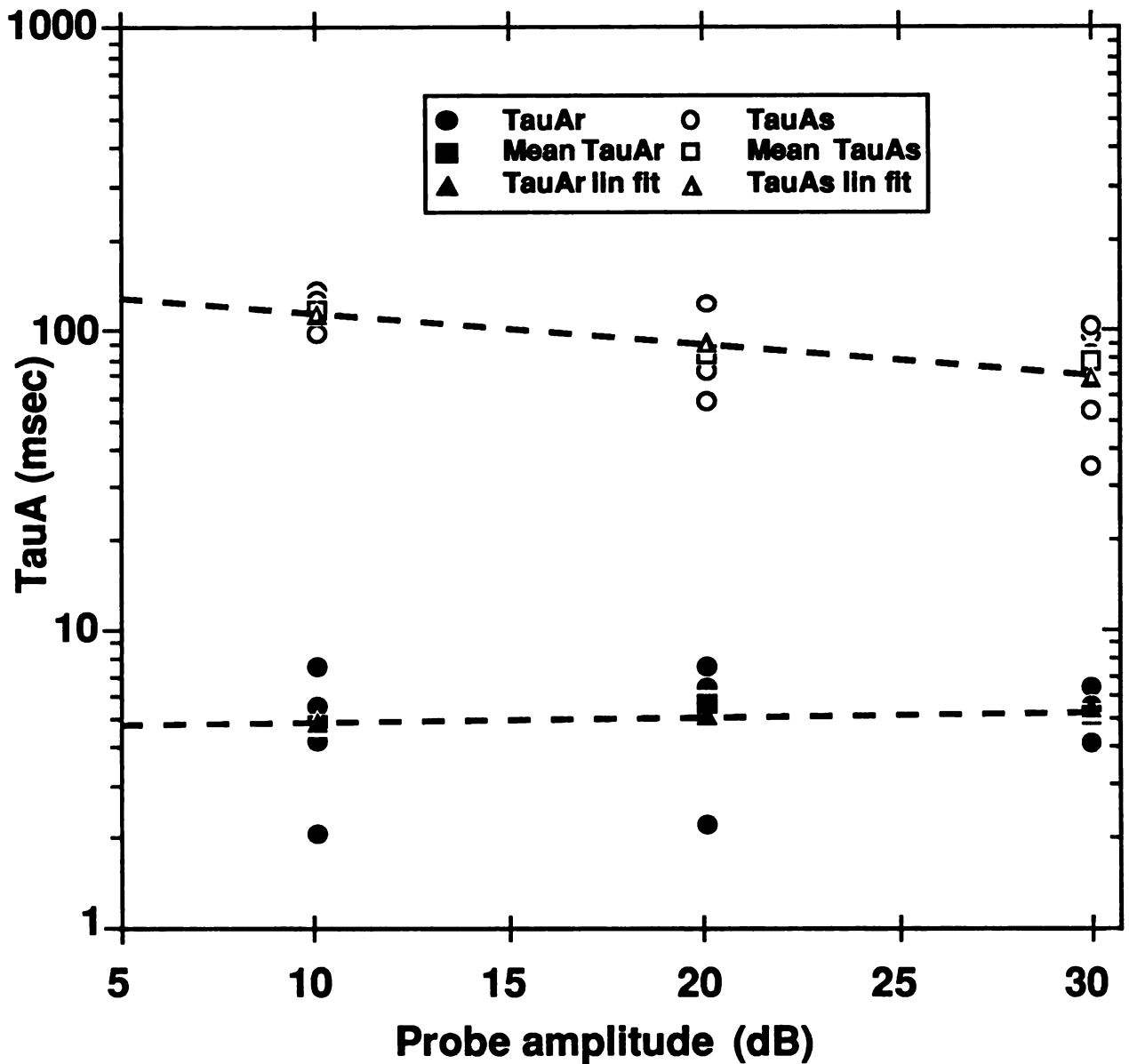


Fig. R22. ANN adaptation time constants. Filled circles are values from each animal for rapid time constant of adaptation ( $TauA_R$ ). These are averages of 3 or 4 traces collected during each experiment. Filled squares are averages across animals at each probe level tested. Filled triangles are values from the regression of all  $TauA_R$  values. Open symbols are the same as above for short term time constant of adaptation ( $TauA_S$ ).

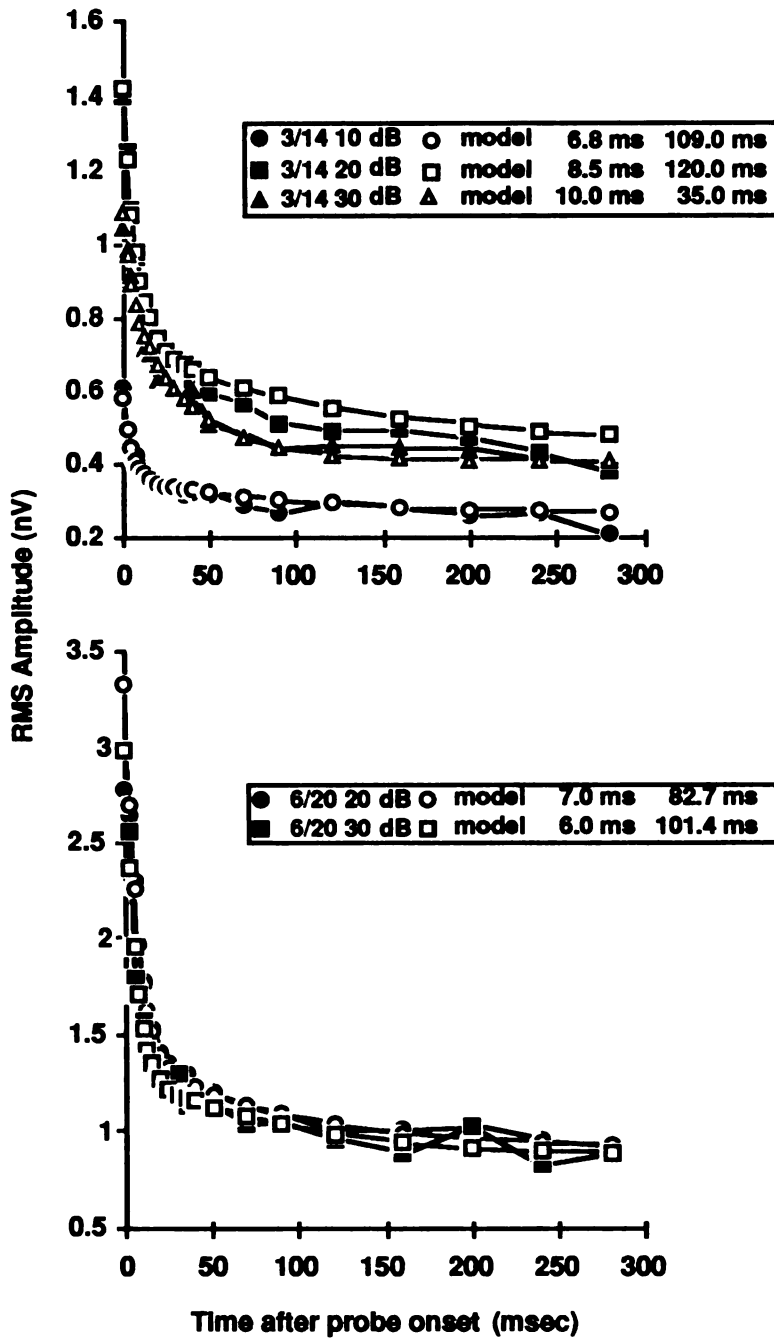


Fig. R23a. RMS amplitude values and model values for adaptation. Filled symbols are data and open symbols are model values generated with Eq. 1. Data has not been shifted vertically. Experiment date, stimulus amplitude in dB above threshold, and the TauAr and TauAs values are presented in the insert of each figure. Data displayed is from two animals.



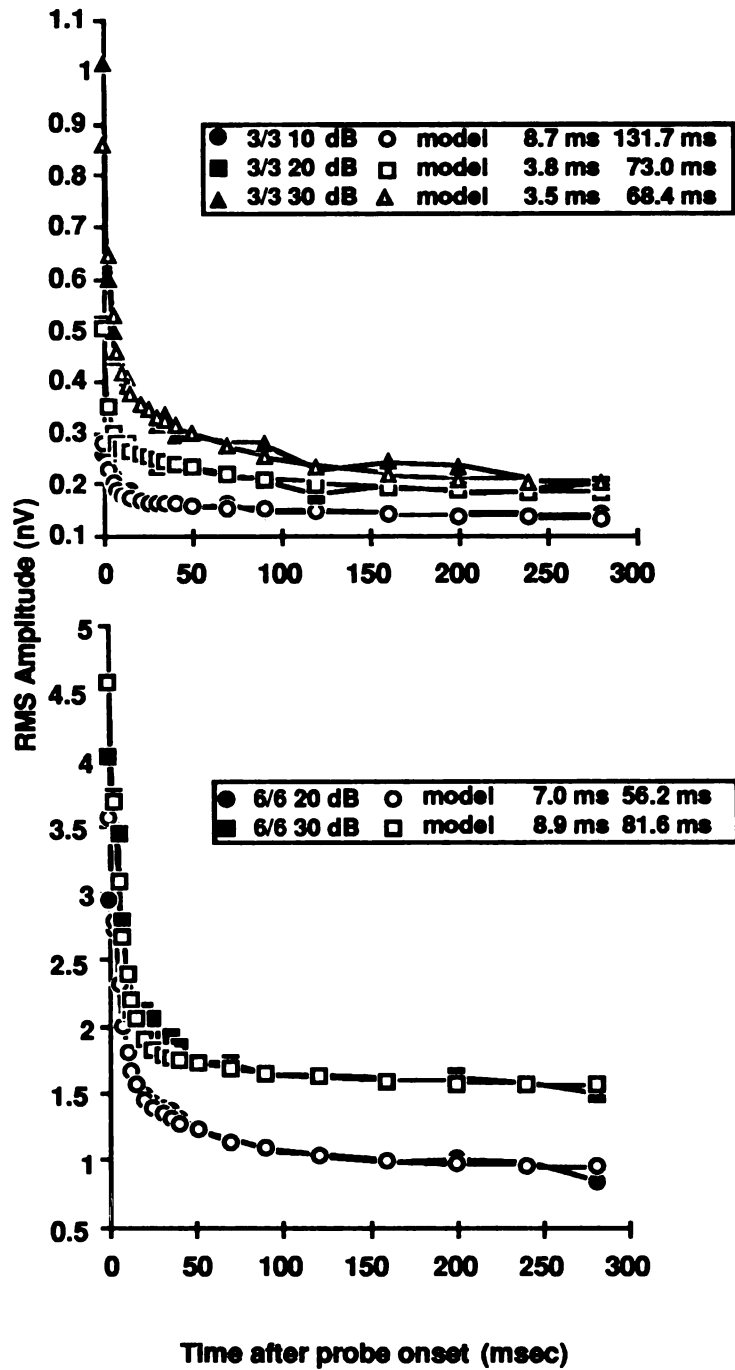


Fig. R23b. RMS amplitude values and model values for adaptation. Same as previous Fig. for two additional animals.

### **Onset Recovery:**

Recovery of the onset amplitude of a response following a masker produces a curve that can be described by the sum of two exponential processes (Eq. 2). The results of estimating the average time constants are shown in Fig. R24. The rapid time constant of recovery ( $\text{TauR}_r$ ) shows no systematic change with relative masker level. The mean value for all cases was 16.2 ( $\pm 9.8$ ) ms. The short term time constant of recovery ( $\text{TauR}_s$ ) shows a slight but statistically not significant increase with relative masker level of 15 ms per 10 dB increase in relative masker level ( $R=0.229$ ,  $N=33$ ,  $p=.20$ ). The mean for all cases was 124.6 ( $\pm 50.1$ ) ms.

Recovery functions determined from two animals, at two probe levels each are presented in Fig. R25. The filled symbols represent data and the open symbols are the result of entering the estimated rapid and short term time constant values into Eq. 2, producing a good fit to the data. The traces have not been normalized. The inset in each set of traces lists the date of the experiment, the masker and probe level relative to threshold and the estimated rapid and short term time constants. The lowest filled symbol in each is the onset amplitude of the probe following a zero ms silent interval. The smallest amplitude always occurs after the loudest masker, but the rate of recovery is not related to the masker amplitude. It is also apparent that the final recovery amplitude at  $\Delta t = 400$  does not always reach the same level. In several cases the probe preceded by the loudest masker recovers to the greatest amplitude even though the amplitude at  $\Delta t = 0$  was always the smallest. Although the end points vary, the individual points within each function do not display any abnormal variations of similar magnitude. Variation in the end point may reflect intrinsic changes in the preparation

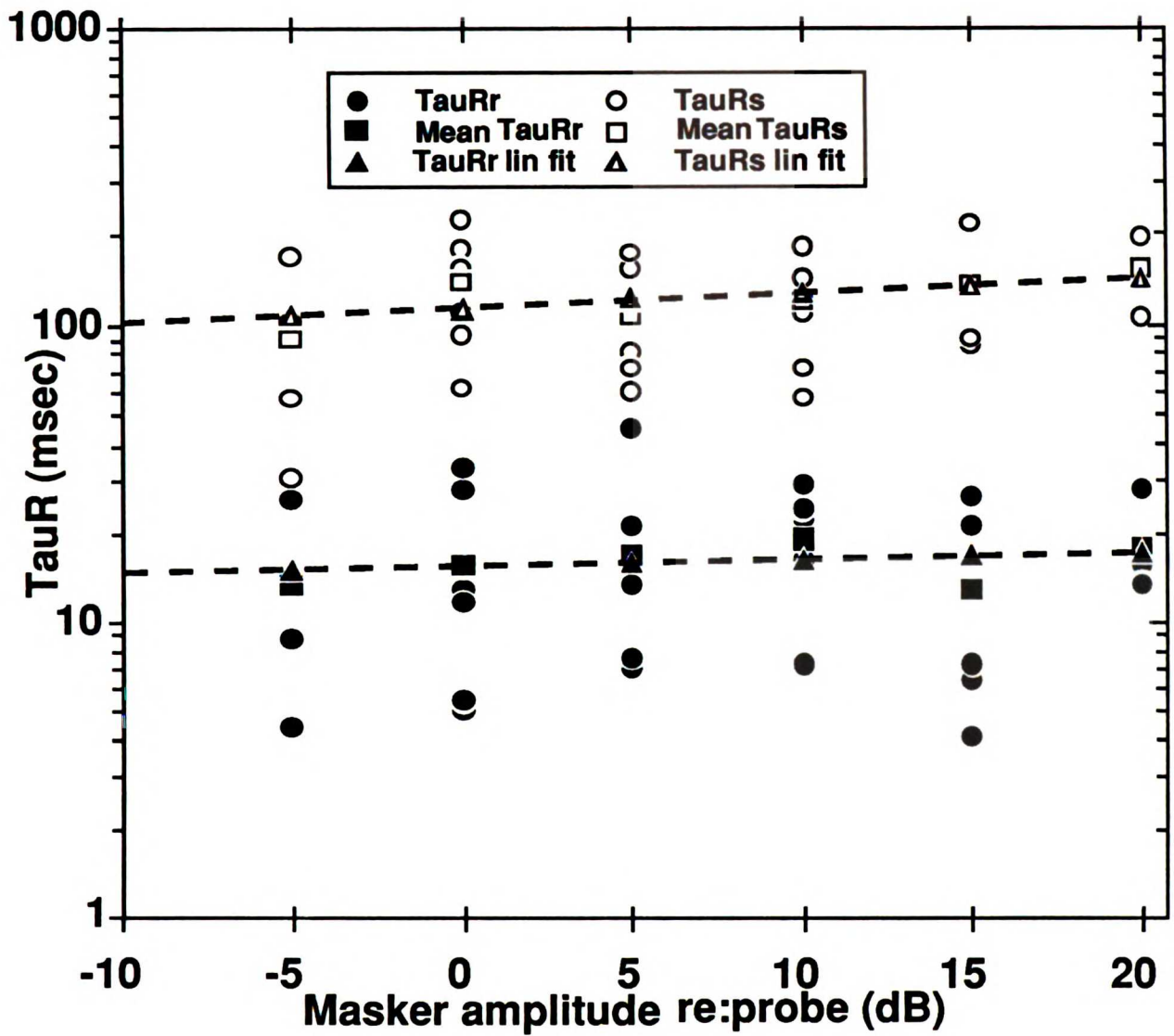


Fig. R24. ANN recovery time constants. All symbols as in Fig. R23. Masker amplitude is in dB relative to probe stimulus level

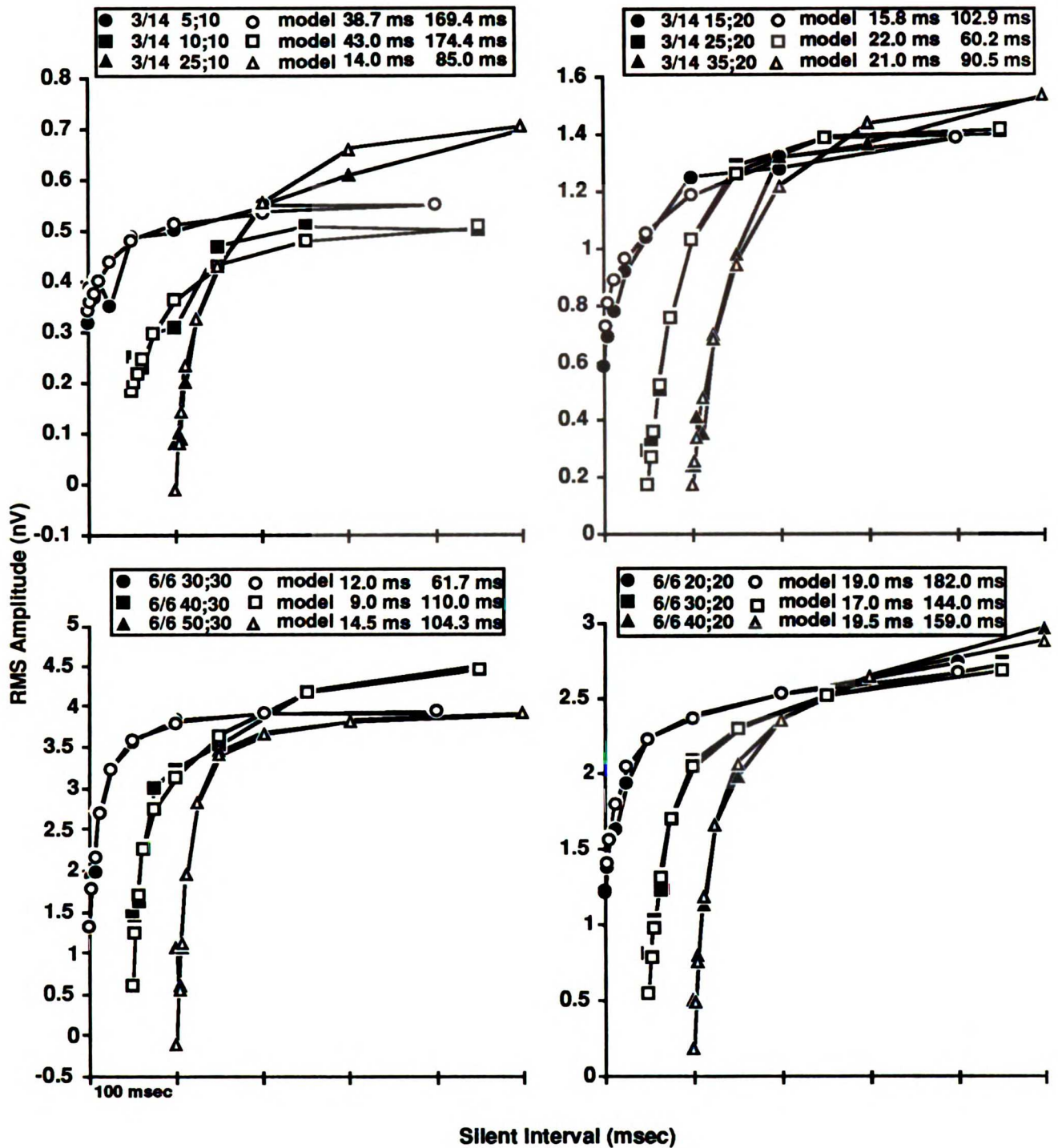


Fig. R25. ANN data and model values for recovery from adaptation. Filled symbols are data and open symbols are model values. The two traces with the highest amplitude maskers have been shifted along the time axis 50 and 100 msec for ease of viewing. Data displayed is from four animals, each at two probe levels. All else as in Fig. 4.

during data collection or slow changes in cochlear function due to stimulation effects.

### **Whole Tone Recovery:**

Fig. R26 displays ANN responses using comparable stimuli to those used for the single unit responses in Fig. R19. The masker was 20 dB louder than the probe which was 10 to 20 dB above the ANN threshold. Probe and masker frequency was always 800 Hz. Note that there is a similar suppression of the first point in the 12.5 ms response as seen in the single unit responses. Likewise, the reversal of the response from a "recovery" function to an "adaptation" function occurs with a silent interval slightly shorter than 12.5 ms.

The sum of all ANN traces with a silent interval of zero ms is displayed in Fig. R27. The parameter is the relative masker/probe level. A progression from traces which follow a "recovery" function to traces which follow an "adaptation" function is evident. The reversal occurs between +5 and +10 dB masker level relative to probe level. An interaction exists between the silent interval during which the system can recover from the masker, and the relative masker/probe level which sets the magnitude of suppression of the system. A flat response will occur at either short silent intervals with relatively quiet maskers or at long silent intervals with relatively loud maskers. Why does the flat response occur between +5 and +10 dB and not at 0 dB? A silent interval of 0 ms with masker and probe at equal levels would be equivalent to presenting one continuous long tone during which only a slight amount of additional suppression of the response amplitude would be expected. In fact, even at  $\Delta t = 0$  ms there is some opportunity for the response to recover as the masker offset and probe onset

each have five ms ramps. Therefore, the flat response would be expected to occur with a masker level somewhat louder than the probe, as seen above.

Four examples of whole tone masking at four different relative masker/probe levels are displayed in Fig. R28. The general pattern of the traces is comparable to the single unit examples. In R28d at  $\Delta t = 12.5$ , ms the first several points are suppressed followed by an onset response which decreases to a steady state level. As in the single unit data, a moderate amount of variation exists within each trace. However, the systematic change seen in Fig. R26 and R22 and the similarity of the ANN and single unit responses recorded with comparable stimuli argues that the ANN can accurately represent a small population of nerve fibers when responses are recorded with low level stimuli.

### ANN Whole Tone Recovery

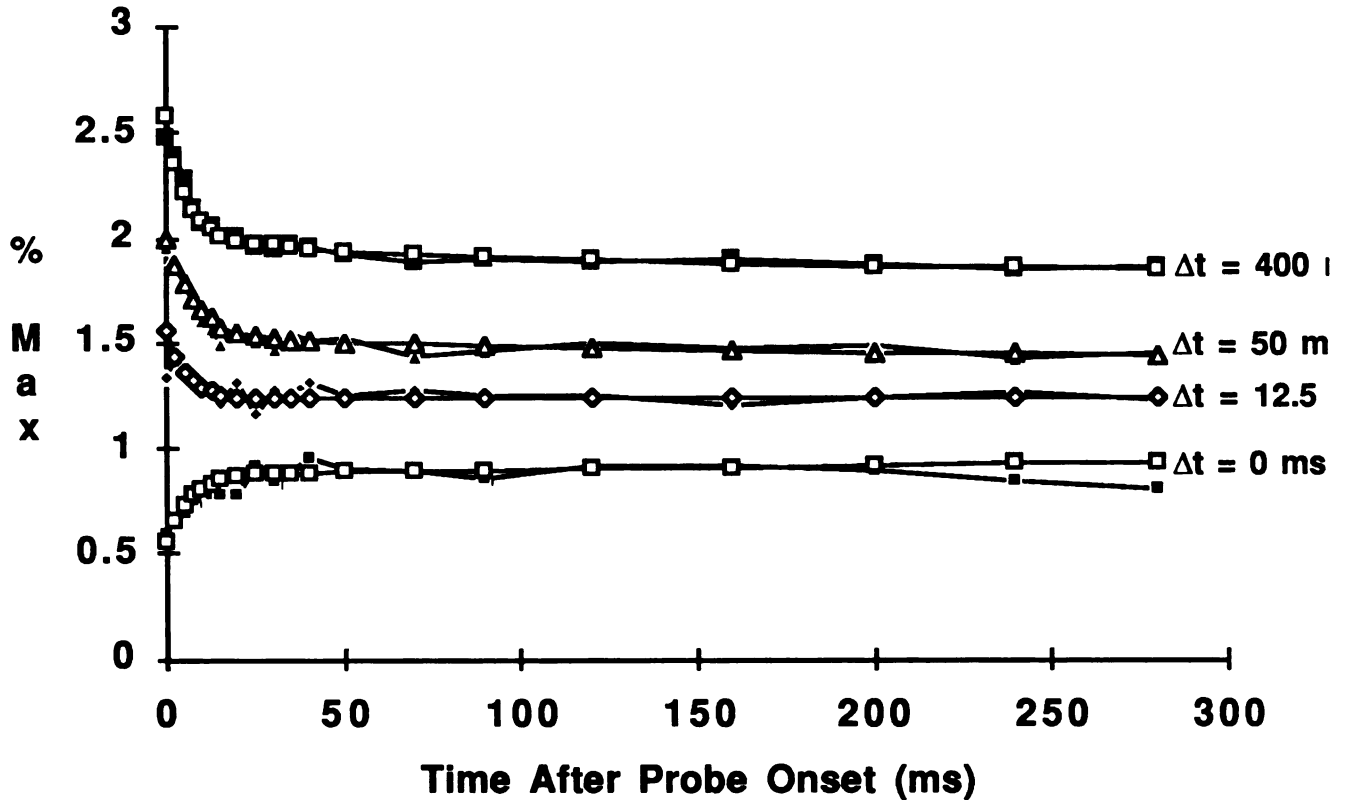


Fig. R26. ANN whole tone recovery. Normalized, averaged data of 4 neurophonic traces with the masker 20 dB louder than the probe. Value to the right of each trace is the silent interval between masker offset and probe onset. Data was fit with a two-time-constant exponential adaptation equation for the top three traces (Eq. 1). The bottom trace is fit with a two-time-constant exponential recovery equation (Eq. 2). All traces have been shifted vertically for ease of viewing. Compare to Fig. R19 of single unit responses.

### ANN Whole Tone Recovery $\Delta t=0$

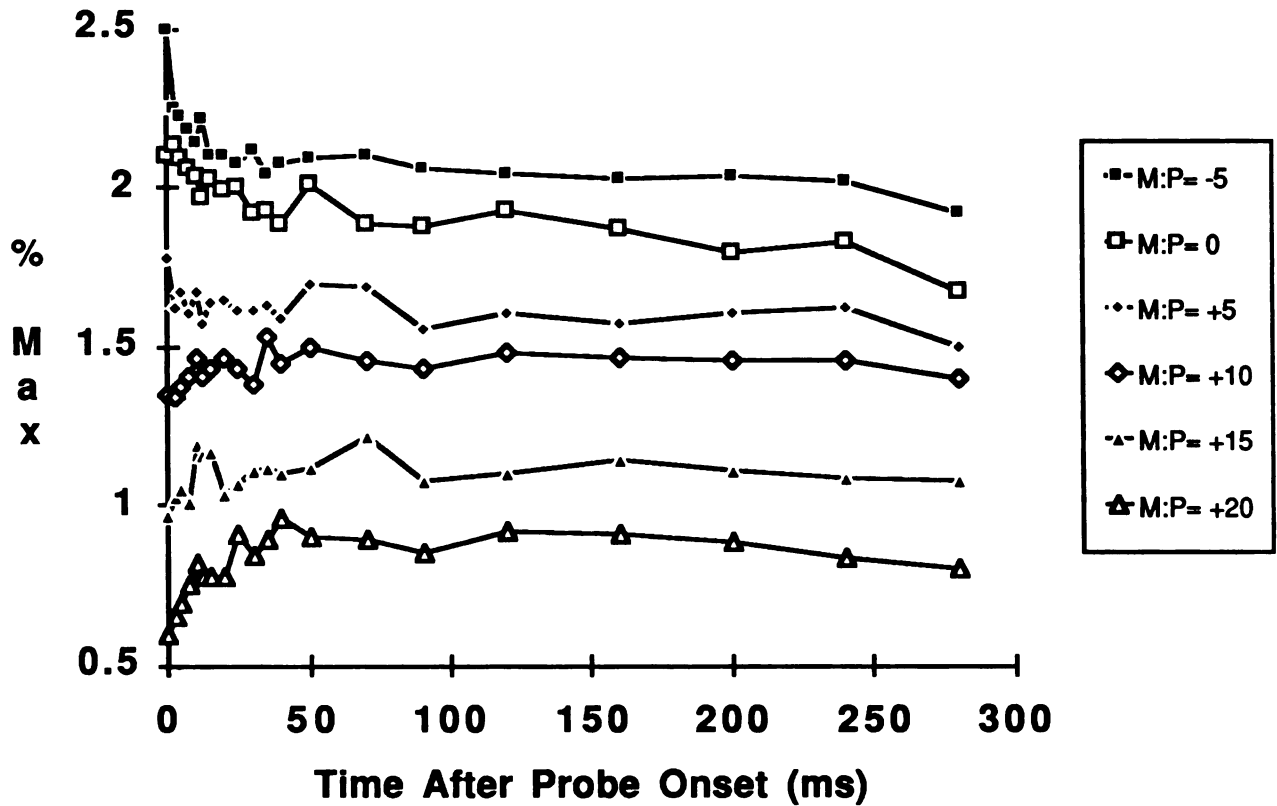


Fig. R27. ANN whole tone recovery at  $\Delta t = 0$ . Normalized, averaged data with the masker varying from - 5 to 20 dB relative to the probe. A systematic shift from an adaptation function to a recovery function is evident in the traces.



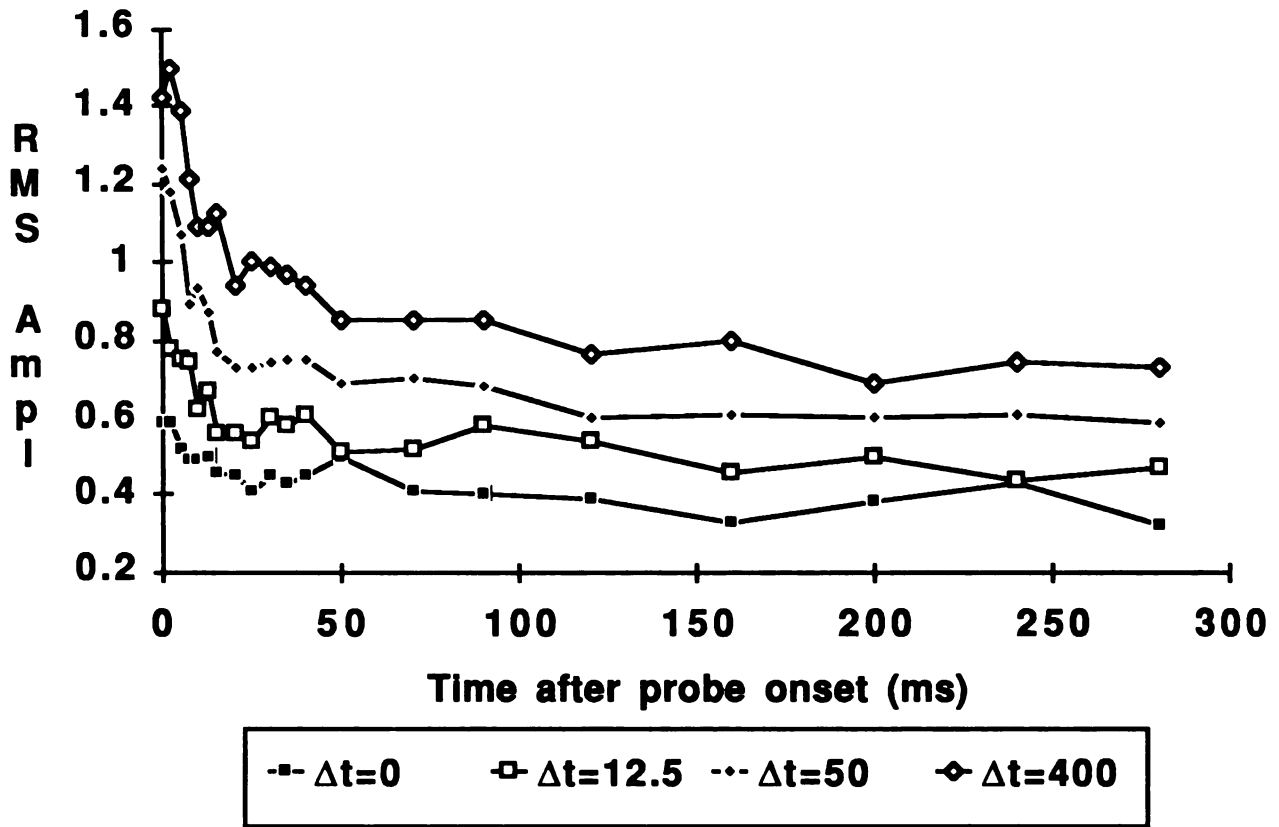


Fig. R28a. Examples of whole tone recovery in four animals. All traces have been shifted vertically. A) Masker level 15 dB SL, probe 20 dB SL.

5/3 30;30

B

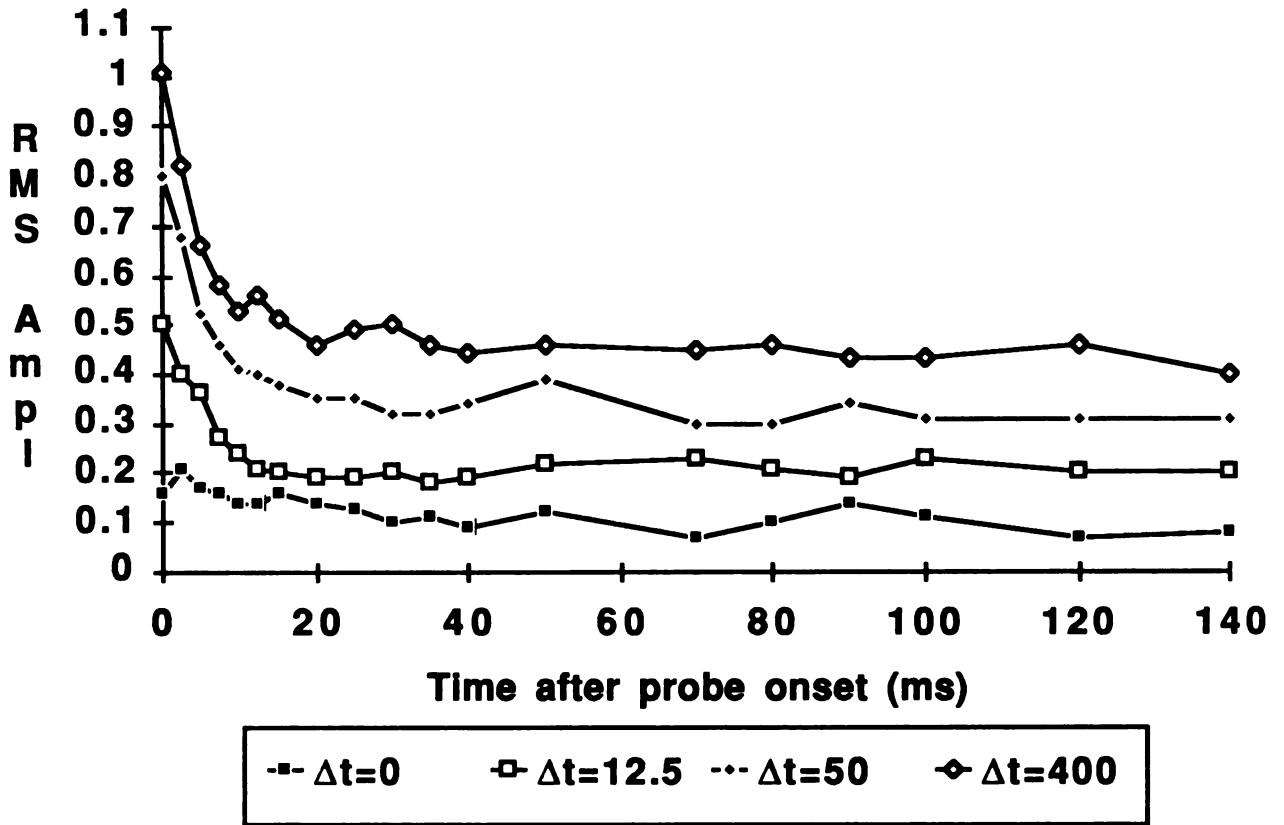


Fig. R28b. Examples of whole tone recovery in four animals. B) Masker level 30 dB SL, probe 30 dB SL.

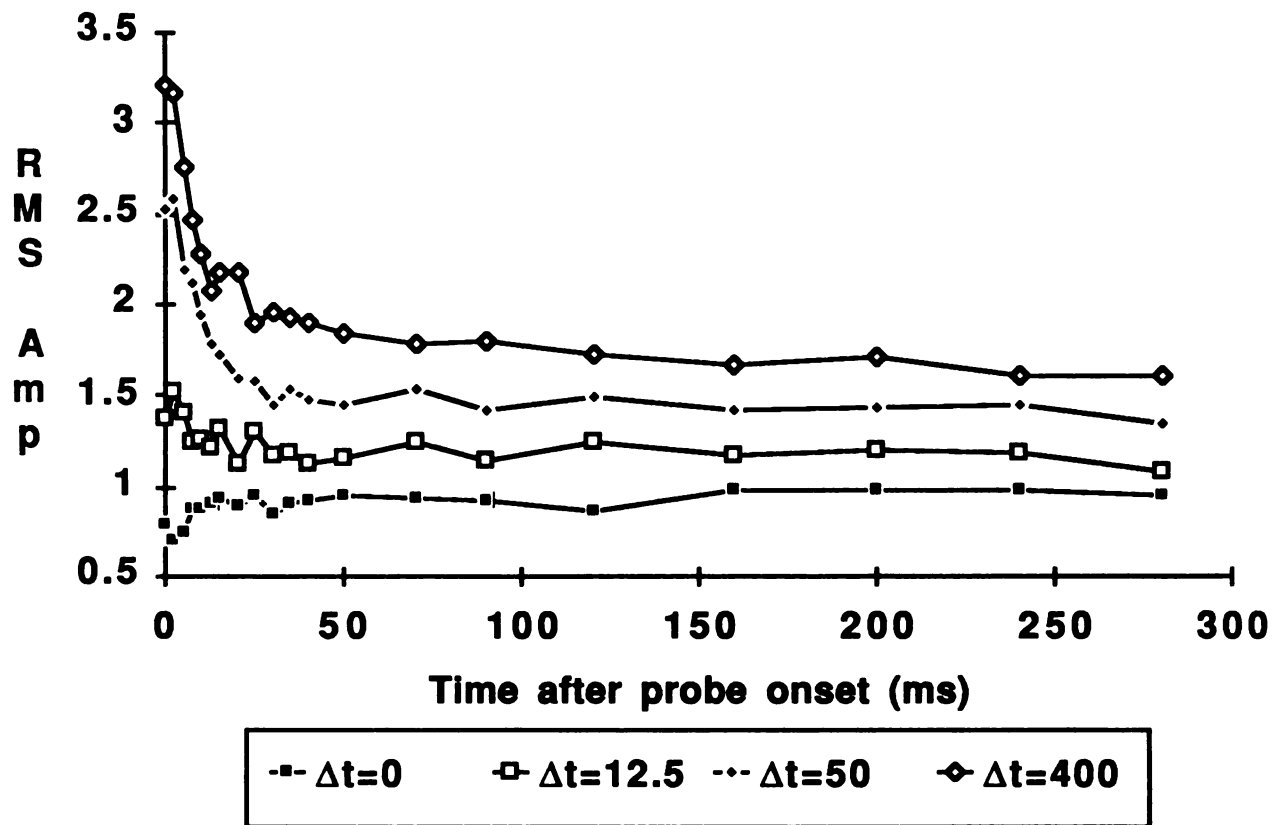


Fig. R28c. Examples of whole tone recovery in four animals. C) Masker level 30 dB SL, probe 20 dB SL.

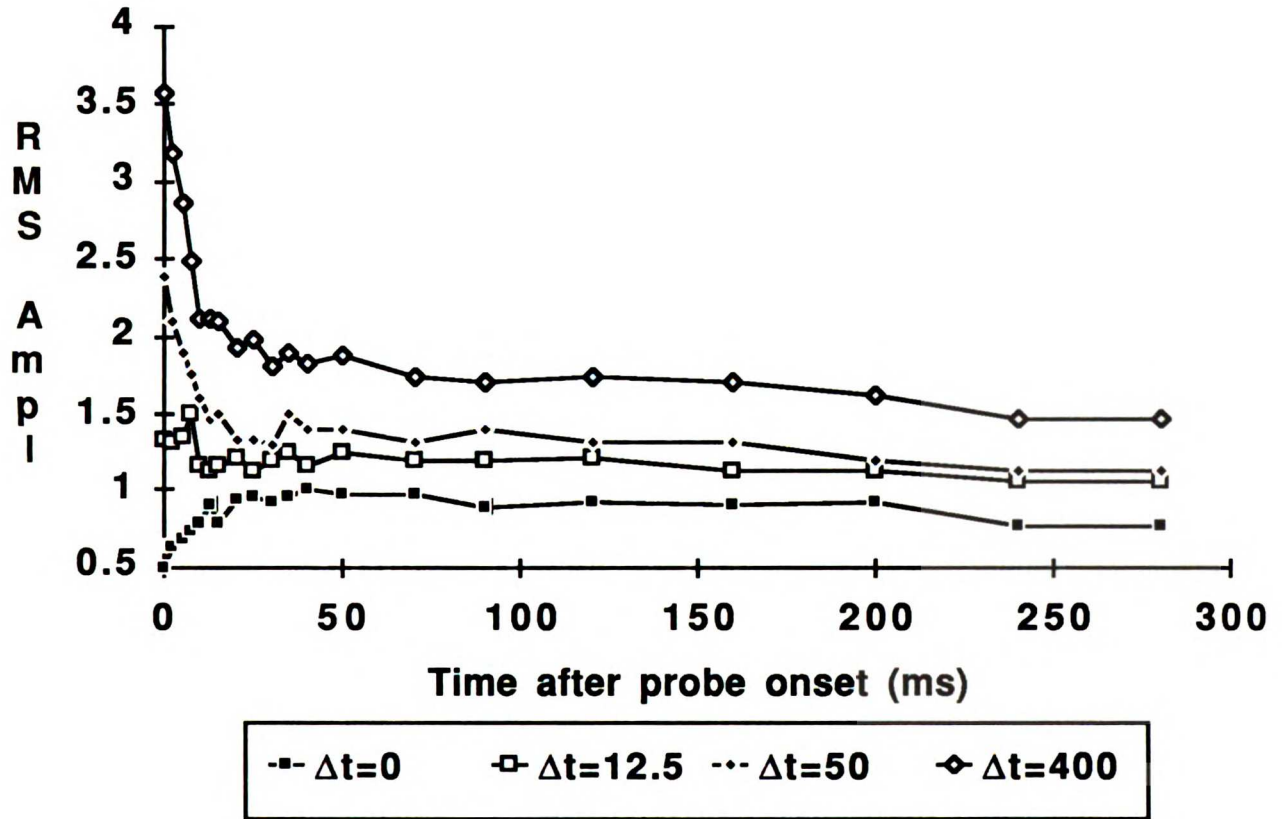


Fig. R28d. Examples of whole tone recovery in four animals. D) Masker level 40 dB SL, probe 20 dB SL.

## **DISCUSSION:**

This study examined the time course of adaptation and recovery from adaptation of the auditory nerve neurophonic (ANN) and single auditory nerve fiber responses of the cat. The conditions studied were: 1) adaptation response using low level 800 Hz or characteristic frequency (CF) stimuli; and 2) onset recovery and whole-tone response recovery following a masker of equal frequency with variable silent intervals between the masker offset and probe onset.

This study has demonstrated that adaptation of the ANN and single unit responses using long duration, low frequency tones can be described as the sum of two exponential processes (Eq. 1). Similarly, recovery from adaptation of the onset can be fitted by two exponential processes with different time constants (Eq. 2) or for some single units by a single exponential process (Eq. 3). The obtained values match, with varying degree, previously reported time constants from compound action potential and single unit data of other species (Eggermont and Spoor, 1973 a,b; Spoor et al. 1976; Smith, 1977; Harris and Dallos, 1979; Huang, 1981; Smith and Brachman, 1982; Westerman and Smith, 1984). Recovery of the whole-tone response can be fit by either a two-time-constant adaptation function (Eq. 1) or a two-time-constant recovery function (Eq. 2). The choice depends on whether the relative masker/probe amplitude and the silent interval produce a response with an large onset which decays to steady state (an "adaptation function") or a suppressed onset which increases to steady state (a "recovery function").

Before discussing the results of this study, several operating assumptions regarding the characteristics of adaptation, onset recovery and

whole-tone recovery and the interactions between these responses need to be considered. In Fig. D1 a schematic representation of the amplitude of each of the afore mentioned responses is shown. A typical adaptation function is represented by the filled squares. This plot is the sum of two exponentially decaying processes with different time constants and a steady state level (Eq. 1). The amplitude values have been arbitrarily chosen. The open squares are the onset values of the response with increasing silent intervals between the masker offset and probe onset (Eq. 2). The filled squares are the amplitude values of the whole tone response with no masker, i.e. an adaptation curve. When the masker amplitude and frequency are equal to the probe amplitude and frequency and the silent interval is zero, no significant change in amplitude will be observed when the probe is presented, i.e. the whole tone response will be a flat line at the steady state amplitude as demonstrated by the horizontal line in Fig. D1. Any onset response that may occur with this stimulus condition is produced by recovery which ensues as the masker tone ramps off and the probe tone ramps on. If there is no offset and no onset ramp this situation is equivalent to presenting one very long tone and examining the last 290 milliseconds. It should be mentioned that some additional decrease in the response amplitude may be observed with very long tones because a true steady state may not have been reached. However, to a first approximation the response has reached a steady state level.

### Schematic of Responses

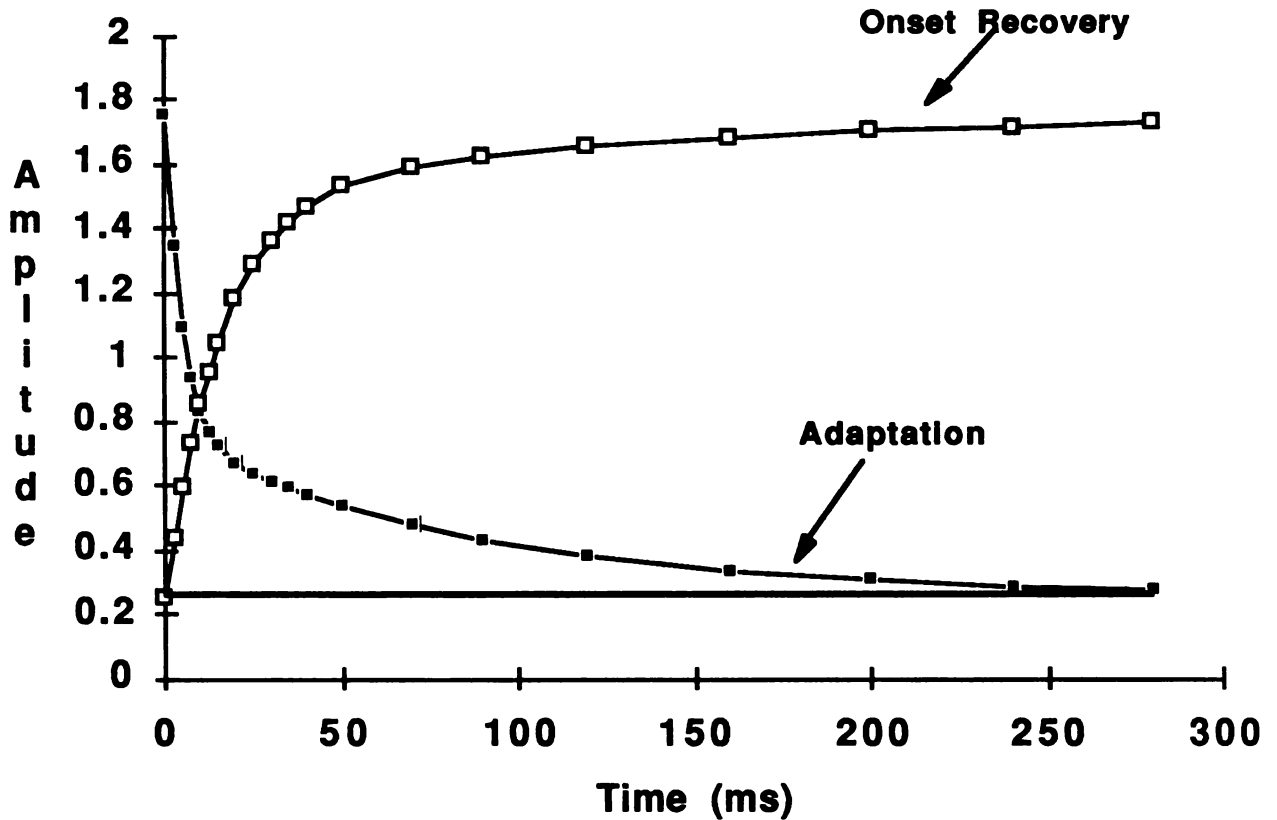


Fig. D1. Schematic of adaptation and onset recovery for the case with masker amplitude and frequency equal to probe amplitude and frequency. Open squares are onset amplitude after silent intervals as listed on abscissa. Filled squares are amplitude of successive windows within an adapting response at post onset times as listed on abscissa. The solid line is the expected response of the whole tone recovery. Amplitude units are arbitrary.

Using the same conditions as above, but measuring the whole tone response at each silent interval, the onset amplitude will recover toward the unmasked amplitude as before and the remainder of the response will adapt to the steady state (Fig. D2). These are not sequential processes; the recovery and adaptation are occurring simultaneously and interacting in some manner to produce the observed response. Finally, if a masker is used which is louder than the probe, the probe onset response with a zero silent interval would be less than the steady state level for that probe level, but would recover to the same onset level as before as the silent interval is increased (Fig. D3). Under these conditions then, the onset will recover from an amplitude below the steady state to the maximum (unmasked) amplitude while the remainder of the whole-tone response will recover to the steady state for that probe level. As the silent interval increases from zero to 400 ms the shape of the whole-tone recovery will change from an "exponential recovery" to an "exponential adaptation".

The same sequence can be attained by changing the relative amplitude of the masker and probe. With a loud masker relative to the probe, the response to the probe will follow a recovery function. Maintaining a constant probe level while decreasing the masker level will produce probe responses that change from recovery to adaptation functions.



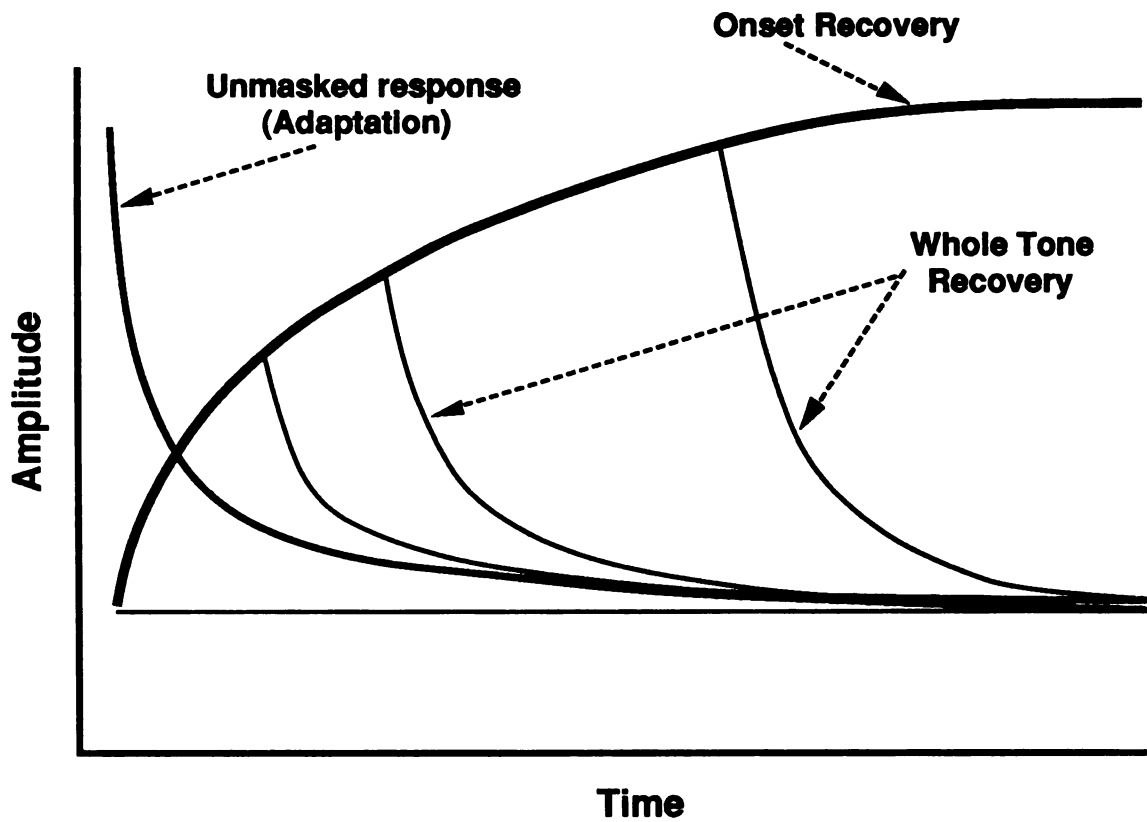


Fig. D2. Schematic of whole tone recovery traces. Correlation between increasing silent intervals with adaptation and onset recovery traces. Masker and probe at equal amplitude and frequency.

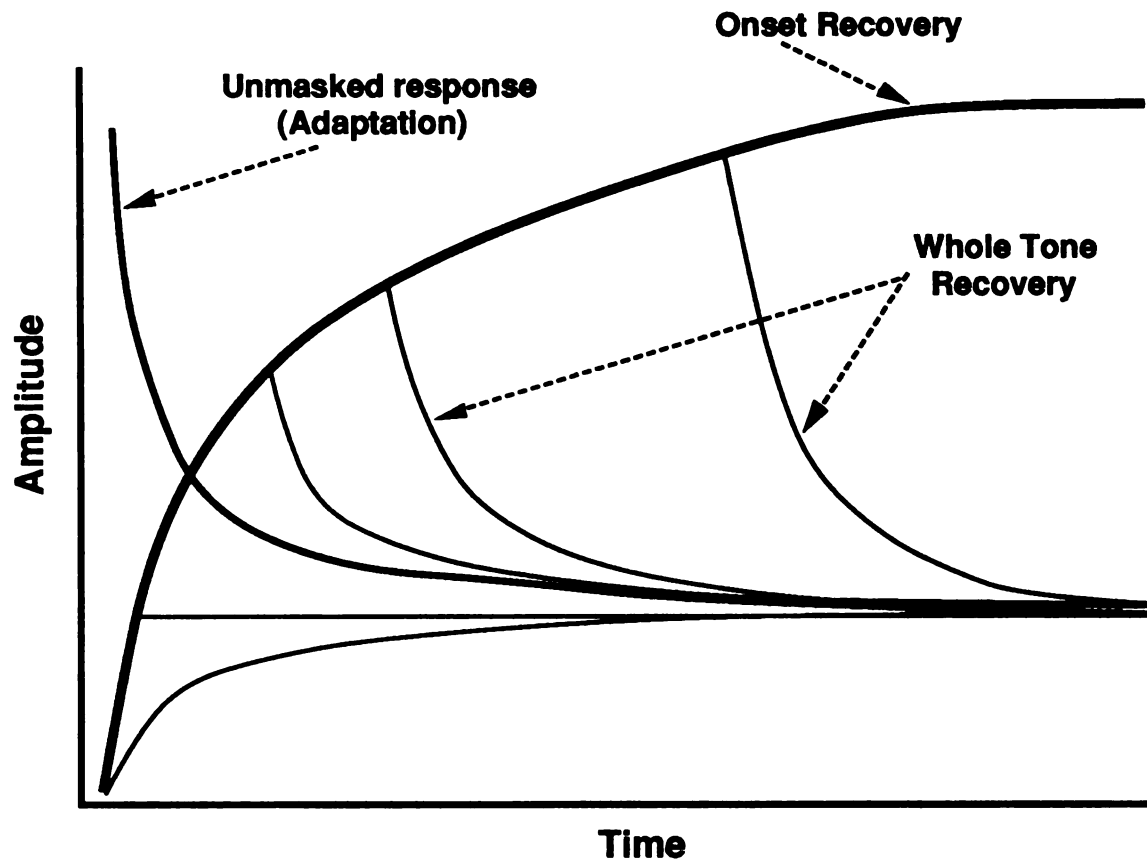


Fig. D3. Same as D2 with masker amplitude greater than the probe amplitude.

**Adaptation:**

In this study no change in either of the two-time-constants of adaptation as a function of CF was noted. This is in contrast to Westerman and Smith (1984) who observed that the rapid time constant of adaptation decreased as fiber CF increased, although they did not observe this for short term adaptation. They tested each fiber using stimuli at CF, not at a constant (low) frequency as used in the present study. The variation of adaptation time constant with stimulus frequency which they observed may be a feature of the stimulus frequency or an inherent characteristic of the fibers or hair cells stimulating those fibers. For example, at low frequencies the time between each cycle may be sufficient to allow some degree of recovery which would result in a decrease of the rate of adaptation (i.e. increase the time constant). This would be a characteristic of the stimulus and not reflect differences in the responses of particular fibers. However, if the adaptation is specific to the fibers, using the same stimulus frequency for all fibers would show a systematic change in TauA as a function of the fiber CF.

These two hypotheses were tested in the present study. Much of the data in this study were collected using 800 Hz stimuli, regardless of the CF of the unit. For units with CF ranging from 400 to 3500 Hz, all stimulated with an 800 Hz tone 20 dB above the threshold at 800 Hz, no variation of TauAr or TauAs with unit CF was observed. A second population of fibers were stimulated at CF, 20 dB above threshold. If a difference existed in the inherent ability of units with a particular CF to follow a stimulus, it should have been evident in Fig. R6. In both cases the single unit results of this study displayed no change in TauAr or TauAs as a function of unit CF. These results contradict the results of Westerman and Smith (1984) and Westerman (1985). They observed a decrease in the rapid

time constant of adaptation with increasing fiber CF. When 12 individual fibers were tested with one tone at CF and a second at one octave below CF, 9 fibers displayed a decrease in TauAr at the lower stimulus frequency while 3 of 12 displayed an increase.

Another factor which may cause the time constant of adaptation to vary is the stimulus intensity. Westerman and Smith (1984) found that the rapid adaptation time constant decreased as stimulus intensity was increased. While the single unit time constants in this study did not vary with stimulus level for stimuli 10 to 40 dB above threshold, the TauAs of the ANN decreased 20.6 ms with each 10 dB increase in probe amplitude. No clear explanation for this systematic variation in the ANN results has been found. The discrepancy between the previous results and the results of this study may be an interspecies difference or a consequence of the analysis methods. Westerman and Smith (1984) and Westerman (1985) present a descriptive analysis of the change in the rapid adaptation time constant such as for "21 of 34 units TauAr declined with increasing stimulus intensity...In about one-third of the units studied the fitted values of TauAr either increased or fluctuated as intensity was increased". In this study all available data were pooled and analyzed for statistical significance with linear regression/correlation analysis.

### **Onset Recovery:**

The same estimation procedures were used for the onset recovery as employed in the adaptation analysis. In this study, two ANN recovery time constants were observed: approximately 16 ms for the rapid and 125 ms for the short term process. Single unit responses had either two-

time-constant cases or one time constant cases. The former had values of approximately 22 ms for  $\tau_{Rr}$  and 184 ms for  $\tau_{Rs}$  and the latter had a value of approximately 95 ms for  $\tau_R$ . The values of the two-time-constants bracket the values observed for recovery functions fit with a single time constant for single-units in the Guinea pig (40 ms: Smith and Zwislocki, 1975), chinchilla (53 ms: Harris and Dallos, 1979) and gerbil (115 ms: Smith, 1977; 48 ms: Westerman, 1985). Separate values for rapid and short term onset recovery time constants have not been previously reported. As discussed previously, the choice of window length for measuring amplitude and calculating time constants can significantly alter the results. It is possible that this is the source of the difference between the present observation and previous reports. Smith (1977) used a 40 ms analysis window to measure the response amplitude which would have obliterated the two-time-constants of recovery observed in this study. Harris and Dallos (1979), using a 15 ms analysis window, observed a second time constant, but only with maskers 30 dB or greater than a 20 dB probe. In addition, a semi-log plot of their data approximated two straight lines with an inflection at 50 ms, while the inflection point in this study occurred at less than 20 ms indicating a clear intraspecies or methodological difference, at least for the rapid time constant. Westerman (1985) utilized a one ms analysis window but chose as the onset of recovery the bin with the highest firing rate in the first 10 ms after stimulus presentation. Statistical noise in the selection of the onset of recovery could easily prevent the rapid recovery time constant from being observed. More importantly, if Westerman's method had been employed in the present study, very different values would have been obtained. In many of the recovery traces, the analysis window which had the greatest amplitude was not the same as the maximum window in the unmasked case. This was

evident in the whole tone data (Figs. R19 and R20). A real reduction in the onset recovery response at the precise time of the original onset response would have been missed by choosing the largest bin in the first 10 ms after stimulus arrival rather than the invariant time used in this study.

In much of the recovery data, the onset amplitude at  $\Delta t = 0$  with equal masker and probe levels shows evidence of recovery. In many cases examination of the whole tone response shows an onset followed by reduction to a steady state level. This recovery observed with a "zero" silent interval is caused by the fact that the silent intervals presented in this study were measured from masker offset to probe onset. However, to reduce spectral effects from abrupt onset, 5 ms linear rise/fall ramps were used on all maskers and probes. Therefore, the silent interval ( $\Delta t$ ), when defined as 0 ms, in fact has a 5 ms offset ramp on the masker followed with no delay by a 5 ms onset ramp on the probe. During the 10 millisecond off/on ramp between masker and probe, some degree of recovery from the masker is occurring, as illustrated by the onset response observed when zero delay is used with a masker and probe of equal amplitude. If no recovery had occurred the probe response should display no onset and no subsequent reduction over time.

These results demonstrate that measuring CAP adaptation with the modified forward masking method used by Westerman (1985) and Abbas and Gorga (1981) has the potential to add an error to the amplitude measurements. One ms rise/fall ramps followed by 5 and 10 ms silent intervals, which were thought to allow no recovery of the response, were used to measure adaptation with CAPs. The amplitude of the probe after the silent interval was measured as a function of masker length to describe the decrement in CAP amplitude with time. However, the present results

demonstrate that in the 5 or 10 msec delay between masker offset and probe onset, measurable recovery of the probe response amplitude can occur. Comparable recovery from adaptation during these small silent intervals has been observed by other investigators (Harris and Dallos, 1979)

### **Whole Tone Recovery:**

In contrast to the previous recovery experiments, which determine the rate of recovery to the maximum onset amplitude, the final part of this study was concerned with recovery of the entire 290 msec response following a 100 msec masker, referred to as the whole-tone response. This response is a combination of onset recovery and peristimulatory adaptation. The assumptions presented above, and displayed in Figs D1, D2, and D3 regarding the general form of whole tone recovery are consistent with the results of this study. Both the ANN and single unit results display a suppressed onset which returns to the steady state level. If the masker is sufficiently loud the response begins below the steady state level and follows an exponential recovery function up to a steady state amplitude. If the onset is above the steady state level the response follows an adaptation function down to the steady state level.

Another feature of the whole tone recovery responses is the presence of an initial suppression of the onset response. The first point in the data is below the second point. This is not an artifact or a spurious response. It is detected due to the procedure of analysis which determine the onset time in the unmasked trace and then applies this onset time to all succeeding traces which are forward masked. In 46 out of 64 cases (72%) at least one PSTH in each series of single unit responses recorded with 0, 12.5, 50 and 400 ms

silent intervals had this reduction in one or more of the initial points. In the normalized mean data presented in Fig. R19 at  $\Delta t = 6, 12.5, 25$  and  $50$  ms the same characteristic can be clearly seen. This phenomenon was also present in the ANN responses as demonstrated in Fig. R27 at  $\Delta t = 12.5$  ms. Previous methods of analysis would preclude this suppression of the onset from being detected.

As mentioned in the results section, the rapid component of the whole tone response in the cases which followed an adaptation function did not vary as the silent interval decreased. However, the short term component increased as the silent interval decreased. This was true until the trace became nearly flat, at which time the rapid component could no longer be estimated and was excluded from the analysis (Fig. R19  $\Delta t = 6$  ms). It was the rate of the rapid dynamic process which remained constant in these cases, not the actual amplitude of the onset response. The onset amplitude decreased as the silent interval decreased, as described in the section covering onset recovery.

### **Comparison of ANN to Single Fiber Responses:**

Comparing the single fiber and ANN data collected using nearly identical procedures and the same species produced very similar results. The presence of two-time-constants was observed in both cases, although there were also onset recovery cases with one time constant in the single unit data. One other anomalous situation is the variation of the ANN TauAs with probe level which is not observed in the single unit TauAs results.

The cycle by cycle characteristics of the responses are also quite similar. In both Fig R1 and Fig R21 the expanded view of the responses display a rapid rise of the response which coincides with the onset ramp of



the stimulus. Although identical analysis methods were applied to both forms of data, the length of time used to determine the short term component of the ANN was systematically shorter than for the single unit data. This means the inflection point between the two straight line segments occurred later in the ANN than in the single units. Even though the ANN rapid component extended further along the response its time constant was slightly shorter than the single units.

The mean  $\text{TauRr}$  was  $16.2 \pm 9.8$  ms for the ANN and  $22.0 \pm 9.6$  ms for the single units, and the mean  $\text{TauRs}$  was  $124.6 \pm 50.1$  for the ANN and  $184.1 \pm 144.8$  for the single units. The greatest difference between the onset recovery results is the presence of a large group of single unit responses which are best described with a single time constant. Attempts were made to separate these two response groups by finding a characteristic of the units which would classify them into two different populations. In one experiment 23 units were isolated and complete response characteristics recorded. The two response groups clustered into those with a CF near the 800 Hz stimulus and those with a CF more distant from the stimulus frequency. Those fibers with a CF near 800 Hz had two-time-constants of recovery while units further away had only one time constant. Perhaps the rapid component of onset recovery is related to the sharpening of tuning of unit response near CF.

In addition to obtaining close values for the ANN and single unit  $\text{TauRr}$  and  $\text{TauRs}$ , the ratio of recovery to adaptation was 3.4 ms for the ANN rapid Tau and 4.0 for the single unit rapid Tau, and 1.5 for the ANN short term Tau and 2.0 for the single unit short term Tau. Note that the mean value used for the ANN short term Tau was 83 ms although the  $\text{TauAr}$  varied systematically with stimulus level.

The ANN is the only compound neural response which can be recorded and analyzed using the same methods as in single unit studies. The extreme difficulty in holding single units long enough to record an entire adaptation, onset recovery and whole tone recovery series with a sufficient number of stimuli to get relatively smooth responses makes the ANN an ideal alternative method of collecting data. Of course this is valid only if the ANN produces results comparable to single unit responses. Comparing Fig R19 and Fig R26 demonstrates the accuracy with which the ANN reflects the single unit responses for the whole tone responses. These cases were recorded with identical stimuli. The pattern of the response are similar even to the point of having a single onset point in both  $\Delta t = 12.5$  ms traces suppressed below the maximum onset value. The rapid component does not systematically vary while the short term component increase as  $\Delta t$  decreases in both data.

The difficulty in analyzing single unit whole tone responses is evident in Fig R20 a-d. Many of the traces could not be fit with a two-time-constant equation because the variance in amplitude resulted in negative values within the rapid component of the response. This prevented the rapid component from being estimated by requiring the log of a negative number to be calculated, which is not possible. If a one time constant equation was substituted, the fit was very poor; the model points missed overlapping any of the initial data points. This problem was not as common in the ANN data. As seen in Fig R28 the data points are sufficiently smooth in most cases to fit the data to the two-time-constant equation.

The ANN provides a direct view into the firing characteristics of the entire auditory nerve for each stimulus presented. By selectively including only the neurons which are phase locked to the stimulus and are in

phase with each other, the ANN offers a direct method for measuring the threshold, dynamic range, and time constants of adaptation and recovery of the ensemble firing of auditory fibers. Our interest in determining the time constants of adaptation and recovery using the ANN was twofold: (1) unlike other compound action potential responses, the ANN can be recorded with low frequency, long duration tones identical to those used in single unit studies, and (2) the ANN can be more easily, quickly, and systematically recorded than single unit responses. Our results are consistent with the results obtained using single unit and compound action potential responses in other mammals. The ability to estimate correctly basic physiological properties of the auditory nerve with the ANN combined with the possibility to record intraoperatively the ANN from the human auditory nerve (Møller and Jho, 1988) offers the opportunity to directly obtain some basic physiological characteristics relevant for the understanding of the processing of auditory information in humans.

### **Where and How?**

The site or sites at which adaptation and recovery from adaptation occur and the mechanisms underlying these phenomenon cannot be specified at this time. However, various responses to appropriate stimuli can be examined to deduce possible sites and mechanisms of transduction and eliminate others which are less likely. The general sequence of sound processing by the auditory system begins with the deflection of the tympanic membrane which sets the ossicles of the middle ear into motion. The relative size of the tympanic membrane and oval window combines with the leverage afforded by the ossicular chain to impedance match the air borne vibrations

to the fluid filled inner ear. The pressure wave transmitted into the scala vestibuli causes the basilar membrane to move up and down, pivoting along the spiral lamina. This produces a shearing of the outer hair cell stereocilia which have their tips embedded in the tectorial membrane (Lim, 1972). The inner hair cell's stereocilia do not have their tips in contact with the tectorial membrane and apparently move as a result of viscous drag in the endolymph. Bending of the inner hair cell stereocilia opens mechanically activated channels near the tip of the stereocilia (Hudspeth, 1982) which depolarize the hair cell opening voltage sensitive  $Ca^{++}$  channels (Lewis and Hudspeth, 1983). The  $Ca^{++}$  activates the release of transmitter into the synaptic cleft (Katz and Miledi 1965; Zucker, 1987; Augustine et al. 1987). Transmitter flows across the cleft, binds to the receptors in the postsynaptic membrane and opens channels which allow entry of positive ions (Stevens, 1968). The cochlear nerve is depolarized and action potentials are initiated which pass along the fiber to the cochlear nucleus.

Which of these steps can be implicated as the source of adaptation and recovery from adaptation and which can be eliminated? The deflection of the outer hair cell stereocilia is the accepted source of the cochlear microphonic (CM) response. The CM displays no adaptation, cannot be forward masked and has a nearly linear stimulus/response input-output function (Synder and Schreiner, 1985). However the outer hair cells do not appear to be instrumental in activating cochlear nerve fibers (Robertson et al. 1984). Intracellular recording from mammalian inner hair cells also do not display adaptation (Russell and Sellick, 1978). Therefore, receptor cell activation plays no role in adaptation and recovery from adaptation.

The first site of recorded adaptation is in the auditory nerve fibers. This focuses the search to the presynaptic release of neurotransmitter

from the hair cell, the postsynaptic activation of the spiral ganglion dendrites, the transmission along the axon, or a combination of these three sites.

The rate of transmission of action potentials along an axon is limited by two factors, the absolute refractory period and the relative refractory period. The absolute refractory period is the 0.3 to 1.0 ms interval following an action potential during which firing cannot occur. The relative refractory period can extend for many milliseconds during which the probability of firing is reduced (Gaumond et al., 1983). This parameter is relevant in some models which describe a rapid adaptation component (Eggermont, 1984; Smith and Brachman, 1982). Perhaps the summed effects of the relative refractory period could be used to explain adaptation.

Axonal transmission along the auditory nerve can be separated from postsynaptic transduction by electrically stimulating the nerve. In single fiber studies of electrical stimulation in the scala tympani using an implanted electrode array, responses to submaximal stimuli produced responses very much like those elicited with acoustic stimuli (Javel et al. 1987). As seen in Fig. D4A PST histograms using submaximal stimuli display a large onset which decreases to a steady state level. The interval histogram demonstrates the source of this adaptation pattern. At submaximal stimulus levels the fiber does not respond to every cycle of the stimulus. As the stimulus intensity is increased the interval histogram consolidates towards responses occurring at an interval equal to the stimulus interval. In this case no adaptation is observed.

**A**

Fig 3. Poststimulus time (PST) and interspike interval (ISI) histograms obtained at various intensities in response to 200- $\mu$ s/phase pulse trains presented at 200 pulses/s for 100 ms. Intensities are in decibels re 1  $\mu$ A.

(From Javel et al., 1987)

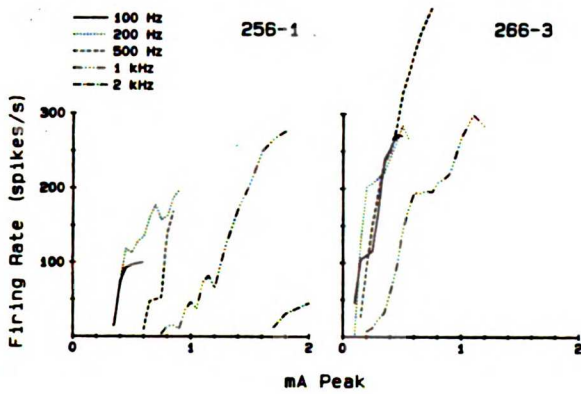
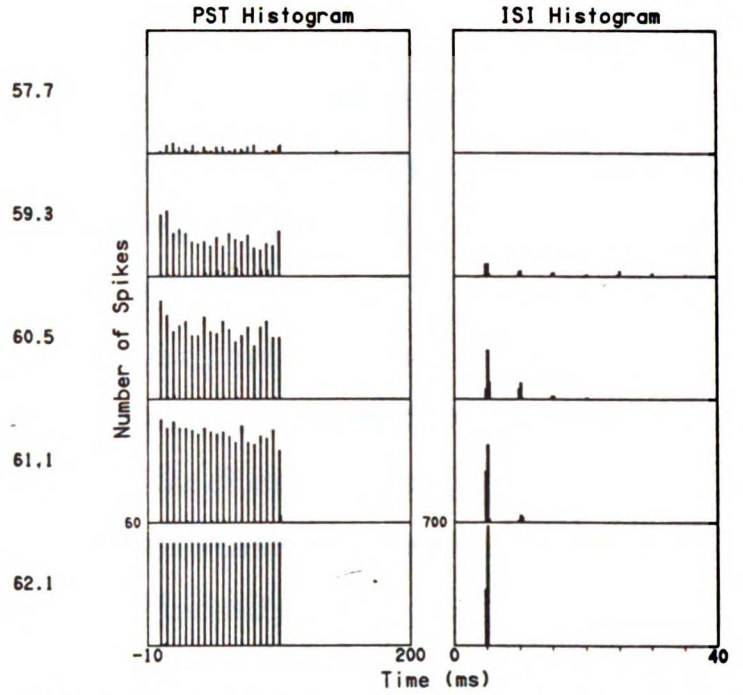


Fig. 2. Firing rate vs. stimulus intensity and time for sinusoidal stimuli. Upper panels show steep rate increase with stimulus intensity at several frequencies. Lower panel shows adaptation with high frequency high intensity stimulation. Electrodes as in Fig. 1.

**B**

(From van den Honert and Stypulkowski, 1987)

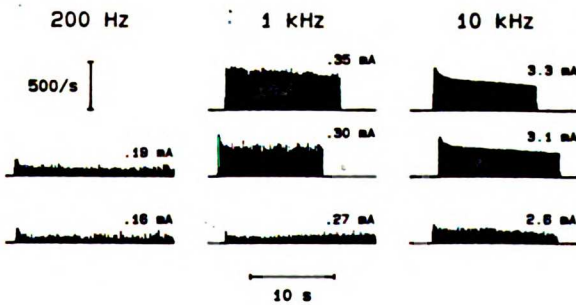


Fig. D4. Electrically stimulated auditory nerve fiber responses.

Van den Honert and Stypulkowski (1987) report similar results for sinusoidal electrical stimuli. Adaptation is clearly observed at frequencies from 200 Hz to 10 kHz. At frequencies above 1 kHz adaptation is seen even with high intensity stimuli (Fig. D4B).

The electrically evoked responses recorded by Javel et al. (1987) were recorded several days after implantation and no acoustic responses or spontaneous activity were present in any of the fibers indicating destruction of the hair cells. This would preclude any transmitter release from the hair cells caused by the electrical stimulus. Additionally, Hartman et al. (1984) compared the activity patterns of fibers in intact and destroyed cochleas and concluded that aside from a lack of spontaneous activity and slightly lower thresholds shown by fibers in the destroyed cochleas, no substantial differences existed between the two preparations. These findings suggest that auditory nerve adaptation has a component contributed by the transmission along the auditory nerve fibers and is therefore not restricted solely to the hair cell / auditory nerve synapse.

Presynaptic transmitter release may also contribute to adaptation. By recording excitatory postsynaptic potentials (e.p.s.p.s) in goldfish saccular fibers in which spike potentials were suppressed with locally applied tetrodotoxin, Furukawa and Matsuura (1978a) developed a model of adaptation restricted to presynaptic depletion of neurotransmitter. A rapid decline in the amplitude of e.p.s.p.s to successive cycles of a tone suggested depletion of transmitter quanta from the release sites as the source of the decline. The rate of decline followed approximately a fixed ratio, was independent of stimulus amplitude and after nearly complete elimination of e.p.s.p.s during a long stimulus, a large, seemingly new response could be elicited when the intensity of the sound was increased.

The general model which used e.p.s.p. amplitude to describe transmitter release states that the mean quantal release ( $m$ ), as defined by the e.p.s.p. amplitude, is equal to the number of available release sites ( $n$ ) times the probability of release ( $p$ ). By applying bimodal statistics the decline in the size of  $m$  was assigned to a decrease in the number of available release sites (vesicles) rather than the probability of release for each site (Furukawa and Matsuura (1978b). This supported the depletion hypothesis of adaptive decline in e.p.s.p. amplitude.

When intracellular responses were recorded in the absence of tetrodotoxin, both action potentials and e.p.s.p.s could be seen in the traces (Furukawa and Ishi, 1967). A wide variation in the rate and degree of adaptation was observed among fibers. Once a fiber ceased firing during a stimulus presentation no further responses occurred. The firing pattern would either follow the stimulus cycle by cycle (or at two times the stimulus frequency) or not fire at all. This is vastly different from the response pattern observed in mammalian auditory fibers. The adaptation of unit firing in response to a steady stimulus is measured by repeatedly presenting the stimulus and summing the responses from each trace. While the fiber may always respond to the first cycle of the stimulus, successive cycles will not necessarily cause firing. Interval histograms demonstrate that no response may be elicited to many successive cycles of a stimulus and then a well phase locked response can occur. Only by summing a group of traces can a reasonably smooth adaptation function be observed. The responses from goldfish saccular S1 fibers do not behave this way. The steady, monotonic, nearly complete decline in the e.p.s.p. amplitude observed in the goldfish is not present in mammalian cochleas. In addition, maximal sustained firing rates of 600 to 1000 Hz. (Furukawa and Ishi, 1967) far



exceed any recorded in cat auditory fibers (Moxon, 1968). The saccular fibers also often respond to both rarefaction and condensation phases of the stimulus. Therefore, although the study of goldfish saccular fiber responses describes a possible process and mechanism for the observed decline in e.p.s.p. amplitude, the lack of correspondence between the firing characteristics of these fibers and those observed in mammalian auditory fibers makes application of the goldfish results to the mammal tentative at best. It seems likely that the presynaptic mechanisms presented by Furukawa and Matsuura (1978 a,b) are not the only sources of adaptation observed in mammalian auditory fibers.

Advances in molecular biology have lead to a fairly detailed understanding of postsynaptic receptor morphology and function (Changeux, et al , 1984). Patch clamp techniques have been used to examine the kinetics of single receptor channels (Kerry et al, 1987). These advances have given insights into the mechanisms which may underlie postsynaptic depolarization and action potential propagation.

The general sequence of events which is believed to occur for the acetylcholine receptor is as follows (Changeux, et al. 1984). Postsynaptic receptors are initially all free, i.e. they do not have transmitter bound to them. In this state they are closed and there is no ionic flow through them. Transmitter released from presynaptic sites crosses the synaptic cleft and binds with the receptors. The channels undergo a conformational change which allows the flow of particular ions into the cell. This depolarizes the cell and produces spike initiation if threshold is reached. These channels are then inactivated or desensitized (closed) but are unavailable for reopening. When the desensitized channels become available again they can open and allow ions to flow once more into the cell. It appears that each channel may

have several open and closed states. The duration of each of the states have different time constants and the transition from one state to another may proceed along several paths. The different states may be caused by the need for more than one transmitter molecule to bind with the receptor to produce the complete open state or the need for other substrates to be present which interact with the transmitter. Similar processes appear to function in the glutamate receptor, which may have as many as three open states of the receptor channel and four closed states (Kerry et al. 1987). There appear to be at least three pathways linking the open states with the closed.

### **Previous Models:**

Brachman (1980) and Smith and Brachman (1982) have developed a model of auditory transduction which assigns all relevant sites of adaptation to the presynaptic side of the hair cell/auditory nerve interface (Fig. D5). The signal which is input to the model (stage 1) is adjusted with a nonlinear input-output function (stage 2) similar to the onset rate intensity function in their data (Fig.s 27 and 28 of Brachman, 1980). The output of stage 2 is low-pass filtered before entering stage 3. Stage 3 is the main part of the model which contains the major sites and mechanisms of adaptation. In this stage the available neurotransmitter is divided into three compartments or stores; a global, local, and immediate store. Adaptation is produced by depleting neurotransmitter from these stores. The global store has a large reservoir of transmitter which can only be depleted with stimuli presented for minutes or longer. This store underlies the steady state firing level. The local store is composed of those vesicles which replace the spent vesicles along the hair cell membrane. The local store is more rapidly depleted than

the global store; at a rate commensurate with the short term time constant. Those vesicles whose contents are available for direct release into the synapse comprise the immediate store, and are modeled by 512 independent sites. Depletion of this supply follows the rapid time constant of adaptation. The transfer rate between these stores is controlled by simple diffusion constants. An important assumption of this model is that the response to an incremental signal causes the release of transmitter from a new pool of previously unavailable transmitter from the immediate store which is depleted at the same rate as the initial onset, i.e. it adapts along the same rapid time course.

The model succeeds in predicting the onset and long window (20 ms) rate intensity functions, the response to increments and decrements measured at onset and at a 30 ms delay, the response to AM stimuli, and period histograms for low-frequency tones. It is not clear from the presentation whether the actual time course of recovery is fit by the model or just the salient characteristics of recovery. No attempt is made to model the response to a long tone following a masker as the silent interval is increased (using Smith's terminology: an incremental or decremental response with a silent interval separating the pedestal tone from the increment or decrement).

An interesting feature of Smith's data is the lack of effect of adaptation on the onset response. Using the terminology developed for the present study, if a masker precedes a probe with a zero ms silent interval and the masker is quieter than the probe, the onset response to the probe will increase the firing rate as if no adaptation had occurred. In other words, if a 20 dB tone produced an onset firing rate of 100 spikes per second and a 26 dB tone produced an onset firing rate of 150 spikes per second the incremental response is 50 spikes per second. If the same 26 dB tone was presented as a probe immediately following a 20 dB masker, that is, after adaptation had

occured, the incremental response would also be 50 spikes per second. In Fig. 1 of Smith and Brachman (1982) the increment in spikes per second vs pedestal (masker) intensity is simply the first derivative of the static non-linear rate-intensity function for the onset response.

If the condition is changed to examine the effect of a 6 dB decrement in the probe during the adapted state, the response is no longer a simple additive feature. The decrement in spikes per second is less during the adapted state than without adaptation. Therefore the system is not linear across the entire range of relative masker/probe levels.

Eggermont (1985) employs some of the characteristics of the previous model, but includes mechanisms occurring postsynaptically as well (Fig. D6). These postsynaptic sites are proposed as the major sites of adaptation and recovery from adaptation. As in the previous model the steady state is achieved with a global store of transmitter termed a general store. In Eggermont's model, transmitter released into the synapse binds with receptors in the postsynaptic membrane causing channels to open which depolarizes the neuron. After a very brief time the channel closes but the

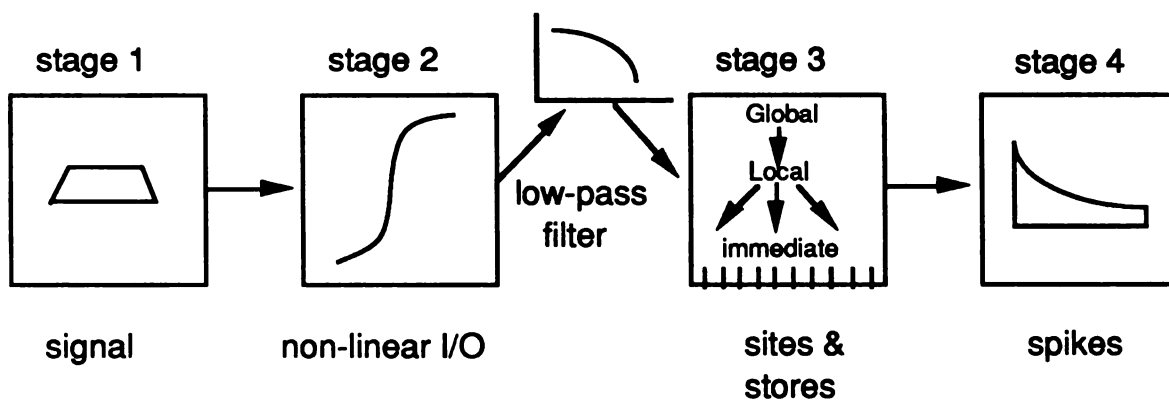


Fig. D5 Schematic of Brachman model (1980) and Smith and Brachman (1982). See text for explanation.

transmitter remains in the receptor site for some time. During this time the channel is inactive (closed) and unavailable (cannot be opened). Eventually the transmitter breaks free of the receptor leaving it available for reactivation and channel opening. The major components of the model are: 1) transmitter release into the synaptic cleft is from an ordered array of vesicles and depends in a non-linear way on stimulus level, 2) rapid adaptation is produced by relative refractory effects, 3) a slower inactivation of the receptor ( $\phi$ ) and a reactivation of the receptor ( $\partial$ ) is the basis of the short term adaptation time constant;  $(\partial+\phi)^{-1}$  and the onset recovery time constant;  $(\phi)^{-1}$ .

In an attempt to explain the interaction process which produced the whole-tone response, Eggermont proposed a simple linear interaction was assumed and subtraction of the equation for onset recovery from adaptation was used. Rewriting his equation to match the form used in this study (but using only one time constant for each section) gives the following equation:

$$A(\Delta t, t_p) = (Y * (\exp(-t_p / \text{TauA})) + A_{SS}) - (a * (Y * (\exp((- \Delta t + t_p) / \text{TauR})))) \quad (3)$$

where all variables are as previously described and 'a' is the magnitude of the masker response relative to the probe

The assumption that the adaptation function is a constant that is linearly combined with to the onset recovery function to describe the whole-tone recovery function is the basis of the Eggermont model. A useful way to think of the underlying processes is to consider the "magnitude of adaptation" at increments of time during the probe ( $t_p$ ). After the offset of a masker the auditory fibers which were firing enter into a period of recovery,

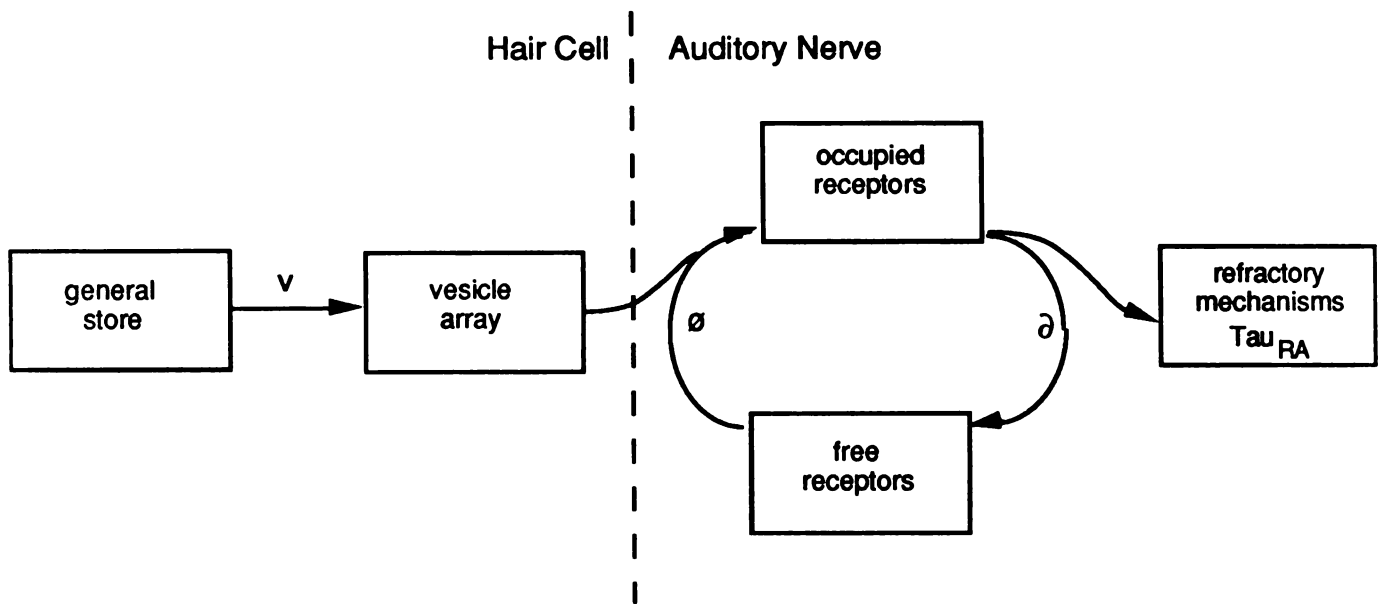


Fig. D6. Schematic of Eggermont model. See text for explanation.

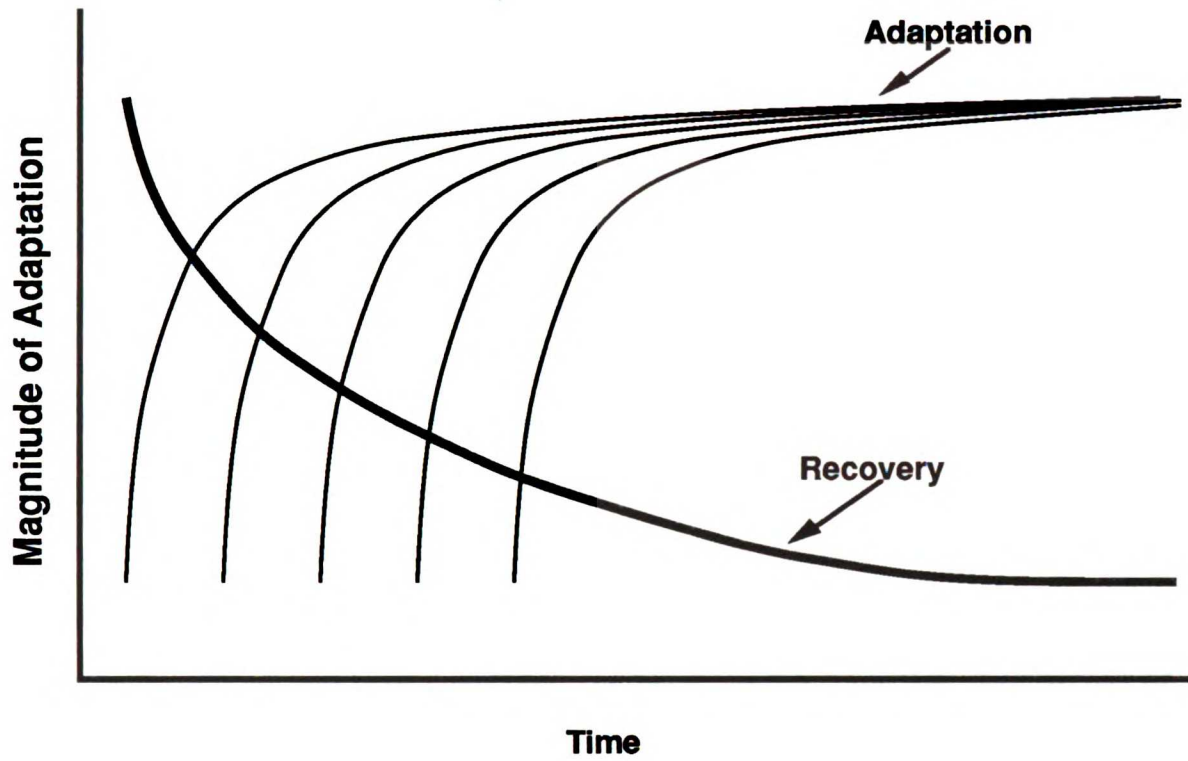


Fig. D7. Schematic of magnitude of adaptation. See text for explanation.



i.e. the magnitude of adaptation is initially at a maximum and exponentially decays to a minimum (Fig. D7). The recovery is "attached" to the time of masker offset, i.e. it begins as soon as the masker ends and is dependent on the amplitude, duration and frequency of the masker. Adaptation is "attached" to the probe and begins with the onset of the stimulus, i.e. the magnitude of adaptation is initially at a minimum and exponentially increases to a maximum. When a probe is preceded by a masker the adaptation function shifts along the time axis as the  $\Delta t$  is increased. Because the time constant of recovery is longer than the time constant of adaptation, linearly combining the two functions will produce the nonmonotonic function displayed in Fig. D8. As presented below, the resulting behavior is not an actual description of the response for either ANN or single units

The equation used by Eggermont employs only one time constant for adaptation and one for recovery, and was tested using the data of Smith and Brachman (1982) and Harris and Dallos (1979) for calculating the fit of the data to the model. The Harris and Dallos (1979) study supplied the onset recovery time constants and the Smith and Brachman (1982) study supplied the adaptation time constants and whole-tone recovery plots. The Smith and Brachman forward masking experiments were limited to 40 msec probe tones presented after a 20 msec silent interval. With these conditions the model appears to fit the data quite well. If however, the same equation used by Eggermont is applied to a long duration probe tone preceded by a masker of equal amplitude with zero silent interval, the model produces a trace which begins with an onset response above steady state, falls abruptly below the steady state and finally recovers up to the steady state amplitude (Fig. D8). If a linear combination of the onset recovery and adaptation is used, the result will always be a nonmonotonic response falling rapidly below the

**E model 20;20 TauA=15 TauR=40 (Chinchilla)**

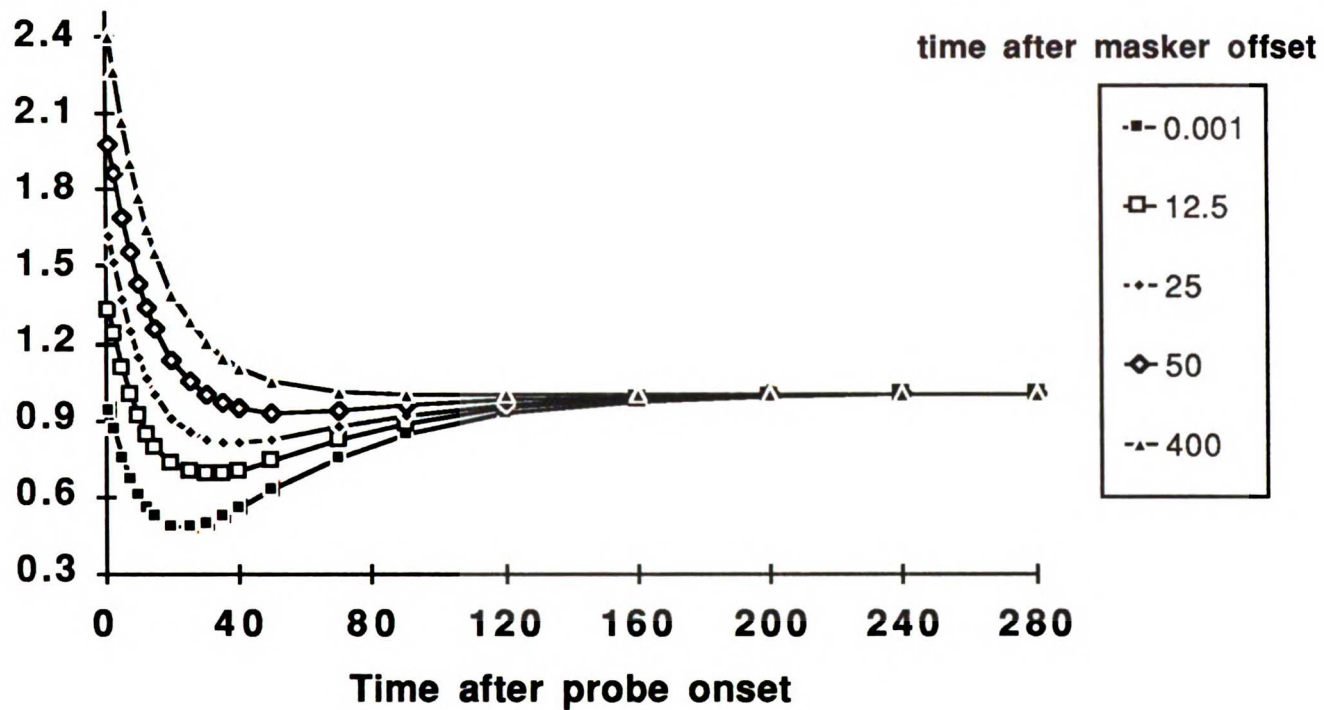
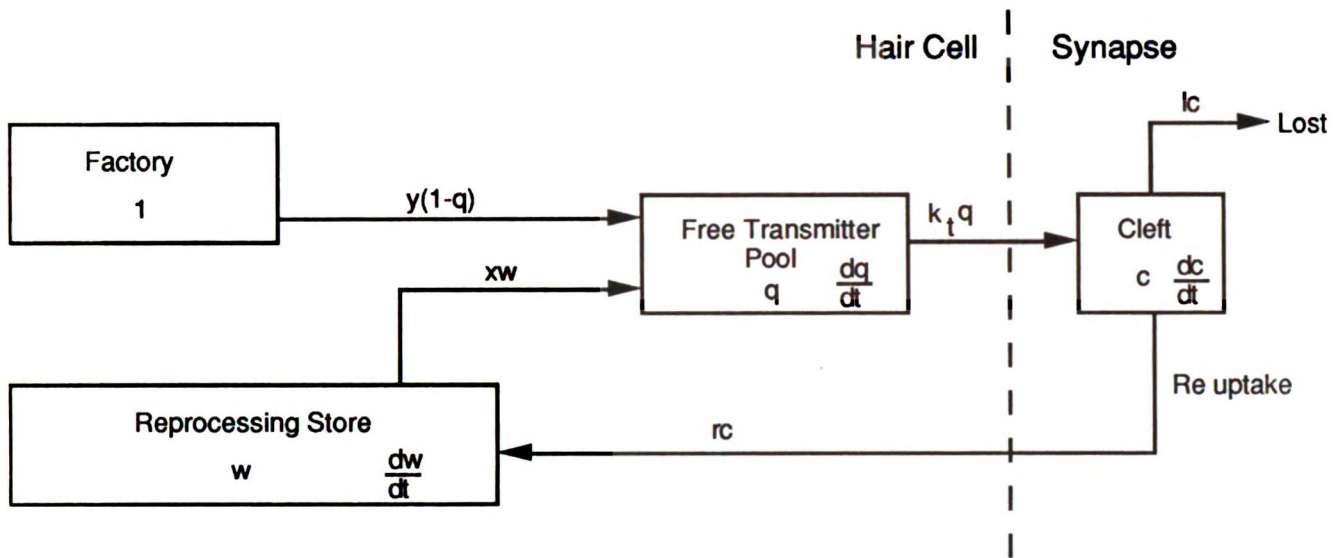


Fig. D8. Results of Eggermont model for whole tone recovery.

steady state and then recovering up to the steady state because the onset recovery time constant is always at least 1.5 times larger than the adaptation time constant. As presented in Fig. D2 the response should progress from a flat line at  $\Delta t = 0$  to an adaptation function with increasing onset values as  $\Delta t$  increases, until the onset amplitude equals the amplitude in the unmasked condition. This is exactly the form of change observed in the neural responses (Fig R28b). Similarly, the schematic results of Fig. D3, in which the masker is louder than the probe are clearly observed in the data presented in Figs R19 and R26. Results such as those described in Fig. D8 are never seen in single unit or compound action potential responses and are inconsistent with the theoretical account presented above. Eggermont's model does not improve by using the two-time-constant description of adaptation and recovery. Rather, the assumption of additivity of the two processes appears to be wrong.

A more recent attempt to model the dynamic processes of auditory transduction by Meddis (1986,1988) restricts adaptation to presynaptic and synaptic sites, avoiding the role of postsynaptic mechanisms. In his model a free transmitter pool releases neurotransmitter as a function of stimulus intensity into the synaptic cleft. After the transmitter has been released from the postsynaptic receptors it is either taken up by the hair cell or lost from the cleft by diffusion. The transmitter taken up by the hair cell is reprocessed and returned to the free transmitter pool. The free transmitter pool is also supplied from a factory which prevents complete depletion due to the lost transmitter. The schematic (Fig D9) is used to generate a series of differential equations which describe the kinetics in each box. Values for the rates of diffusion, uptake, reprocessing, release, etc. are chosen by the investigator and a simulation is run on a computer.



$$\frac{dq}{dt} = y(1-q(t)) + xw(t) - k(t)q(t)$$

$$\frac{dc}{dt} = k(t)q(t) - lc(t) - rc(t)$$

$$\frac{dw}{dt} = rc(t) - xw(t)$$

Fig. D9. Schematic of Meddis model. (1986) See text for explanation

The model succeeds in describing rate intensity functions, interval and period histograms, incremental responses, two-time-constant adaptation, recovery of spontaneous activity and frequency-limited phase locking. The model fails to accurately describe onset and whole tone recovery.

Each of the three models presented above approaches the problem of describing the observed dynamics of auditory transduction as reflected in the firing pattern of the auditory nerve in a different way. Smith and Brachman impart static non-linearities and low pass filters to the early stages of their model as necessary adjustments to account for the responses to the wide range of stimuli used to collect data. The later stages of their model present possible sites and mechanisms underlying the dynamics of adaptation and recovery observed within each response. These are described by a set of differential equations: one for the rapid and short term adaptation and another for the steady state. Eggermont develops a detailed description of synaptic transduction which eventually is described by a relatively simple set of exponential equations. Meddis applies classical multi-compartment dynamic process models (often used in drug uptake and clearance studies) to propose a physiological sequence of events which can be described by a series of differential equations. By choosing diffusion constants and other values of appropriate magnitude and solving the differential equations, some of the characteristics of auditory nerve responses are well described while others cannot be fit by the model.

### **Features of a model of synaptic transduction:**

The invariance of the rapid component of the whole tone recovery responses, up until the abrupt disappearance of that component, implicate relative refractory effects as a possible source. Relative refractory period effects only become significant at high response frequencies, such as the onset of a response (Eggermont, 1985). The degree of recovery from the masker will change the magnitude of the onset response of the probe, but will not add to the refractory period effects which are fixed to the time of stimulus onset. Therefore, the rapid component of whole tone recovery and adaptation may result from relative refractory period effects.

Short term adaptation may be related to the rundown in available transmitter in the presynaptic stores or to postsynaptic receptor channel dynamics. There is currently no way to determine from the available data which of these choices is correct. Several models, which were presented above, have tried to apply these sites in various combinations. These models have met with varying success and failure in describing the observed sequence of events presented in this and previous studies of adaptation and recovery from adaptation. Until more is known about the transmitter released from the mammalian hair cells and the details of postsynaptic depolarization by this neurotransmitter, one can only speculate which is the "true" sequence of events.

There is general agreement that the steady state firing rate depends on some large store of neurotransmitter. This store may be dependent upon the hair cells ability to manufacture transmitter at a rate sufficient to replace that which is released into the synaptic cleft or may reuse released transmitter by endocytotic uptake and reprocessing.

In summary, each of the models presented above fails to account for all of the observed features of adaptation and recovery from adaptation. Any model of synaptic transduction and action potential transmission in the auditory periphery must include pre- and post-synaptic mechanisms and axonal transmission characteristics. This will require a better understanding of the kinetics of presynaptic transmitter release, postsynaptic channels, and axonal refractory effects.

## **BIBLIOGRAPHY:**

- Abbas, P.J., and Gorga, M.P. (1981) "AP responses in forward-masking paradigms and their relationship to responses of auditory-nerve fibers." *J. Acoust. Soc. Am.* 69, 492-499.
- Augustine, G.J., Charlton, M.P., Smith, S.J. (1987) "Calcium action in synaptic transmitter release." *Ann. Rev. Neurosci.* 10,633-693.
- Brachman, M.L. (1980) "Dynamic response characteristics of single auditory-nerve fibers." Ph.D. Dissertation, Institute for Sensory Research, Syracuse University, Syracuse, New York.
- Changeux, J-P., Devillers-Thiery, A. (1984) "Acetylcholine receptor: An allosteric protein." *Science* 225,1335-1345.
- Chimento, T.C., and Schreiner, C.E. (1989) "Selectively eliminating cochlear microphonic contamination from the frequency following response." in press: *EEG and clin. Neurophysiol.*
- Delgutte, B. (1982) "Some correlates of phonetic distinctions at the level of the auditory nerve." in *The representation of speech in the peripheral auditory system.* edited by R Carlson and B. Granstrøm. (Elsevier Biomedical Press, Amsterdam) pp. 131-149.
- Delgutte, B. (1984) "Speech coding in the auditory nerve: II. Processing schemes for vowel-like sounds." *J. Acoust. Soc. Am.* 75,879-886.
- Delgutte, B., and Kiang, N.Y.S. (1984a) "Speech coding in the auditory nerve: I. Vowel-like sounds." *J. Acoust. Soc. Am.* 75,866-878.
- Delgutte, B., and Kiang, N.Y.S. (1984b) "Speech coding in the auditory nerve: III. Voiceless fricative consonants." *J. Acoust. Soc. Am.* 75,866-878.



- Delgutte, B., and Kiang, N.Y.S. (1984c) "Speech coding in the auditory nerve: IV. Sounds with consonant-like dynamic characteristics." *J. Acoust. Soc. Am.* 75,897-907.
- Delgutte, B., and Kiang, N.Y.S. (1984d) "Speech coding in the auditory nerve: V. Vowels in background noise." *J. Acoust. Soc. Am.* 75,908-918.
- Eggermont, J.J. (1985) "Peripheral auditory adaptation and fatigue: A model oriented review." *Hearing Res.* 18,57-71.
- Eggermont, J.J., and Spoor, A. (1973a) "Cochlear adaptation in Guinea pig." *Audiology* 12,193-220.
- Eggermont, J.J., and Spoor, A. (1973b) "Masking of action potentials in the Guinea pig cochlea, its relation to adaptation." *Audiology* 12,221-241.
- Furukawa, T, Hayashida, Y., Matsuura, S. (1978) "Quantal analysis of the size of excitatory post-synaptic potentials at synapses between hair cells and afferent nerve fibres in goldfish." *J. Physiol (London)* 276,211-226.
- Furukawa, T, Ishi Y. (1967) "Neurophysiological studies on hearing in goldfish." *J. Neurophys.* 30(6),1377-1403.
- Furukawa, T., Matsuura, S. (1978) "Adaptive rundown of excitatory post-synaptic potentials at synapses between hair cells and eight nerve fibres in the goldfish." *J. Physiol (London)* 276,193-209.
- Gardi, J.N., Merzenich, M.M., McKean, C. (1979) "Origins of the scalp-recorded frequency-following responses in the cat." *Audiology.* 18,353-381.
- Gaumond, R.P., Kim. D.O., Molnar, C.E. (1983) "Response of cochlear nerve fibers to brief acoustic stimuli: Role of discharge-history effects." *J. Acoust. Soc. Am.* 74,1392-1398.

- Harris, D.M., and Dallos, P. (1979) "Forward masking of auditory nerve fiber responses." *J. Neurophys.* 42,1083-1107.
- Hartman, R., Topp, G., Klinke, R. (1984) "Discharge patterns of cat primary auditory fibers with electrical stimulation of the cochlea. *Hearing Res.* 13,47-62.
- Huang, C. (1981) "Time constants of acoustic adaptation." *EEG and clin. Neurophysiol.* 52,394-399.
- Hudspeth, A.J. (1982) "Extracellular current flow and the site of transduction by vertebrate hair cells." *J. Neuroscience.* 2,1-10.
- Javel, E., Tong, Y.C., Shepherd, R.K., Clark, G.M. (1987) "Responses of cat auditory nerve fibers to biphasic current pulses." *Ann. Otol. Rhinol. Laryngol.* 96(suppl. 128),26-30.
- Katz, B., Miledi, R. (1965) "The effect of calcium on acetylcholine release from motor nerve terminals." *Proc. R. Soc. Lond. B. Biol. Sci.* 161,496-503.
- Kerry, C.J., Karel, S.K., Ramsey, R.L., Sansom, M.S.P., Usherwood, P.N.R. (1987) "Single channel kinetics of a glutamate receptor." *Biophys. J.* 51,137-144.
- Kiang, N.Y.S., Watanabe, T., Thomas, E.C., Clark, L.F. (1965) *Discharge patterns of single fibers in the cat auditory nerve Research Monograph No. 35* (The M.I.T. Press, Cambridge, Mass.)
- Kim, D.O., and Molnar, C.E. (1979) "A population study of cochlear nerve fibers: Comparison of spatial distributions of average-rate and phase-locking measures of responses to single tones." *J. Neurophys.* 42,16-30.

- Lewis, R.S., Hudspeth, A.J. (1983) "Voltage- and ion-dependent conductances in solitary vertebrate hair cells." *Nature* 304,538-541.
- Lim, D.J. (1972) "Fine morphology of the tectorial membrane." *Acta Otolaryngol*, 96,199-215.
- Meddis, R. (1986) "Simulation of mechanical to neural transduction in the auditory receptor." *J. Acoust. Soc. Am.* 79(3),702-711.
- Meddis, R. (1988) "Simulation of auditory-neural transduction: Further studies." *J. Acoust. Soc. Am.* 83(3),1056-1063.
- Miller, M.I., and Sachs, M.B. (1983) "Representation of stop consonants in the discharge patterns of auditory-nerve fibers." *J. Acoust. Soc. Am.* 74,502-517.
- Møller, A. and Jho, H.D. (1988) "Responses from the the exposed human auditory nerve to low-frequency tones: Basic characteristics " *Hear. Res.* 38,163-176.
- Moxon, E.C. (1968) "Auditory nerve responses to electrical stimuli." *M.I.T.,E.R.L. Q.P.R.* 90,270-275.
- Robertson, D. (1984) "Horseradish peroxidase injection of physiologically characterized afferent and efferent neurones in the guinea pig spiral ganglion." *Hearing Res.* 15,113-122.
- Sachs, M.B., Young, E.D., Miller, M.J. (1982) "Encoding of speech features in the auditory nerve." in *The Representation of speech in the peripheral auditory system.* edited by R. Carlson and B. Granstrom (Elsevier Biomedical Press, Amsterdam) pp. 115-130.
- Sachs, M.B., Young, E.D., Miller, M.J. (1983) "Speech encoding in the auditory nerve: implications for cochlear implants."in *Cochlear prostheses: An international symposium* edited by C.W. Parkins and

- S.W. Anderson (Annals of the New York Academy of Sciences, New York) pp. 94-113.
- Sinex, D.G., and Geisler, D.C. (1983) "Responses of auditory-nerve fibers to consonant-vowel syllables." J. Acoust. Soc. Am. 73,602-615.
- Sinex, D.G., and Geisler, D.C. (1984) "Comparison of the responses of auditory nerve fibers to consonant-vowel syllables with predictions from linear models." J. Acoust. Soc. Am. 76,116-121.
- Smith, R.L. (1977) "Short -term adaptation in single auditory nerve fibers:some poststimulatory effects." J. Neurophys. 40,1098-1112.
- Smith, R.L. (1979) "Adaptation, saturation, and physiological masking in single auditory-nerve fibers." J. Acoust. Soc. Am. 65 ,166-177.
- Smith, R.L., and Zwislocki, J.J. (1975) "Short-term adaptation and incremental responses of single auditory-nerve fibers." Biol. Cybern. 17,169-182.
- Smith, R.L., and Brachman, M.L. (1982) "Adaptation in auditory-nerve fibers: A revised model." Biol. Cybern. 44,107-120.
- Snyder, R.L. and Schreiner, C.E. (1984) "The auditory neurophonic: basic properties." Hearing Res. 15: 261-280.
- Snyder, R.L. and Schreiner, C.E. (1985) "Forward masking of the auditory nerve neurophonic (ANN) and the frequency following response (FFR)." Hearing Res. 20: 45-62.
- Spoor, A., Eggermont, J.J., Odenthal, D.W. (1976) "Comparison of human and animal data concerning adaptation and masking of eighth nerve compound action potential." in *Electrocochleography* edited by Ruber, Elberling and Solomon (Univ. Park Press, Baltimore, MD) pp.183-198.

- Stevens, C.F. (1968) "Synaptic physiology." *Proceed. IEEE.* 56,916-930.
- van den Honert, C. Stypulkowski, P.H., (1987) "Temporal patterns of single auditory nerve fibers elicited by periodic electrical stimuli." *Hearing Res.* 29,207-222.
- Westerman, L.A. (1985) "Adaptation and recovery of auditory nerve responses." Ph.D. Dissertation, Institute for Sensory Research, Syracuse University, Syracuse, New York.
- Westerman, L.A., and Smith, R.L. (1984) "Rapid and short-term adaptation in auditory nerve responses." *Hear. Res.* 15,249-260.
- Zucker, R.S. (1987) "The calcium hypothesis and modulation of transmitter release by hyperpolarizing pulses." *Biophys. J.* 53,347-350.



562372



3 1378 00562 3726

**FOR REFERENCE**

**NOT TO BE TAKEN FROM THE ROOM**

**CAT. NO. 23 012**

**PRINTED IN U.S.A.**

UC  
San Francisco  
LIBRARY

UC  
San Francisco  
LIBRARY

UC  
San Francisco  
LIBRARY



